

DUCTILE LIGHTWEIGHT CONCRETE FOR LIGHTWEIGHT  
STRUCTURAL APPLICATION

by

AKE PIYAMA KONGDECH

Presented to the Faculty of the Graduate School of  
The University of Texas at Arlington in Partial Fulfillment  
of the Requirements  
for the Degree of

MASTER OF SCIENCE IN CIVIL ENGINEERING

THE UNIVERSITY OF TEXAS AT ARLINGTON

December 2007

Copyright © by Ake Piyamaikongdech 2007

All Rights Reserved

## ACKNOWLEDGEMENTS

I wish to express my sincere thanks to Dr. Ali Abolmaali for his guidance and remarkable patience throughout the supervision of this research. I am also grateful to Dr. Ali Abolmaali for providing a great deal of suggestions and corrections during the preparation and completion of my thesis.

I would like to extend my appreciation to Professor Guillermo Ramirez and Professor J. H. Matthys in the Department of Civil Engineering for their comments and suggestions for this study.

My gratitude goes to Joe Lundy, Professor David Yeih, Vartan Babakhanian, and Kim Spahn for providing invaluable suggestion in understanding the concrete behavior, useful cooperation for equipment and machines for experiments.

I especially wish to thank the Hanson Pipe and Precast, one of the largest precast concrete producer, and Department of Civil and Environmental Engineering of the University of Texas at Arlington for their financial assistance throughout the careers of this study.

Finally, I thank my mother, and father for their support from my country, Thailand. I also extend my appreciation to my friends here, in USA, without whom the completion of this thesis was not possible.

December 1, 2007

## ABSTRACT

### DUCTILE LIGHTWEIGHT CONCRETE FOR LIGHTWEIGHT STRUCTURAL APPLICATION

Publication No. \_\_\_\_\_

Ake Piyamaikongdech, M.S.

The University of Texas at Arlington, 2007

Supervising Professor: Ali Abolmaali

This study developed a ductile concrete for precast wall systems which are capable of resisting high wind in excess of 500 mph. The developed concrete mix design consists of sand, cement, glass fiber, and a foaming agent to produce lightweight concrete in the range of 87 pcf ( $1392 \text{ kg/m}^3$ ) to 90 pcf ( $1440 \text{ kg/m}^3$ ).

A comprehensive testing program for evaluation of the developed concrete material was undertaken. The mix designs were prepared both in the laboratory and in the mix truck with drum capacity of  $27 \text{ ft}^3$  ( $0.77 \text{ m}^3$ ), and  $177.6 \text{ ft}^3$  ( $5 \text{ m}^3$ ), respectively. The large concrete batches using trucks were prepared at the Hanson plants in Grand Prairie, Texas and News Orleans, Louisiana.

The material test included: 188 compressive strength tests (ASTM C39); 166 Modulus of rupture tests (ASTM C78); and 310 Pull-out test (ASTM C234-86) for both

sites. From each mix design, three specimens for 1, 3, 7, 14, 28, 56, and 90 day(s) were prepared and tested on the designated test day. The relationships between the concrete unit weight and each of the aforementioned properties were obtained and recorded.

Two types of pull out test (ASTM C234-86) were conducted: (1) the steel bar (#4) was embedded at 4 in. (10.16 cm.) in the 6 in.(152.4 mm.) x 12 in.(304.8 mm.) cylinders and (2) the steel bar was embedded at 12 in.(304.8 mm.) in the 6 in.(152.4 mm.) x 12 in.(304.8 mm.) cylinders. This was done to document both the pull-out and fracture mode of the failure during the pull-out test.

Full-scale beam tests with specimen sizes of 8 in.(20.32 cm.)x 20 in.(50.8 cm.) x 96 in.(243.8 cm.) were conducted with and without reinforcements. A total of 124 beams (95 without reinforcement and 29 with reinforcement) were tested in four-point bending. The crack patterns and failure loads were identified and recorded. Also, the behavior of the non-reinforced full-size test beams were compared with the ASTM C78 beams. The full-scale testing was continued by testing lightweight precast wall panel with two types of opening configurations: (1) window opening and (2) door opening. Four full-scale walls were tested by being subjected to a single concentrated load at the center of the panel and being loaded to failure. These wall panels were cast at the Hanson's News Orleans's site (Site 2) and were transported for testing to the University of Texas at Arlington structural field laboratory at the Hanson's Grand Prairie plant (site 1). The wall panels were loaded to failure in an incremental manner and the crack initiation and propagations were identified and recorded. Also the load-deformation plots were obtained.

Finally, a three dimensional nonlinear finite element model (FEM) of the wall panels were developed which included elements for the lightweight ductile concrete and the reinforcements. The material geometric and contact algorithms were coupled with the smeared crack model was incorporated in the analysis. The developed FEM is capable of predicting crack initiation and propagation which verified against the experimental tests. Also, the load-deformation plots from the experimental results were compared with those obtained from the FEM analysis, which showed very close correlations

## TABLE OF CONTENTS

ACKNOWLEDGEMENTS .....	iii
ABSTRACT.....	iv
LIST OF ILLUSTRATIONS.....	x
LIST OF TABLES .....	xvi
Chapter	
1. INTRODUCTION .....	1
1.1 Introduction.....	1
1.2 Literature review.....	4
1.2.1 Aggregate for lightweight concrete .....	5
1.2.2 Compressive strength of concrete.....	8
1.2.3 Tensile strength of concrete.....	10
1.2.4 Bond strength between concrete and rebar .....	10
1.2.5 Behavior of concrete structure under severe loads .....	11
1.3 Objective.....	13
2. EXPERIMENTAL PROGRAM.....	14
2.1 Introduction.....	14
2.2 Mix design and Mix procedure.....	17
2.3 Laboratory tests.....	25

2.3.1 Compressive strength test (ASTM C39).....	26
2.3.1.1 Compressive strength test set-up.....	26
2.3.1.2 Compressive strength test result.....	27
2.3.2 Tensile strength test .....	32
2.3.2.1 Tensile strength test set-up .....	33
2.3.2.2 Tensile strength test result.....	34
2.3.3 Relationship between compressive strength and modulus of rupture.....	39
2.3.4 Pull-out test .....	44
2.3.4.1 Pull-out test set-up.....	46
2.3.4.2 Pull-out test result.....	49
3. FULL-SCALE TEST .....	61
3.1 Introduction.....	61
3.2 Full-scale beam tests .....	61
3.2.1 Full-scale beam tests .....	61
3.2.2 Full-scale beam test set-up.....	63
3.2.3 Result for beam tests without reinforcement .....	66
3.2.4 Result for beam tests with reinforcement .....	69
3.2.5 Reinforced beam test designation .....	70
3.3 Full-scale panel tests .....	77
3.3.1 Full-scale panel tests set-up .....	77
3.3.2 Wall panel test designation .....	82



3.3.3 Result for concrete panel tests .....	83
4. FINITE ELEMENT MODELING AND ANALYSIS.....	87
4.1 Introduction.....	87
4.2 FEM model .....	88
4.3 Elements .....	88
4.4 Result for FEM model .....	101
5. SUMMARY, CONCLUSION, AND RECOMMENDATION.....	110
5.1 Summary.....	110
5.2 Conclusion .....	112
5.3 Recommendations.....	116
Appendix	
A. PICTURES FOR MIX-DESIGN PANEL, BEAM, AND SPECIMEN CASTING.....	119
B. FULL-SCALE BEAM TEST.....	132
C. WALL TEST, PICTURE BEFORE AND AFTER TESTING, AND DRAWING OF EACH PANEL .....	170
REFERENCES .....	181
BIOGRAPHICAL INFORMATION.....	183

## LIST OF ILLUSTRATIONS

Figure	Page
1.1 World production of cement during the twentieth century .....	5
2.1 Foaming agent used for mixing concrete .....	15
2.2 Truck used for mixing procedures.....	15
2.3 Launch fine aggregate into the truck .....	15
2.4 Mixing machine used for foaming agent.....	16
2.5 Put forming agent from mixing machine to the truck .....	16
2.6 Casting concrete in prepared form work .....	16
2.7 Compression machine for compressive strength test .....	27
2.8 Failure of specimens for compressive test .....	27
2.9 Graph relationship between compressive strength and unit weight for concrete mixed at Site 1 .....	30
2.10 Graph relationship between compressive strength and unit weight for concrete mixed at Site 2 .....	30
2.11 Graph relationship between compressive strength and unit weight on the 28 <sup>th</sup> day by comparing concrete mixed at Site 1 and Site 2 .....	31
2.12 Comparison of compressive strength for concrete unit weight 90, 95, and 150 pcf.....	31
2.13 Third-point loading for flexural test following ASTM; (a) actual test photograph and (b) Set-up detail.....	34
2.14 Graph relationship between modulus of rupture and unit weight for concrete mixed at Site 1 .....	37

2.15 Graph relationship between modulus of rupture and unit weight for concrete mixed at Site 2 .....	37
2.16 Graph relationship between modulus of rupture and unit weight on the 28 <sup>th</sup> day by comparing concrete mixed at Site 1 and Site 2 .....	38
2.17 Comparison of modulus of rupture for concrete unit weight of 90, 95, and 150 pcf .....	38
2.18 Graph relationship between $\alpha$ and unit weight for concrete mixed at Site 1...	42
2.19 Graph relationship between $\alpha$ and unit weight for concrete mixed at Site 2..	42
2.20 Graph relationship between $\alpha$ and unit weight on the 28 <sup>th</sup> day by comparing concrete mixed at Site 1 and Site 2.....	43
2.21 Pull out failure pattern .....	45
2.22 Splitting failure pattern.....	45
2.23 Pull-out test with universal material testing machine.....	47
2.24 Graph relationship between bond strength and unit weight for concrete mixed at Site 1 .....	52
2.25 Graph relationship between bond strength and unit weight for concrete mixed at Site 2 .....	52
2.26 Graph relationship between bond strength and unit weight on the 28 <sup>th</sup> day by comparing concrete mixed at Site 1 and Site 2 .....	53
2.27 Comparison of bond strength for concrete unit weight of 90, 95, and 150 pcf .....	53
2.28 Typical load-displacement curve.....	54
2.29 Graph relationship between bond stiffness and unit weight for concrete mixed at Site 1 .....	58
2.30 Graph relationship between bond stiffness and unit weight for concrete mixed at Site 2.....	58
2.31 Graph relationship between bond stiffness and unit weight on	

the 28 <sup>th</sup> day by comparing concrete mixed at Site 1 and Site 2.....	59
2.32 Comparison of Bond stiffness for concrete unit weight of 90, 95, and 150 pcf .....	59
3.1 Reinforcement detail for big beam tests.....	62
3.2 Casting for beams with and without reinforcement .....	62
3.3 Load cell set-up at the middle of the steel beam above concrete beam .....	64
3.4 Displacement sensor attached to the middle under the beam with wooden protection after concrete beams were failed .....	64
3.5 Detail for beam test set-up.....	65
3.6 Set up position for loading and displacement sensor .....	65
3.7 Failure mode for big beam tests without reinforcement compare concrete beams made from regular weight concrete and ductile lightweight concrete; Figure 3.7 (a) and (c) failure mode for Regular weight concrete (150 pcf(2400 kg/m <sup>3</sup> )), Figure 3.7 (b) and (d) failure mode for Ductile lightweight concrete (90 pcf(1450 kg/m <sup>3</sup> )) .....	66
3.8 Graph relationship between load and displacement compare concrete beams without reinforcement made from regular weight concrete and ductile lightweight concrete .....	67
3.9 Failure mode for big beam tests with reinforcement compare concrete beams made from regular weight concrete and ductile lightweight concrete; Figure 3.9 (a) and (c) failure mode for Regular weight concrete (150pcf(2400 kg/m <sup>3</sup> )), Figure 3.9 (b) and (d) failure mode for Ductile lightweight concrete (90pcf(1450 kg/m <sup>3</sup> )).....	69
3.10 Graph relationship between load and displacement compare concrete beams with reinforcement made from regular weight concrete and ductile lightweight concrete for unit weight 93.3 pcf.....	75
3.11 Installation of load cell at the top of the concrete panel and displacement sensor at the opening; (a) load cell installation, (b) displacement sensor set up.....	78

3.12 Set up equipment for wall with window opening test .....	79
3.13 Set up equipment for wall with door opening test.....	79
3.14 Detail drawing for concrete panel with window opening .....	80
3.15 Detail drawing for concrete panel with door opening .....	81
3.16 Wall panel with window opening after test.....	84
3.17 Big crack 45 degree at the corner of the window opening occur at failure load .....	84
3.18 Wall panel with door opening after test .....	85
3.19 Graph load and displacement compare concrete panel with door and window openings.....	86
4.1 8-node linear brick, reduced integration (C3D8R).....	89
4.2 The 8-noded quadrilateral in-plane general purpose continuum shell, reduced integration, (SC8R), .....	90
4.3 Tension stiffening model.....	91
4.4 Post-failure stress-strain relation .....	92
4.5 Post-failure stress-strain relation applied for model.....	92
4.6 Tension stiffening model used for this study .....	93
4.7 Typical Unstable Static Response .....	95
4.8 Finite element models for concrete element for window opening model .....	96
4.9 Finite element models for concrete element for door opening model.....	96
4.10 Finite element models for rebar element for window opening model.....	98
4.11 Finite element models for rebar element for door opening model .....	98
4.12 Finite element models for assembled element for window opening with 2636 nodes and 2128 elements.....	99

4.13 Finite element models for assembled element for door opening with 3145 nodes and 2610 elements .....	99
4.14 Boundary condition for panel with window opening model .....	100
4.15 Boundary condition for panel with door opening model.....	100
4.16 Van Mises stress for concrete panel with window opening .....	101
4.17 S11 for concrete panel with window opening .....	102
4.18 S22 for concrete panel with window opening .....	102
4.19 S33 for concrete panel with window opening .....	102
4.20 Van Mises stress for concrete panel with door opening.....	103
4.21 S11 for concrete panel with door opening.....	104
4.22 S22 for concrete panel with door opening.....	104
4.23 S33 for concrete panel with door opening.....	104
4.24 The first cracks of the panel with window opening by FEM model .....	105
4.25 The failure cracks of the panel with window opening by FEM model: (a) failure crack from FEM and (b) failure crack from experiment .....	106
4.26 The cracks of the panel with window opening by FEM model: (a) at 20 kip load and (b) at 120 kip load .....	106
4.27 The first cracks of the panel with door opening by FEM model.....	107
4.28 The failure cracks of the panel with door opening by FEM model: (a) failure crack from FEM and (b) failure crack from experiment .....	107
4.29 The cracks of the panel with window opening by FEM model: (a) at 28 kip load and (b) at 140 kip load .....	108
4.30 Comparison of FEM with experiment for concrete panel with window opening .....	109
4.31 Comparison of FEM with experiment for concrete panel with door opening.....	109

5.1	Graph relationship between compressive strength and unit weight for ductile lightweight concrete at 28 day .....	112
5.2	Graph relationship between modulus of rupture and unit weight for ductile lightweight concrete at 28 day .....	113
5.3	Graph relationship between $\alpha$ and unit weight for ductile lightweight concrete at 28 day .....	114
5.4	Graph relationship between bond strength and unit weight for ductile lightweight concrete at 28 day .....	114
5.5	Graph relationship between bond stiffness and unit weight for ductile lightweight concrete at 28 day .....	115
5.6	Full scale beam test with varied a/d ratio.....	117

## LIST OF TABLES

Table	Page
2.1 Mix proportion for concrete 1 yard <sup>3</sup> (0.7646 m <sup>3</sup> ) .....	17
2.2 Compressive strength for concrete mixed at Site 1 (Grand Prairie).....	28
2.3 Compressive strength for concrete mixed at Site 2 (New Orleans) .....	29
2.4 Modulus of rupture for concrete mixed at Site 1 (Grand Prairie) .....	35
2.5 Modulus of rupture for concrete mixed at Site 2 (New Orleans).....	36
2.6 $\alpha$ for concrete mixed at Site 1 (Grand Prairie) .....	40
2.7 $\alpha$ for concrete mixed at Site 2 (New Orleans).....	41
2.8 Failure mode for concrete cylinder.....	48
2.9 Bond strength for concrete mixed at Site 1 (Grand Prairie).....	50
2.10 Bond strength for concrete mixed at Site 2 (New Orleans).....	51
2.11 Bond stiffness for concrete mixed at Site 1 (Grand Prairie) .....	56
2.12 Bond stiffness for concrete mixed at Site 1 (New Orleans) .....	57
3.1 Mechanical properties for regular and lightweight concrete beams without reinforcement .....	67
3.2 Summary of Test Results for 96 in. (244 cm.) length and 20 in. (50.2 cm.) reinforced concrete beams mixed on 2/8/07 .....	71
3.3 Summary of Test Results for 96 in. (244 cm.) length and 20 in. (50.2 cm.) reinforced concrete beams mixed on 2/20/07 .....	72
3.4 Summary of Test Results for 96 in. (244 cm.) length and 20 in. (50.2 cm.) reinforced concrete beams mixed on 2/27/07).....	73



3.5	Summary of Test Results for 96 in. (244 cm.) length and 20 in. (50.2 cm.) reinforced concrete beams mixed on 3/6/07.....	74
3.6	Mechanical properties for regular and lightweight concrete for 93.3 pcf unit weight beams with reinforcement .....	75
3.7	Summary of Test Results for 78 in. (199 cm.) length and 144 in. (366 cm.) wall panel .....	93

## CHAPTER 1

### INTRODUCTION

#### 1.1 Introduction

Concrete is a construction material that consists of cement, aggregate (fine and coarse), water, and admixtures such as fly ash, silica fume, and other chemical agents. After the mixing process, concrete is hardened by a chemical process called hydration. Concrete can be used for several applications such as pavements, buildings, foundations, pipes, dams, and other civil infrastructural structures. Concrete is one of the most popular construction materials. According to the ASCE (2005), every year approximately six billion cubic meters of concrete is produced. In addition, more than 55,000 miles of roads and highways in America are built by using concrete. Usually, concrete has an outstanding compressive strength but very low tensile strength. Therefore, steel reinforcement is applied in concrete structures to handle the tensile strength of structures.

Precast construction is one of the most popular construction methods. There are several benefits from using precast construction such as optimum use of materials, less construction time, and other advantages. Precast concrete can keep down costs, and save time of construction. Even though the materials needed to produce precast concrete are rather expensive, compared to the regular concrete, precast concrete saves labor cost. Furthermore, the factory engineers delivery the precast concrete framework to be assembled in-site, so the contractors do not need to hire extra labors.

Another advantage is the short duration period of construction because of complete portions of precast concrete delivered from the industry. The site engineers do not need to spend time casting those portions. Therefore, it saves time and money.

In addition, precast concrete can improve some components better and stronger such as wall panels. New wall panels with precast concrete makes the performance of the panels better by including a core of insulation in the units to enhance their thermal performance. Another significant feature of precast concrete is its flexibility to approach different consulting situation. When the construction site is in business areas or traffic zones, the contractors need to finish building as quickly as possible. The construction can not take a long time because it is a barrier to traffic. Precast concrete is the solution to this problem. The building process is done in a very short time by the using of the cranes.

Lightweight construction used in residential houses, and other lightweight structural application has also been developed by researchers and engineers. The reduction of dead load of entire structures have also decreased steel reinforcements significantly. Therefore, cost of the projects have reduced substantially with the decreasing of reinforcements in columns and beams. Some of the material properties have also improved due to lightweight construction, such as thermal insulation, sound insulation, durability, permeability, and other structural properties. Moreover, the method of precast construction can be applied in lightweight construction. For example, a hollow core slab which is one of the most popular construction techniques. Using precast slabs that have a hollow core inside, can decrease dead load by almost half of normal slabs, while electrical wires or conduits can be installed in precast slabs easily.

Ductile lightweight concrete is another popular construction material. Because of severe damages from catastrophes such as earthquakes and hurricanes, the need for new types of concrete with more ductility and strength have substantially increased. To improve ductility and strength of concrete, researchers and engineers have been trying to develop characteristics for specialist applications by certain methods, such as changing the composition of concrete, developing mixed method, or adding some chemical agents in the concrete. Lightweight concrete is one of the most interesting concretes that researchers have been conducting. Generally, lightweight concrete has a density range of less than 120 pcf. Lightweight concrete has traditionally been made by several types of aggregates such as clay, volcanic fly ash, oil palm, and other materials. Using lightweight aggregates instead of these conventional aggregates, many properties of concrete can be improved because of its low weight and density. Moreover, various preformed foams have been added to concrete to decrease its unit weight. Cellular concretes have unit weight between 20 pcf to 60 pcf because of the use of foams as aggregates. Due to high ductility, lightweight concrete can also be applied for dynamic type loading applications in areas of high risk of earthquakes or in severe weather conditions.

The precast panels produced for this research are ductile lightweight structural elements used lightweight structural application. A lightweight concrete of about 90 pcf unit weight was used, so that the concrete panels have more ductility. To determine the stiffness of the ductile lightweight structural elements, full-scale tests such as full-scale beam tests with and without reinforcement, and reinforced concrete panel tests were conducted. Alongside, finite element models for reinforced concrete panels were used to simulate the behavior of concrete panels during loading by using

the ABAQUS software. Stiffness results of the reinforced concrete panels from the experiment and ABAQUS were compared to each other after the analysis process. To identify material properties, such as compressive strength, tensile strength, bond strength between concrete and rebar, and other properties, many specimens were prepared by following the ASTM standard.

### 1.2 Literature review

Aitcin (2000) stated that concrete is the most popular construction material. Because of new development in technologies, concrete has new improved material properties in several ways such as strength, durability, ductility, etc. Yet, concrete will have to improve more to adapt to the environment by using natural materials mixed with it.

According to CEMBUREAU in 1900, the total world production of cement was about 10 million tons; in 1998 it increased to 1.6 billion tons. In less than a century, concrete has become the most widely used construction material in the world. The progression of the amount of cement produced in the world is presented as shown in Figure 1.1. The Graph shows that during the second half of the 20<sup>th</sup> century, the consumption of cement increased substantially. This increase is due to the reason that concrete can be applied in many ways such as buildings, bridges, and other infrastructures.

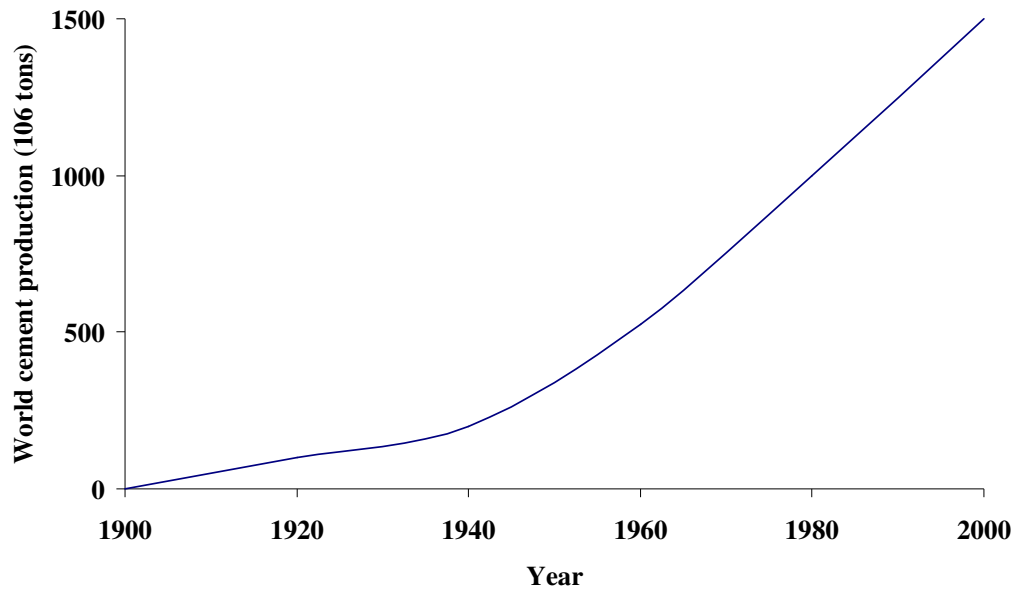


Figure 1.1 World production of cement during the twentieth century

### *1.2.1 Aggregate for lightweight concrete*

Many researchers who have aimed to produce lightweight concrete have conducted their research in several different ways. Some researchers applied new materials for aggregates. Several scientists used chemical agents in the mixing process to lower the weight of concrete. Many specimens such as concrete cubes, concrete cylinders, and concrete beams have been made to test the specific properties of the new lightweight concrete. There are invaluable advantages for using lightweight concrete instead of regular concrete, such as decrease in building weight, improvement of thermal and sound insulation, etc.

Topcu (1996) investigated the properties of semi-lightweight concretes produced by using volcanic slag as coarse aggregate. Topcu (1996) reported that the unit weight of regular concrete is very high related to the dead load of the buildings

that designers have to be concerned with. Moreover, Topcu (1996) also stressed that earthquakes and foundation problems would increase, if the weight of the building is high and construction cost might also be effected by these problems. Therefore, by using lightweight concrete instead of regular weight concrete, the weight of construction can be decreased. Reinforced steel bars used for reinforced concrete structures will be reduced as well because of decreased dead load. Lightweight concrete not only decreases building weight but also improves thermal insulation properties. However, volcanic slag as an aggregate has some disadvantages, such as decreased workability and low strength. Yet, volcanic slag can decrease unit weight of concrete as much as 20 percent of regular concrete.

Pioro, and Pioro (2005) used a technology of processing non-self bloating clays into expanded-clay aggregate for lightweight concrete in a melting converter with submerged combustion. Submerged burners can melt products at a very high temperature. Moreover, submerged burners improve mixing and also increases the rate of chemical reactions.

Unal et al. (2005) showed that the production of lightweight concrete has been expanding in many parts of the world. In their research, block elements were produced with diatomite taken from the region of Afyon with different aggregate granulometries and cement contents. This experiment mentions that the effect of these parameters on physical and mechanical properties of block elements include compressive strength, thermal conductivity, ultrasonic velocity tests, bulk density and specific porosity. According to the result of this study, lightweight concretes with diatomite can be used in constructions to obtain high insulation and reduce self-weight of dead load in buildings.

Qiao et al. (2006) tested an experiment to investigate the properties of mixes produced from crushed medium fraction IBA and Portland cement for lightweight concrete using incinerator bottom ash. This research mentions several properties of concrete, such as the effects of thermally treated crushed IBA, varying the water to solids ratio and the PC to  $\text{Ca}(\text{OH})_2$  ratio used in the binder phase, bulk density, compressive strength, and X-ray diffraction tests.

Mun (2006) conducted a research about lightweight concrete mixed from lightweight aggregate made from a sewage sludge, mixed with various mass ratios of clay to sewage sludge in a rotary kiln, and tested it for density, water absorption, abrasion loss, crushing value, impact value, and heavy metal leaching. Therefore, it proved that lightweight concrete using sewage sludge as an aggregate could be used as an environment conscious artificial lightweight aggregate.

Gesoglu et al. (2006) studied about the effects of physical and chemical properties of fly ash and the characteristics of cold-bonded fly ash lightweight aggregates. To determine the microstructural and mineralogical properties, the produced fly ash aggregates were then examined by several methods such as ESEM micrograph, EDX spectrum, and XRD. The research showed that the fly ash with higher specific surface and with lower CaO content yielded higher strength.

Teo et al. (2006) produced a research to determine structural bond and durability properties of lightweight concrete made from oil palm shell. The split tensile strength, modulus of rupture and modulus of elasticity were determined for this study. Moreover, the structural bond properties were determined by pull-out tests and durability properties of water were characterized by permeability and water absorption tests.



Topcu and Uygunoglu (2006) studied properties of autoclaved lightweight aggregate concrete. This project investigated physical and mechanical properties of lightweight concrete using diatomite and pumice as lightweight aggregates after autoclave curing at different temperature, and curing time.

Mannan et al. (2006) used oil palm shell as the coarse aggregate in lightweight concrete. The purpose of this research was to determine material properties such as water absorption and aggregate impact value. The tests conducted on the oil palm shell concrete were the slump, remolded density and compressive strength.

### *1.2.2 Compressive strength of concrete*

Elfahal et al. (2004) describes a multi-national collaborative study including both numerical and experimental experiments about geometrically similar normal strength concrete cylinders by applying different forces of axial impact. This research studied about high strength concrete. The study investigated the size effect phenomenon for regular strength concrete cylinders under impact loads. However, the tests are different from the study on high strength concrete using only soft impact. Results from the tests and simulations showed the existence of a size effect in regular strength concrete cylinders under both hard and soft impact loading.

Qasrawi (2000) produced a research including estimation of concrete strength by combining methods of non-destructivity. Both the traditional well-known rebound hammer and ultrasonic pulse velocity tests were used in this study. The research was summarized in one simple chart. The method can be easily applied to concrete specimens as well as existing concrete structures. The final results were compared with previous results from literature and also with actual results obtained from samples extracted from existing structures.

Qasrawi (2000) said that the direct method to determine the strength of concrete is loading specimens until failure. Hence, special specimens are required to determine concrete strength and need to be tested at laboratories. This procedure may result in the actual strength of concrete, but may cause trouble and delay in evaluating existing structures. Therefore, special techniques have been developed to measure some of the concrete properties such as hardness, resistance to penetration or projectiles, rebound number, resonance frequency, and the ability to allow ultrasonic pulses to propagate through concrete and relate them to strength, durability, or other properties. Concrete electrical properties, ability to absorb, scatter, and transmit X-rays and gamma rays, response to nuclear activation and acoustic emissions allow researchers to estimate concrete moisture content, density, thickness, and cement content. However, a successful nondestructive test is the one that can be applied to concrete structures in the field, and less investment can be spent on other test methods.

Rajamane et al. (2006) studied about the prediction of compressive strength of concrete with fly ash as the sand replacement material. Fly ash performs as a partial replacement material for both Portland cement and fine aggregate. This research mentions a determination and a formula to predict the compressive strength of concrete on the 28<sup>th</sup> day. Application of the formula to the test data in published literature shows that compressive strength of concrete on the 28<sup>th</sup> day contained different levels of sand replaced by fly ash can be assessed.

Miled et al. (2004) investigated the size effects and failure mechanism of an idealized lightweight expanded polystyrene concrete under compression. There were two types of idealized 2D- expanded polystyrene concrete specimens obtained. Therefore, the specimens were tested by standard uniaxial compressive tests. The

results show that similar compressive strengths for the two specimens were obtained. Moreover, a specimen's tensile failure mode with no crack localization was observed. So, results show that no size effect was engendered by the quasibrittle behavior of the considered idealized expanded polystyrene lightweight concrete. Finally, uniaxial compressive tests on the two specimens were simulated and non-local model parameters were fitted to reproduce in satisfactory manner similar compressive strengths for the two specimens, matching those obtained experimentally.

Kewalramani, and Gupta (2005) conducted research about using ultrasonic pulse velocity (UPV) as a measure of compressive strength of concrete for non-destructive testing methods. This study was conducted to forecast the compressive strength of concrete for different unit weight of concrete and UPV for two different concrete mixtures. The prediction applied multiple regression analysis and artificial neural networks for the results. A comparison between the two methods demonstrated that the artificial neural networks can be used to predict the compressive strength of concrete with high accuracy.

### *1.2.3 Tensile strength of concrete*

Iskhakov, and Ribakov (2006) studied about a design method for two-layer beams consisting of normal and fibered high strength concrete. This research mentioned at two-layer fibered concrete beam analysis by using conventional methods for composite elements. The compressive zone of the beam section used high strength concrete and the tensile zones of the beams used regular strength concrete. The compatibility conditions between high strength and normal strength concrete related to the shear deformations equality on the layers border in a section with maximal

depth of the compression zone. Moreover, fibers were mixed in with high strength concrete to solve the problem of low ductility.

#### *1.2.4 Bond strength between concrete and rebar*

Yeih et al. (1997) researched about a pull-out test for determining interface properties between rebar and concrete. In this study, the rebar-concrete interface properties were investigated by using the single rebar pull-out test. The corresponding material parameters were determined by applying a combination of the stress approach and the fracture mechanical theory.

The single rebar pull-out test's purpose was to determine some material properties about interface behaviors. Pull-out behaviors and the interface properties can be predicted by several theories. However, before using the model to define bond strength between concrete and rebar, researchers have to make assumption that is suitable for experimental models.

#### *1.2.5 Behavior of concrete structure under severe loads*

Watanabe (1997) said that under severe earthquakes, first story columns will collapse due to lack of lateral strength and ductility. Therefore, to prevent failure for first story columns, construction materials have to be more ductile. Moreover, Mitche et al. (1995) mentioned that most of the collapsed buildings from earthquakes at Northridge in 1994 were non-ductile structures with high dead load. Hence, when earthquake occurs, a mix of gravity load and lateral load from the earthquake cause the damages. In addition, Dogangun (2003) described this as one of the main reasons that caused the damage of the structures during the earthquakes that occurred in different regions of the World. During an earthquake, the floor's deformation

significantly increases and transfers the loads to the first floor columns. Thus, lack of ductility of columns is the cause of a building's failure.

Luccioni et al. (2004) studied about the collapse of buildings due to blast loads by using numerical simulation program compare to actual effect of blasting. Analysis results demonstrated that collapse of reinforced concrete buildings happens due to gravitational mechanism at the first floor columns.

Moreover, Yankelevsky, and Avnon(1998) conducted research about Autoclaved aerated concrete behavior under explosive action. This experiment mentioned the crack patterns and explosion response of concrete. This examination can be summarized to say that tensile strength and ductility are one of the factors that can resist tensile wave spall cracking in concrete walls.

Schenker et al. (2006) tested full-scale concrete slabs subjected to blast loads to verify dynamic response of concrete structures to blast loads. In the research, numerical simulation models were conducted to compare results to the field tests.

### 1.3 Objective

The main objective of this research is to develop a lightweight ductile concrete with optimum weight in the range of 90 pcf (1450 kg/m<sup>3</sup>) to 95 pcf (1530 kg/m<sup>3</sup>) for lightweight construction with minimum compressive strength of 1500 psi ( 105 kg/cm<sup>2</sup>). To achieve this objective, the following are at the forefront;

1) To develop a mix design and a mix design procedure to consistently produce the lightweight concrete. It should be noted that lightweight, in this study, does not refer to lightweight aggregate, which means that the mix design consists of sand, cement, water, and a foaming agent.

2) To conduct all the necessary material tests to identify the material behavior. This test includes compressive test (ASTM C39), flexural tensile test (ASTM C78), and pull-out test (ASTM C234).

3) To conduct the necessary ASTM structural tests to identify the behavior of structural members built with the developed lightweight concrete, full-scale beams test and panel test were conducted.

CHAPTER 2  
EXPERIMENTAL PROGRAM

2.1 Introduction

This chapter presents a series of experimental studies to develop and optimize the material properties of the lightweight ductile concrete. Several experiments were conducted to develop a mix design procedure in both small batch laboratory setting and large batch field mixing. The laboratory mixes used 27 ft<sup>3</sup> (0.77 m<sup>3</sup>) mix drum and the field mixing used 177.6 ft<sup>3</sup> (5 m<sup>3</sup>) mix drum in two locations: Hanson Grand Prairie, Texas (Site 1) and Hanson New Orleans, Louisiana (Site 2).

The mixing procedure consisted of identifying the order and increments in which the ingredients (sand, cement, foaming agent, and water) are placed and added, at a mixing duration of each increment. This was done to identify the mixing design procedure which reached to the targeted unit weight of 90 lb/ft<sup>3</sup> (1450 kg/m<sup>3</sup>) and the compressive strength of 1500 lb/in<sup>2</sup> ( 105 kg/cm<sup>2</sup>).

The material tests included : Compressive strength test (ASTM C39), Tensile test (ASTM C78), and Pull-out test (ASTM C234). All the tests were conducted for 1, 3, 7, 14, 28, 56, and 90 day(s) tests. The numerical and graphical representations of the test results are presented as functions of the unit weight of each mix.



Figure 2.1 Foaming agent used for mixing concrete



Figure 2.2 Truck used for mixing procedures



Figure 2.3 Launch fine aggregate into the truck





Figure 2.4 Mixing machine used for foaming agent



Figure 2.5 Put forming agent from mixing machine to the truck



Figure 2.6 Casting concrete in prepared form work

## 2.2 Mix design and Mix procedure

To investigate the characteristic properties of the ductile lightweight concrete, several tests have been conducted such as compressive tests, tensile tests, and pull-out tests. For this research, the material tests are classified into two groups. First, the lab test mixes were made in the forms of small specimens such as 4 in.(101.6 mm.) x 8 in.(203.2 mm.) cylinders, 6 in.(152.4 mm.) x 12 in.(304.8 mm.) cylinders, and non-reinforced 6 in.(152.4 mm.) x 6 in.(152.4 mm.) x 24 in.(609.6 mm.) beams. All of specimens were cast from Hanson concrete plants at Site 1 and Site 2 and delivered to the Structural Laboratory at the University of Texas at Arlington immediately after the concrete hardened. The specimens were tested for 1, 3, 7, 14, 28, 56, and 90 day(s). A second series of the test is full-scale mix tests. Full scale mixes were produced with the mixing truck with 177.6 ft<sup>3</sup> (5 m<sup>3</sup>) concrete when samples are loaded by testing machines, such as 8 in.(20.32 cm.)x 20 in.(50.8 cm.) x 96 in.(243.8 cm.) beams and the wall panel tests.

### **Mix design**

To produce desired concrete unit weight (90 lb/ft<sup>3</sup> (1450 kg/m<sup>3</sup>)), mix design for concrete 1 yard<sup>3</sup> (0.7646 m<sup>3</sup>) is shown in the below Table. 2.1.

Table 2.1 Mix proportion for concrete 1 yard<sup>3</sup> (0.7646 m<sup>3</sup>)

<b>Materials (concrete)</b>	<b>Mix proportion</b>
Cement	675 Lb (307 Kg)
Sand	1440 Lb (655 Kg)
Water	300 Lb (137 Kg)
NEOPOR (foaming agent)	40 Lb (19 Kg)

## Mix procedures

### 1. Calibration

- a. To calibrate the foam generator, a container of known quantity was prepared.
  - i. Take a 55 gallon drum and weigh it. Take the scale.
  - ii. Fill the drum with water and weigh it.
  - iii. Divide the weight of the water-filled drum by 8.34, (the weight of water per gallon in pounds).
- b. The ratio of water to the Neopor foaming agent is 40:1.
- c. Connect the water supply to the foam generator using a ¾" hose. The minimum flow of water from the supply is 15 gal/min with a minimum pressure of 58 psi.
- d. Disconnect the green discharge hose.
- e. Place the container close to the opening of the discharge hole.
- f. Turn on the water supply and open the water valve on the foam generator.
- g. Turn on the foam generator.
- h. Place the container under the flow and start timing. Stop the time when it reaches 40 gallons. Turn off the generator.
- i. Empty the container and repeat the above step.
- j. After successfully completing step h, turn off the pump and water supply, and close the water valve on the generator.
- k. Drop the clear siphon hose into the bucket.

- l. On the bottom of the foam generator motor, there is a round, black dial. On this dial are lines or “tic marks”. These marks represent ones. The “shaft” of this dial has lines that represent tens. The center line on the shaft is the target line or zero line. Turn the dial until to 50.
- m. Get the one gallon container and the funnel ready. Turn on the generator. The siphon hose will begin to fill and a small stream of water will start to come out of the discharge hole. When it looks like the stream is steady, place the funnel under the flow. Place the one gallon container under the funnel and start the stopwatch.
- n. At one gallon, stop timing. Check the time. You are trying to match the time it took to reach 40 gallons. Remember the ratio – 40:1. If it took longer to reach one gallon than it did for 40 gallons, then increase the amount of flow from the siphon hose. Turn the black dial to 60. If it did not take as long, decrease the flow from the siphon hose. Adjust the flow from the siphon hose accordingly until the time for 40 gallons is the same as 1 gallon (within 1 second).
- o. After successfully obtaining the correct ratio, the Neopor is ready to be introduced. Hook up the air supply. The air supply needs to maintain a constant pressure of at least 87 psi, and the air must be oil and vapor free.
- p. Get a container of known volume, weigh and tare. Connect the green discharge hose, open the air supply valve and water supply valve on the generator, and place the siphon hose in a container of Neopor.

- q. Turn on the generator. When foam starts to come out of the discharge hose, fill up the container. Strike off any excess from the top of the container, leaving a flat surface. Weigh the container full of foam. The density of the foam should be 5lbs/ft<sup>3</sup>. Adjust the air on the generator air supply valve and fill the barrel again. Repeat this procedure until a density of 5lbs/ft<sup>3</sup> is achieved.
- r. Next, determine the output of the foam generator. Again, a container of known volume is needed, as well as a stopwatch.

## 2. Batching

### a. Manual batching system

- i. Place mixer truck under plant and throttle up for loading.
- ii. Determine number of yards to be loaded.
- iii. Multiply number of yards by 36 (gallons of water per yard).
- iv. Discharge 80% of water into truck this is the head water.
- v. Multiply number of yards by 675 (pounds of cement per yard).
- vi. Weigh up cement into scale – do not discharge. Depending on the number of yards to be loaded and the scale capacity, this may take 2 batches of cement, or “double batch”.
- vii. Multiply number of yards by 1440 (pounds of sand per yard).
- viii. Turn on load conveyor and start loading the sand.
- ix. Within 5 seconds of the sand entering the truck, start the cement.  
Try to complete the cement just before the completion of the sand.

If the cement has to be double batched, stop the sand until the second round of cement is ready to be loaded.

- x. After the sand and cement are loaded, put the remaining 20% of water into the truck. This is the tail water.
- xi. Let the truck mix at full throttle for 2-3 minutes.
- xii. Check the load. The consistency should be that of hot caramel.
- xiii. Proceed to the foam generator.

b. Computerized batching system

- i. Determine number of yards to be loaded.
- ii. Set water to load at 80% head and 20% tail.
- iii. Set computer to load cement at 90% of aggregate load rate.
- iv. Start batching sequence.
- v. After truck is loaded, let the load mix in truck for 2-3-minutes.
- vi. Check load.
- vii. Proceed to foam generator.

3. Administering the Neopor foam

- a. Assuming the output has been calculated, set the timer on the generator for the appropriate time to coincide with the yards batched
  - i. The mixer should be turning at engine idle speed.
  - ii. Climb up the ladder on the back of the truck and place the green discharge hose into the back of the mixer. Do not let it lay or

dangle freely. It will have to be held in place. This is critical for a good mix.

- iii. When the “hose man” is ready, the person on the ground can start the foam generator, making sure to watch the output gauge, which is located just above the coupling of the discharge hose. Optimum output is 0.6 bar or 8.7 psi.
- iv. Employees make sure that the foam is going as far into the truck as possible.
- v. Once the timer has stopped the foam, allow the truck to mix for approximately 30 revolutions. Then, have workers keep an eye on the load while the mixer truck operator runs the mix up and down the drum by charging and discharging (forward and reverse) the drum. Do this 8-12 times. After doing this, allow the drum to mix for approximately 2-3 minutes more.
- vi. Discharge a small amount into a wheelbarrow (careful-it will flow like water) and check and record the weight for proper density. If the proper density has been achieved, allow the drum to mix another 3-4 minutes and check again to make sure the mix has stabilized. If the weights are the same or within 2%, make 2 cylinders and pour it out.
- vii. If the mix has not stabilized, then the foam is breaking down, either due to not being mixed well enough, or because there was

not enough foam to begin with. Add more foam, but only in small time increments, like one minute at a time. Mix as mentioned above.

#### 4. Placement of concrete

- a. Attach as many chutes as the truck will properly allow. Remember, putting on more chutes than for which the truck is rated. It may damage the hydraulic lift cylinder.
- b. Position the truck alongside the forms.
- c. Reverse the drum and slowly pour the mixture into the form, starting at one end and moving to the other. Move the chute back and forth in a sweeping motion. The mixer truck driver will need to pay close attention to the chute man, as he will signal the driver as to when to pull up, stop, etc.
- d. If the table is equipped with vibrators, turn them on as soon as the concrete hits the form and run them for approximately 30 seconds. Turn off the vibrators for about 30 seconds, then back on again for about 30 seconds. Repeat this pattern for the entire pour.
- e. When the truck is approximately half empty, take a sample of the poured concrete from inside the form and check and record the weights. Make four more cylinders. If the weights are close to the weights taken at the beginning of the load, continue to pour.



- f. If the weights are significantly more, stop. The foam is breaking down. Mix the concrete for a few more minutes and check and record the weight. If the weight continues to rise, add more foam and check the weight again. If the load does not stabilize, then it must be discarded and a new load put into the truck.
- g. Assuming that the weight is still stable, take a sample at the end of the load from inside the form. Make two more cylinders. Check and record the weight.
- h. After the truck is empty, discharge all of the water in the truck's water tank into the drum. If another load is required, dump this water into the reclamation pit and reload. If another load is not required, dump this water into the reclamation pit and add another 300 gallons of water to the drum, plus, add about 5000 pounds of ¾" or larger gravel to the drum and let it mix for about 5 minutes. This water/gravel mixture can be used again and again to "rock" the drum. The Neopor mixture is very sticky and will cling to the blades of the mixer drum. This "rocking" will help keep the blades clean. Clean blades result in a better and more consistent mix.

## 5. Finishing the surface

- a. After filling a form, strike off any excess with a screeder.
- b. Cover the form with a plastic thermal blanket or some other type of plastic sheeting. Try to keep the cover from resting on the concrete.

- c. Ambient temperature and humidity will play a part in how long it will be before the product can receive the final troweling, floating, raking, brooming, or whatever finish is needed.
- d. About every 15 minutes, lift the cover and perform the “finger” test. Touch the top of the concrete. If it feels like gritty soft serve ice cream, then it is still too early.
- e. After the desired finish is achieved, recover the product with the plastic sheeting, again trying to avoid letting it rest on the product.

### 2.3 Laboratory tests

To identify the design parameter of the ductile lightweight concrete such as the compressive strength, the tensile strength, and the bond strength between concrete and rebar, 91 4 in.(101.6 mm.) x 8 in.(203.2 mm.) cylinders for Site 1 and 90 cylinders for Site 2, 91 6 in.(152.4 mm.) x 6 in.(152.4 mm.) x 24 in.(609.6 mm.) beams for Site 1 and 75 beams for Site 2, and 168 6 in.(152.4 mm.) x 12 in.(304.8 mm.) cylinders for Site 1 and 144 cylinders for Site 2 were prepared and tested. Each test was repeated three times to obtain additional data for verification.

Since the aim of the study is to produce ductile lightweight concrete with optimum weight of 90 pcf ( $1450 \text{ kg/m}^3$ ) with minimum compressive strength of 1500 psi ( $105 \text{ kg/cm}^2$ ), concrete with different unit weight were produced and tested which resulted in developing relationships between the concrete unit weight and the compressive strength for a given test. This, off course, yields to additional relationships with regard to the age at which the concrete was tested.

### *2.3.1 Compressive strength test (ASTM C39)*

In order to characterize the compressive strength of concrete, 91 specimens and 90 specimens were tested from the mix designs produced in Site 1 and 2, respectively. Cylinders were produced from each mix design for 1, 3, 7, 14, 28, 56, and 90 days.

#### *2.3.1.1 Compressive strength test set-up*

Following ASTM C39, three cylinders were tested on each age test. In test procedure, to provide the uniform distributed load, cylinders are capped generally on the top and the bottom of the concrete cylinders by steel caps as shown in Figure 2.7. Cylinders have to be centered in the compression testing machine and loaded to complete failure. The 500 kips (226.8 tons) compression machine using hydraulic system is used for this test. Steel caps are put at the top and the bottom of the concrete cylinders before tests.

The loading rate on the hydraulic machine should be maintained at a range of 20 psi (0.138 MPa) to 50 psi (0.345 MPa) per second during the latter half of the loading phase. Types of failure are recorded at the end of every test. A common failure pattern of concrete cylinders for compressive test is conical fracture. Finally, the compressive strength of concrete is calculated by dividing the maximum load at failure by the average cross sectional area of concrete cylinders.

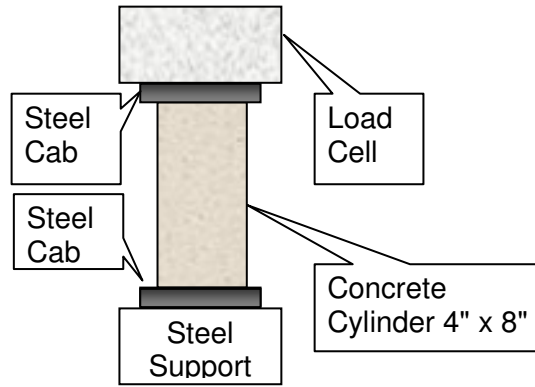


Figure 2.7 Compression machine for compressive strength test



Figure 2.8 Failure of specimens for compressive test

From the Figure 2.8, the concrete cylinder had fracture failure at the top of the specimens. The acquisition system used for the compressive test collected the highest load during the tests. The computer automatically stopped and showed the results after the concrete cylinder reached the failure point.

### 2.3.1.2 Compressive strength test result

The results from compressive strength tests are shown in Tables, 2.2 and 2.3. Comparison between concrete mixed at Site 1 and Site 2 also are shown in Figures, 2.12 and 2.13.

Table 2.2 Compressive strength for concrete mixed at Site 1 (Grand Prairie)

Site1														
Mix date	1day		3days		7days		14days		28days		56days		90days	
	fc	weight	fc	weight	fc	weight	fc	weight	fc	weight	fc	weight	fc	weight
	psi	pcf	psi	pcf	psi	pcf	psi	pcf	psi	pcf	psi	pcf	psi	pcf
2/27/07	667.65	99.87	909.57	99.36	908.77	93.51	1279.61	99.55	1115.68	91.89	1126.83	92.21	1183.17	91.71
2/27/07	520.44	93.22	876.15	99.71	869.78	93.22	1209.00	93.22	1200.00	92.30	1212.00	92.97	1272.60	92.30
2/27/07	670.04	99.87	715.40	93.22	1105.33	99.34	1368.73	100.27	1446.72	99.68	1461.19	99.33	1534.24	100.62
2/27/07	502.13	93.22	715.40	93.22	1260.51	100.66	1317.00	92.83	1429.21	96.77	1443.50	97.30	1515.68	96.77
3/6/07	678.00	95.88	780.10	95.88	838.75	95.88	1220.72	97.31	1273.24	95.06	1285.97	95.06	1350.27	95.56
3/6/07	679.00	95.88	826.65	95.88	1008.25	95.88	1147.51	91.95	1407.73	94.65	1421.80	94.19	1492.89	94.65
3/6/07	673.00	95.88	826.65	95.88	1231.06	95.88	1292.00	93.67	1155.46	91.33	1167.02	90.86	1225.37	91.33
3/20/07	366.85	87.731	670.84	87.99	875.35	87.35	964.48	87.35	861.00	86.01	734.27	85.23	770.98	85.09
3/20/07	396.30	88.488	549.08	87.99	720.97	88.52	996.31	88.18	939.01	88.109	948.40	87.91	995.82	87.89
3/20/07	387.54	87.731	627.87	89.05	872.96	88.41	977.21	87.62	915.14	88.83	924.29	89.04	970.51	88.56
3/27/07	346.16	88.60	521.23	86.18	721.77	86.94	795.77	87.62	992.33	86.94	1002.25	86.94	1052.37	87.66
3/27/07	534.00	92.04	545.90	86.86	651.74	86.71	826.81	86.52	875.35	86.71	884.11	86.71	928.31	86.71
3/27/07	350.94	87.96	519.64	88.22	596.83	87.01	904.00	86.63	915.14	87.01	924.29	87.01	970.51	86.61

Table 2.3 Compressive strength for concrete mixed at Site 2 (New Orleans)

Site2														
Mix date	1day		3days		7days		14days		28days		56days		90days	
	fc	weight	fc	weight	fc	weight	fc	weight	fc	weight	fc	weight	fc	weight
	psi	pcf	psi	pcf	psi	pcf	psi	pcf	psi	pcf	psi	pcf	psi	pcf
3/29/07	NA	NA	1025	92.609	1046.4	92.81	1450.7	92.91	939	88.30	828.72	90.59	1125	88.299
3/29/07	NA	NA	1203.2	97.034	1089.4	92.63	1529.5	98.92	1219	89.78	1159.9	88.866	1188.9	88.866
3/29/07	NA	NA	868.99	89.32	1143.5	93.79	1339.3	92.72	1318.6	91.31	1351.6	91.31	1385.4	91.31
3/30/07	NA	NA	879.33	90.98	853.07	84.70	1766	101.12	1400	91.94	1435	91.94	1470.9	91.94
3/30/07	NA	NA	805.32	90.07	810.89	89.13	921.51	84.933	1290	90.79	1322.3	90.79	1355.3	90.79
3/30/07	NA	NA	839.54	91.05	1394.2	99.89	1556.5	99.832	1254.1	90.21	1285.5	90.21	1317.6	90.21
3/30/07	NA	NA	2981.8	146.31	3017.6	144.45	3489.5	143.43	3489.5	143.43	3576.7	143.43	3666.1	143.43
3/30/07	NA	NA	2252.8	142.57	3724.2	145.21	3565.1	143.62	3565.1	143.62	3654.2	143.62	3745.6	143.62
3/30/07	NA	NA	2751.8	142.94	3191.1	146.16	3591.3	141.58	3591.3	141.58	3681.1	141.58	3773.1	141.58
4/3/07	NA	NA	631.85	73.74	890.47	85.94	1028.1	86.12	1332	93.28	1084	86.116	1543	94.46
4/3/07	NA	NA	858.64	87.32	728.13	80.27	1040.9	86.46	1070.3	86.46	1097.1	86.459	1124.5	86.459
4/3/07	NA	NA	647.76	78.55	980.39	88.35	545.11	79.93	1062.4	86.46	1088.9	87.54	1116.1	87.07
4/4/07	NA	NA	1232.7	95.82	1289.2	93.32	2263.2	104.68	2188.4	97.98	2243.1	97.976	2299.2	97.976
4/4/07	NA	NA	736.89	91.61	1538.2	98.49	2047.5	97.98	1599.5	97.19	1639.5	95.79	1680.5	96.38
4/4/07	NA	NA	1601.1	105.71	1476.2	97.45	1562.9	88.18	2115.2	97.98	2168	97.976	2222.2	97.976

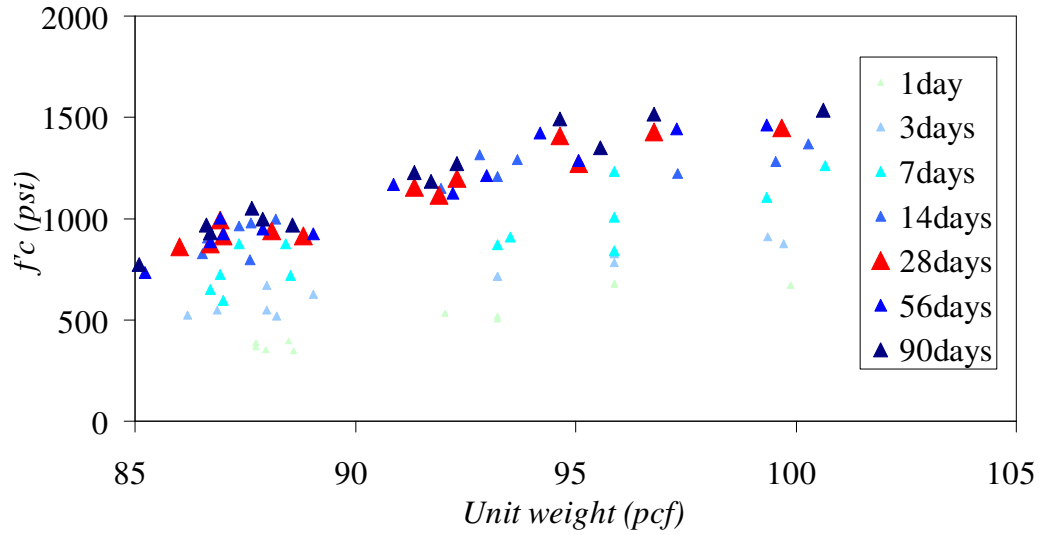


Figure 2.9 Graph relationship between compressive strength and unit weight for concrete mixed at Site 1

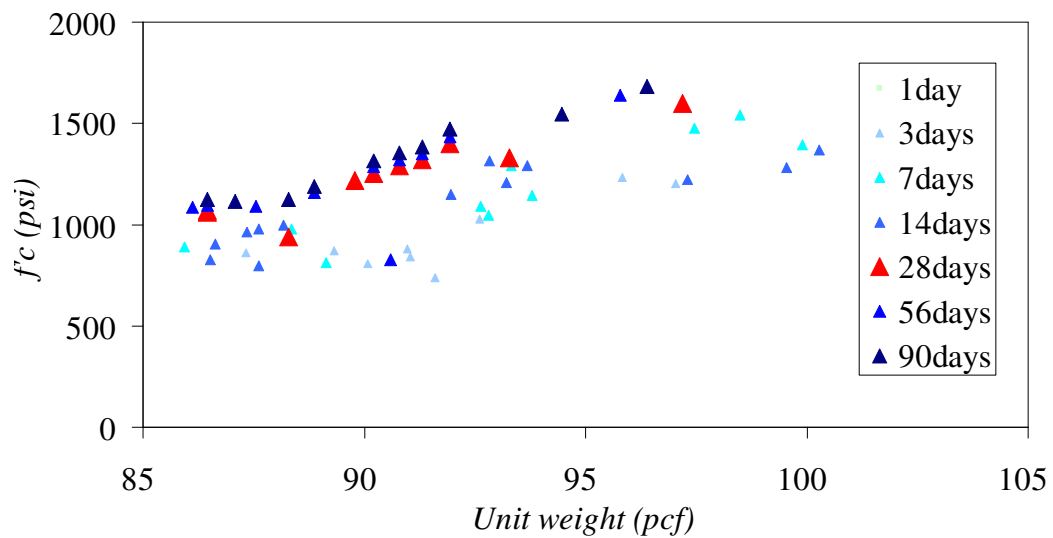


Figure 2.10 Graph relationship between compressive strength and unit weight for concrete mixed at Site 2

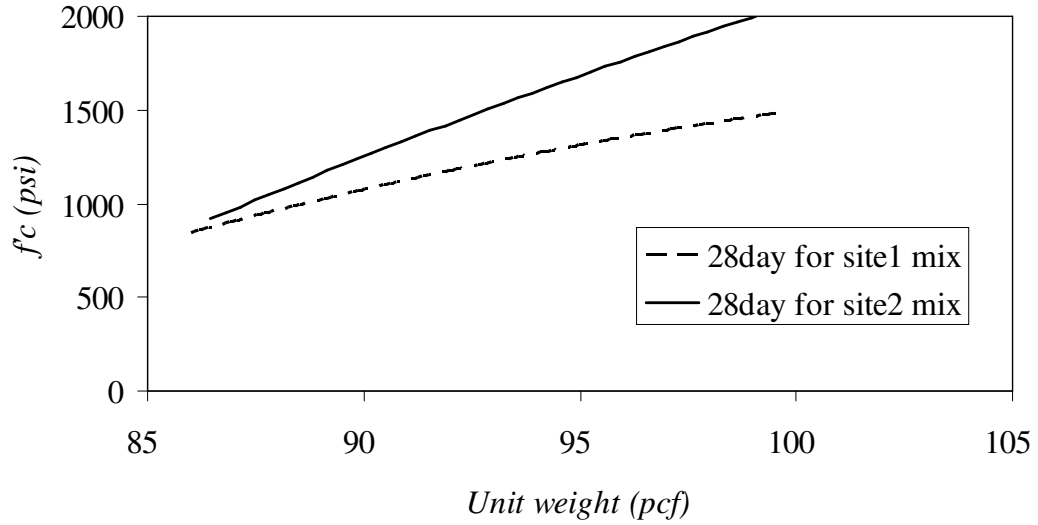


Figure 2.11 Graph relationship between compressive strength and unit weight on the 28<sup>th</sup> day by comparing concrete mixed at Site 1 and Site 2

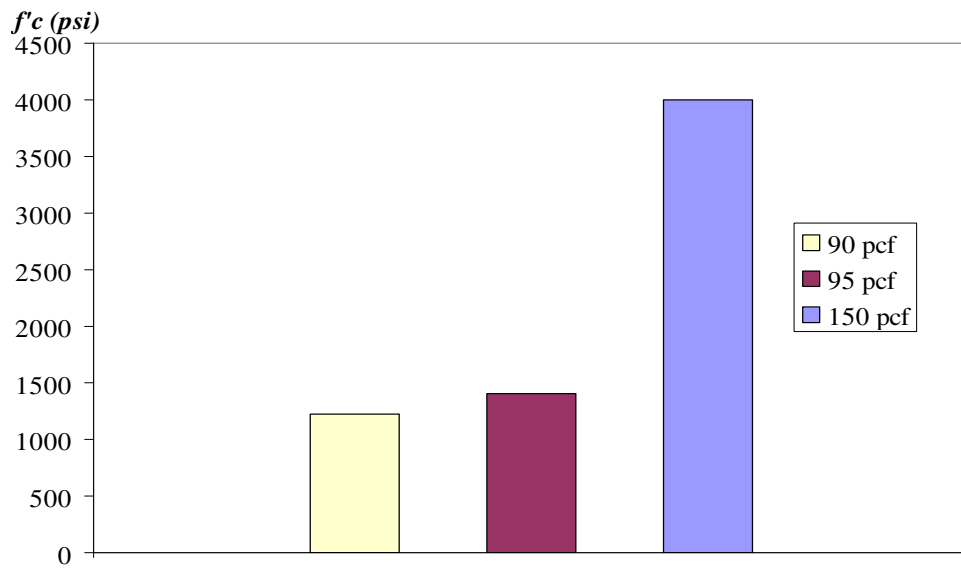


Figure 2.12 Comparison of compressive strength for concrete unit weight 90, 95, and 150 pcf.



From the result, compressive strength of ductile lightweight concrete from site 1 and Site 2 are very close to each other.

Compressive strength on the 28<sup>th</sup> day and unit weight of concrete for Site 1 are related by the following equation

$$f'_c = -1.0541w^2 + 242.6w - 12220 \quad (2.1)$$

Compressive strength on the 28<sup>th</sup> day and unit weight of concrete for Site 2 are related by the following equation

$$f'_c = -0.8949w^2 + 251.89w - 14170 \quad (2.2)$$

$f'_c$  = compressive strength of concrete on the 28<sup>th</sup> day (psi)

$w$  = unit weight of concrete (pcf)

### 2.3.2 Tensile strength test

Concrete has relatively high compressive strength, but significantly lower tensile strength about 10% of the compressive strength. As a result, concrete always fails from tensile stress. Flexural strength is one measure of tensile strength of concrete. Flexural strength can be measured by a non-reinforced concrete beam to resist failure in bending. Concrete specimens were cast on 6 in.(152.4 mm.) x 6 in.(152.4 mm.) x 24 in.(609.6 mm.) for 21 molds for each mixed design for 1, 3, 7, 14, 28, 56, and 90 day(s) test. The flexural strength is expressed as *Modulus of Rupture* (MR) in psi unit by following the standard test method ASTM C78 (third-point loading) as shown in Figure 2.15. There are two loading methods for the beam test. First method is third-point loading and another method is center-point loading. Usually, MR determined by third-point loading is lower than MR determined by center-point loading by 15 percent. Therefore, third-point loading was chosen for this research because this method is more conservative.

### 2.3.2.1 Tensile strength test set-up

Following ASTM C78, third-point loading method is used for this project. Beam specimens were marked at points for supports at three inches from the edges of the beams. And then, the top of the beams were located at the point for loads by 6 in. (152.4 mm.) from the support positions. Finally, the beams were placed on the hydraulic compression machine by placing the loads on the top of the beams at the marked point. The 500 kips compression machine using hydraulic system is used for this test. Beam supports and loading equipments were applied for this machine before placing beam specimens.

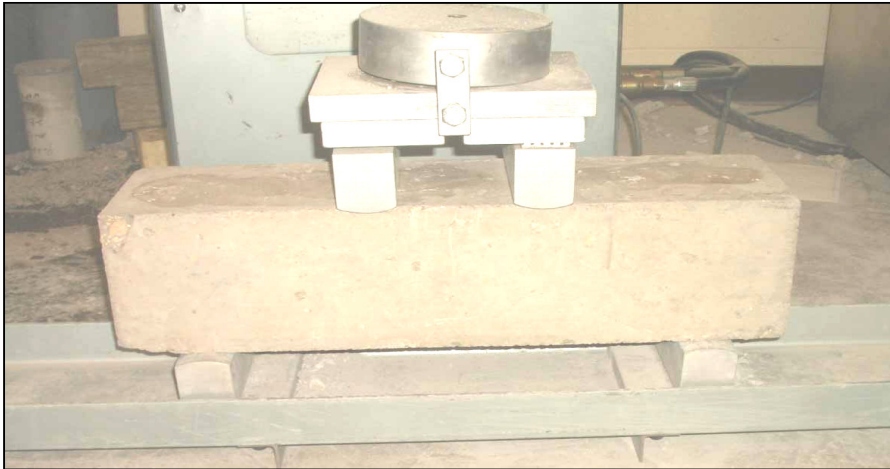
The loading rate on hydraulic machines should be maintained in a range of 20 psi (0.138 MPa) to 50 psi (0.345 MPa) per second during the tests. Maximum load for each test was recorded to calculate the maximum moment for the tests. Finally, modulus of rupture of concrete can be determined by the equation below.

$$f_t = \frac{Mc}{I} \quad (2.3)$$

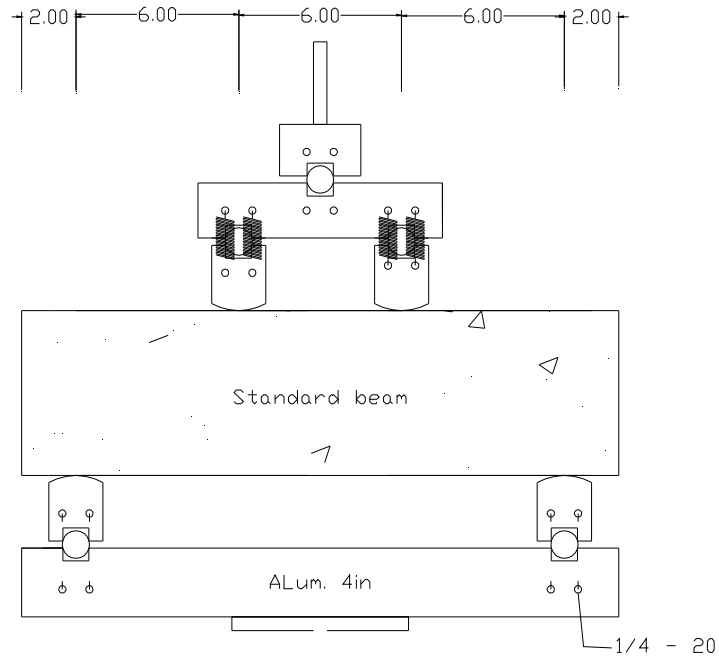
M = maximum moment calculated from maximum load

c = distance from neutral axis of the beam to the bottom of the beam that equals to 3 inches

I = moment of inertia of concrete beam



(a)



(b)

Figure 2.13 Third-point loading for flexural test following ASTM;  
 (a) actual test photograph and (b) Set-up detail

*2.3.2.2 Tensile strength test result*

The results from compressive strength tests are shown in Tables, 2.4 and 2.5. Comparison between concrete mixed at Site 1 and Site 2 also shows in Figure. 2.18.

Table 2.4 Modulus of rupture for concrete mixed at Site 1 (Grand Prairie)

Site1														
Mix date	1day		3days		7days		14days		28days		56days		90days	
	f <sub>t</sub>	weight	f <sub>t</sub>	weight	f <sub>t</sub>	weight	f <sub>t</sub>	weight	f <sub>t</sub>	weight	f <sub>t</sub>	weight	f <sub>t</sub>	weight
	psi	pcf	psi	pcf	psi	pcf	psi	pcf	psi	pcf	psi	pcf	psi	pcf
2/27/07	158.33	93.22	195.83	93.22	200.14	93.22	215	93.22	221	95.90	198.52	95.25	241	95.90
2/27/07	154.17	93.22	206.17	93.22	212.87	93.45	206.11	92.69	284	96.60	286.84	96.33	289.71	96.99
2/27/07	154.17	93.22	206.67	93.22	226.8	93.22	228.79	93.66	305	98.90	308.05	98.90	311.13	98.48
2/27/07	173.9	95.88	254.17	104	252	93.2	330	104.63	370.83	103.44	374.54	103.44	378.28	103.44
3/6/07	187.3	95.88	247.5	105	244	94.5	364.7	110	269.3	95.85	283	96.13	274.71	96.13
3/6/07	182.3	95.88	207.1	95.88	240	93.4	320	104.3	298.42	99.65	301.4	100.08	304.41	99.65
3/6/07	137.5	89.4	175.83	92.33	190.19	91	233.9	92.99	243	89.50	229	89.50	247.88	89.87
3/20/07	135.83	88.92	172.5	89.84	188.6	90.6	212	91.5	234	91.4	236.34	91.4	238.7	91.78
3/20/07	135	89.448	196.67	92.05	187.01	90.4	189.39	88.93	215	89.1	217.15	89.1	219.32	89.1
3/20/07	144	91.51	170	89.5	200.54	91.3	218.84	89.44	237.94	88.43	240.32	88.73	242.72	88
3/27/07	143.33	90.38	176.67	90.2	178.1	88.43	178	86.75	218	90.54	220.18	90.54	222.38	90.3
3/27/07	138.33	90.5	162.5	89.9	174.6	88.43	188	87.47	234.75	91.08	237.1	91.08	251	91.08
3/27/07	137	90.5	165	89.9	165	88.43	190	87.47	231	91.08	215	91.08	237	91.08

Table 2.5 Modulus of rupture for concrete mixed at Site 2 (New Orleans)

Site2														
Mix date	1day		3days		7days		14days		28days		56days		90days	
	f <sub>t</sub>	weight	f <sub>t</sub>	weight	f <sub>t</sub>	weight	f <sub>t</sub>	weight	f <sub>t</sub>	weight	f <sub>t</sub>	weight	f <sub>t</sub>	weight
	psi	pcf	psi	pcf	psi	pcf	psi	pcf	psi	pcf	psi	pcf	psi	pcf
3/29/07	NA	NA	234.17	96.46	163.13	85.29	155.97	84.936	230	90.43	208.97	86.29	211.06	87.18
3/29/07	NA	NA	208.33	96.36	171.09	92.74	205.31	86.736	220.43	87.78	222.63	88.67	224.86	88.22
3/29/07	NA	NA	220.83	98.49	160.75	85.68	158.36	88.584	215.65	84.07	217.81	84.07	219.99	84.07
3/30/07	NA	NA	244.17	97.2	287.7	100.25	258.63	99.744	266.58	92.18	269.25	92.7	271.94	91.02
3/30/07	NA	NA	265	99.24	274.8	100.51	249.87	97.56	282.5	97.83	285.33	97.05	288.18	96.35
3/30/07	NA	NA	262.5	99.79	253.85	100.51	234.75	98.96	276.93	94.48	279.7	93.55	282.5	93.55
3/30/07	NA	NA	225	93.75	385.95	105.07	337.41	104.8	346.16	103.30	349.62	103.30	353.12	103.30
3/30/07	NA	NA	364.17	107.6	245.1	93.12	203.72	88.224	338.2	104.8	341.59	104.8	345	104.8
3/30/07	NA	NA	315.83	105.82	319.9	98.832	264.99	102.3	206.9	89.39	208.97	89.14	211.06	88.54
4/3/07	203.33	102.32	209.17	97.68	187.01	91.815	346.16	104.8	346	102.24	349.46	102.24	352.95	102.24
4/3/07	210.83	97.11	163.33	87.6	282.5	102.53	338.2	104.8	314	99.91	317.14	99.44	320.31	100.38
4/3/07	151.67	86.76	249.17	96.96	237.94	97.68	206.9	88.224	337	101.05	340.37	100.57	365	101.05

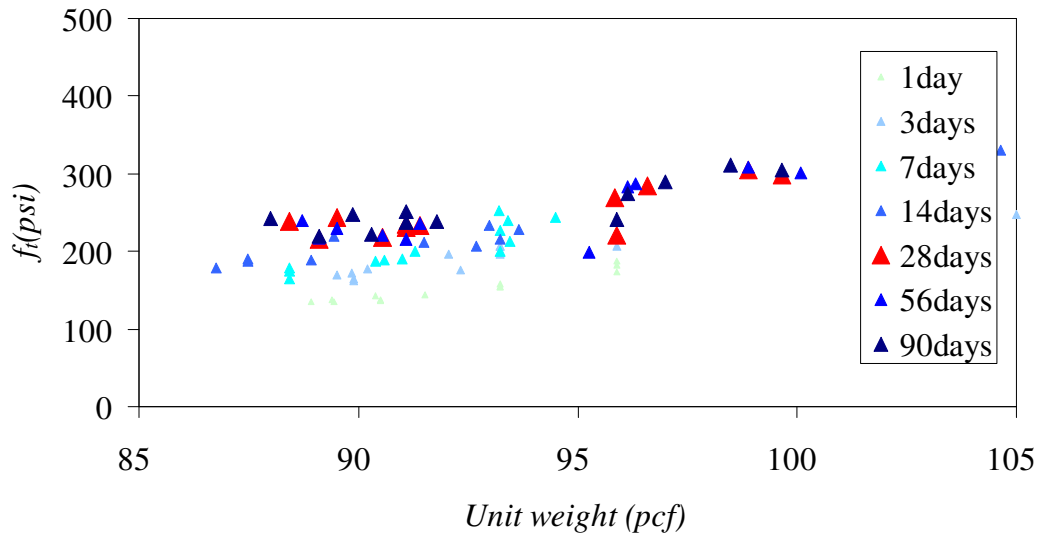


Figure 2.14 Graph relationship between modulus of rupture and unit weight for concrete mixed at Site 1

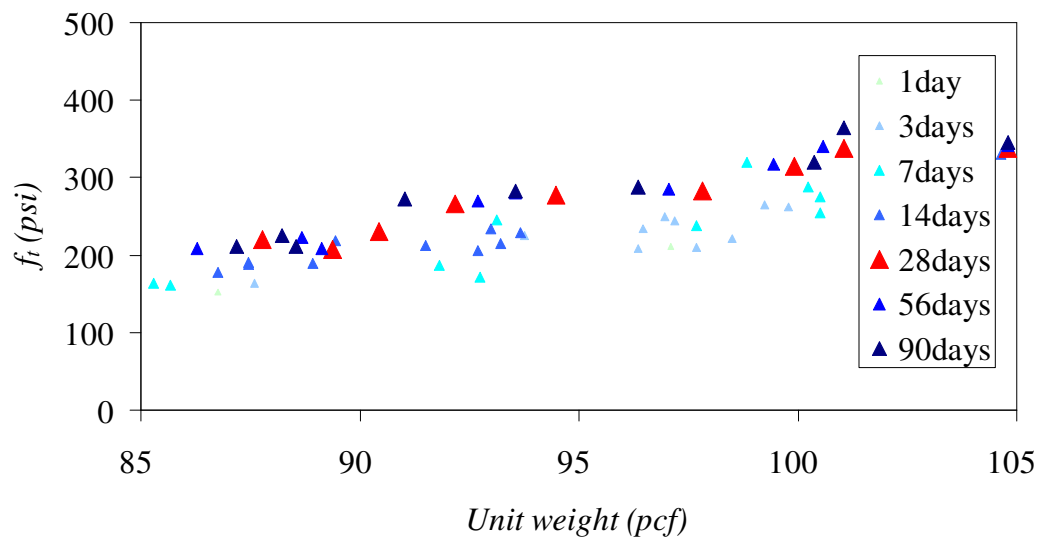


Figure 2.15 Graph relationship between modulus of rupture and unit weight for concrete mixed at Site 2

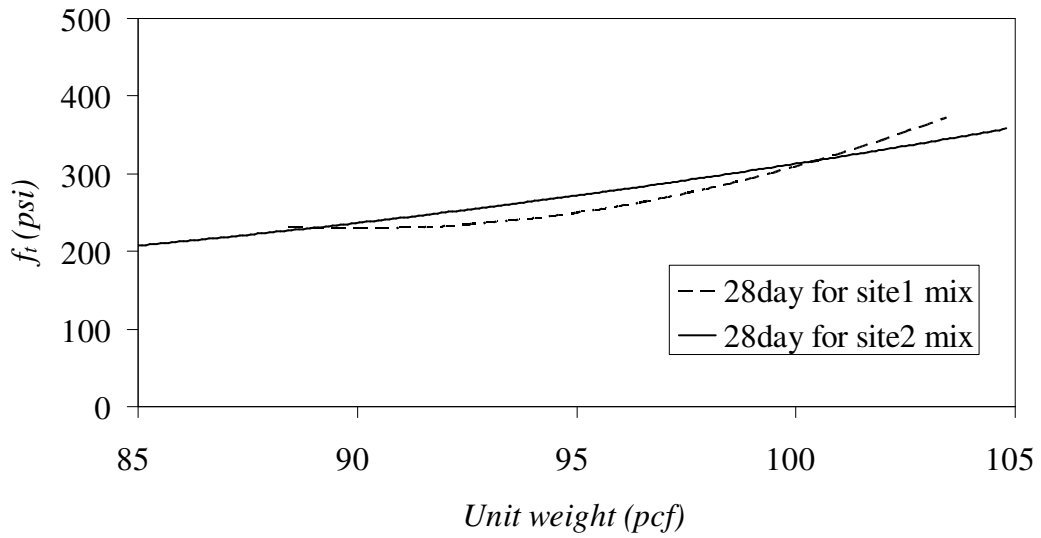


Figure 2.16 Graph relationship between modulus of rupture and unit weight on the 28<sup>th</sup> day by comparing concrete mixed at Site 1 and Site 2

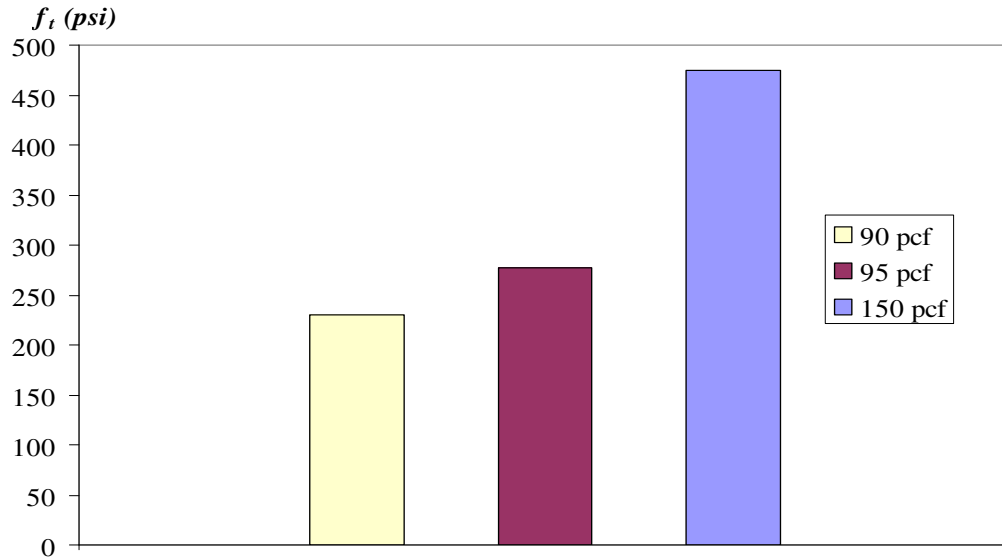


Figure 2.17 Comparison of modulus of rupture for concrete unit weight of 90, 95, and 150 pcf

From the result, modulus of rupture of ductile lightweight concrete from site 1 and Site 2 are very close to each other.

Modulus of rupture of concrete on the 28<sup>th</sup> day and unit weight of concrete for Site 1 are related by the following equation

$$f_t = 0.7797w^2 - 140.12w + 6524.9 \quad (2.4)$$

Modulus of rupture of concrete on the 28<sup>th</sup> day and unit weight of concrete for Site 2 are related by the following equation

$$f_t = 0.1179w^2 - 14.76w + 610.41 \quad (2.5)$$

$f_t$  = modulus of rupture of concrete at 28 day (psi)

$w$  = unit weight of concrete (pcf)

### 2.3.3 Relationship between compressive strength and modulus of rupture

Theoretically, compressive strength has a relationship with flexural strength. From the experiment, compressive and flexural strength of concrete are collected to determine their relationship by the following equation. Usually, value of  $\alpha$  is around 7.5 for regular weight concrete.

$$f_t = \alpha \sqrt{f'_c} \quad (2.6)$$



Table 2.6  $\alpha$  for concrete mixed at Site 1 (Grand Prairie)

Site1														
Mix date	1day		3days		7days		14days		28days		56days		90days	
	$\alpha$	weight	$\alpha$	weight	$\alpha$	weight	$\alpha$	weight	$\alpha$	weight	$\alpha$	weight	$\alpha$	weight
	psi	pcf	psi	pcf	psi	pcf	psi	pcf	psi	pcf	psi	pcf	psi	pcf
2/27/07	6.5181	93.22	6.9059	93.22	6.2177	93.22	5.7	93.22	6.3438	95.90	6.3438	93.95	7.45	95.90
2/27/07	6.3466	93.22	7.2703	93.22	6.6132	93.22	6.3116	93.22	6.5	92.42	6.5	93.22	6.5	91.91
2/27/07	6.3466	93.22	7.288	93.22	7.0459	93.22	7.0062	93.22	6.64	98.90	6.64	93.85	6.64	97.83
2/27/07	8.771	95.88	8.9243	104	7.3288	93.2	5.9089	104.63	8.2204	103.44	8.2204	104.63	8.2204	103.44
3/6/07	8.65	95.88	8.6902	105	6.68	94.5	6.9835	110	7.3156	92.46	7.3156	110	7.3156	91.4
3/6/07	8.1939	95.88	8.7194	95.88	6.4841	93.4	5.8685	104.3	7.7966	99.65	7.7966	104.3	7	99.65
3/6/07	7.0208	89.4	7.0221	92.33	6.6296	91	5.1094	92.99	5.93	90.48	4.779	92.99	5.8	89.50
3/20/07	6.9357	88.92	6.889	89.84	6.5741	90.6	5.8212	91.5	5.1349	89.5	5.1349	91.5	6.01	90
3/20/07	7.2335	89.448	7.8541	92.05	6.5187	90.4	6.05	88.93	5.1603	89.1	5.1603	88.93	6.55	89.1
3/20/07	8.6465	91.51	7.282	89.5	7.8296	91.3	7.8377	89.44	7.8149	88.43	8.24	89.44	7.8149	88.92
3/27/07	7.7056	90.38	7.5676	90.2	8.6374	88.43	8.2367	86.75	5.68	88.43	4.8353	86.75	4.8353	87.83
3/27/07	7.4368	90.5	6.9607	89.9	8.2646	88.43	8.1227	87.47	7.7103	89.44	7.7103	87.47	7.7103	89.87
3/27/07	350.94	87.96	6.9607	88.22	8.2646	87.01	8.1227	86.63	7.7103	87.01	7.7103	86.63	7.04	87.01

Table 2.7  $\alpha$  for concrete mixed at Site 2 (New Orleans)

Site2														
Mix date	1day		3days		7days		14days		28days		56days		90days	
	$\alpha$	weight	$\alpha$	weight	$\alpha$	weight	$\alpha$	weight	$\alpha$	weight	$\alpha$	weight	$\alpha$	weight
	psi	pcf	psi	pcf	psi	pcf	psi	pcf	psi	pcf	psi	pcf	psi	pcf
3/29/07	NA	NA	8.0747	96.46	5.7319	85.29	5.138	84.936	6.1522	89.31	5.68	89.31	6.1522	88.66
3/29/07	NA	NA	7.1839	96.36	6.0115	92.74	6.7633	86.736	6.5545	89.94	5.93	90.21	6.5545	90.69
3/29/07	NA	NA	7.6149	98.49	5.6481	85.68	5.2167	88.584	6.4125	84.07	6.4125	84.07	6.4125	84.07
3/30/07	NA	NA	7.8196	97.2	7.0147	100.25	6.6777	99.744	5.961	97.75	5.35	99.744	5.961	98.7
3/30/07	NA	NA	8.2252	99.24	7.2864	100.51	6.4517	97.56	6.3169	93.28	6.3169	93.28	6.3169	93.28
3/30/07	NA	NA	8.1476	99.79	7.8792	100.51	6.0613	98.96	6.1923	95.37	5.64	95.37	6.1923	96.19
3/30/07	NA	NA	7.8793	93.75	6.9431	105.07	6.7482	104.8	6.9232	104.80	6.9232	104.80	6.9232	104.27
3/30/07	NA	NA	7.7924	107.6	6.9324	93.12	6.4421	88.224	6.7641	103.93	6.7641	103.93	6.7641	103.93
3/30/07	NA	NA	7.105	105.82	7.8281	98.832	6.2459	102.3	5.9727	88.224	6.75	87.73	5.4	88.224
4/3/07	7.3515	102.32	7.3268	97.68	5.0897	91.815	6.9232	104.8	6.0614	101.13	6.0614	101.13	6.75	101.13
4/3/07	7.6227	97.11	5.9841	87.6	6.3974	102.53	6.7641	104.8	6.66	94.45	6.01	94.45	6.66	94.98
4/3/07	5.9811	86.76	8.7279	96.96	6.7299	97.68	5.9727	88.224	6.63	99.4	7	99.72	6.1252	100.55

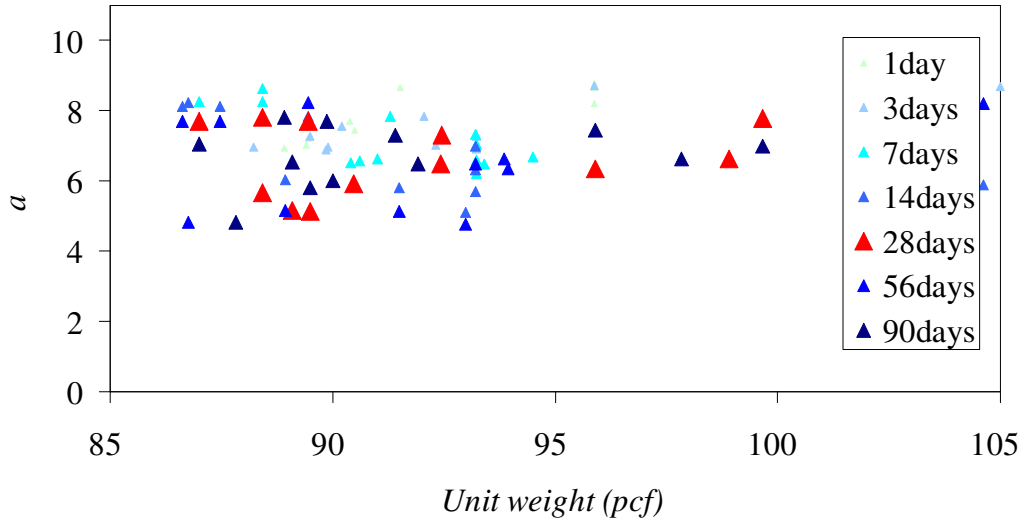


Figure 2.18 Graph relationship between  $\alpha$  and unit weight for concrete mixed at Site 1

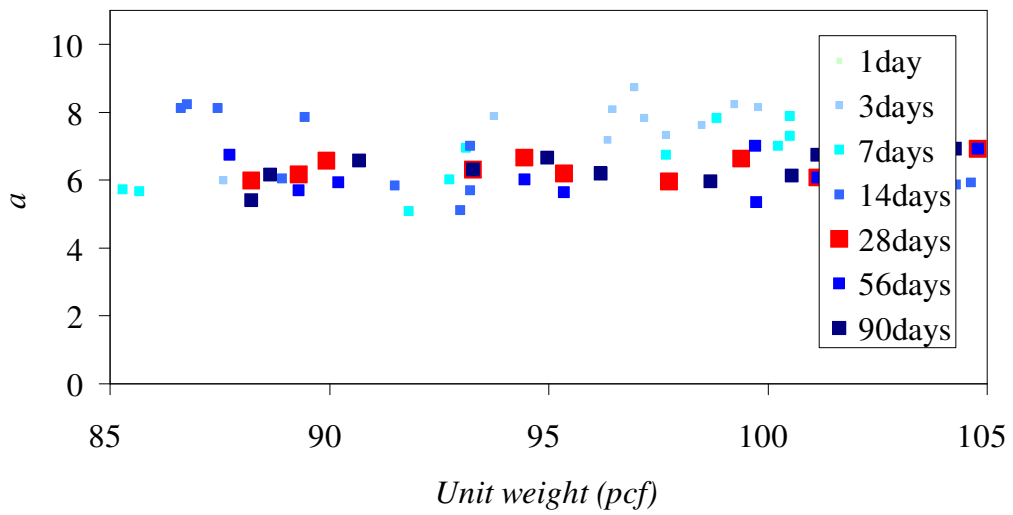


Figure 2.19 Graph relationship between  $\alpha$  and unit weight for concrete mixed at Site 2

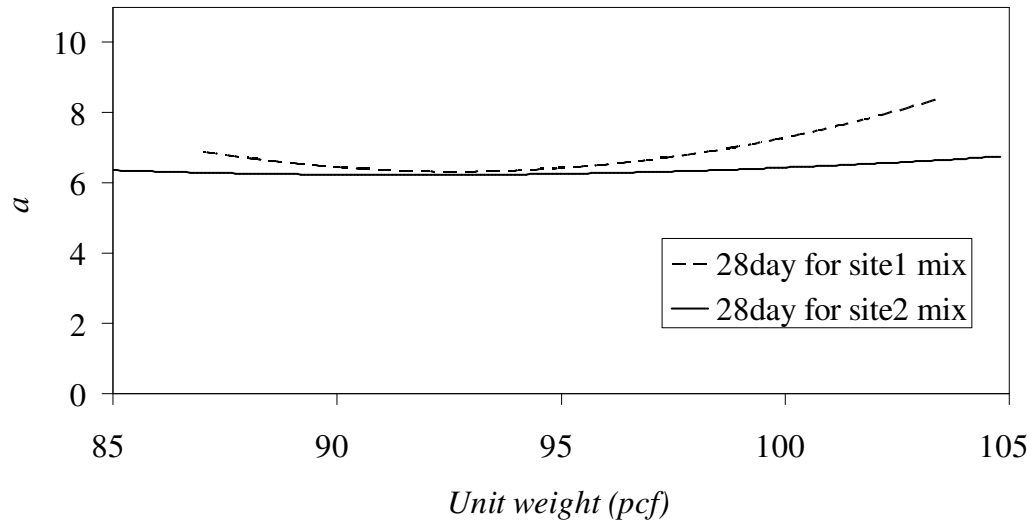


Figure 2.20 Graph relationship between  $\alpha$  and unit weight on the 28<sup>th</sup> day by comparing concrete mixed at Site 1 and Site 2

From the results from tests,  $\alpha$  has value from 5 to 8 for both Site 1 and Site 2.

$\alpha$  of concrete on the 28<sup>th</sup> day and unit weight of concrete for Site 1 are

related by following equation

$$\alpha = 0.0178w^2 - 3.2995w + 159.17 \quad (2.7)$$

$\alpha$  of concrete on the 28<sup>th</sup> day and unit weight of concrete for Site 2 are

related by following equation

$$\alpha = 0.0031w^2 - 0.563w + 32.056 \quad (2.8)$$

$\alpha$  = relationship between modulus of rupture and compressive strength of concrete on the 28<sup>th</sup> day (psi)

$w$  = unit weight of concrete (pcf)

#### *2.3.4 Pull-out test*

The bond between rebar and concrete is one of the most important mechanical behaviors of composite material. There are several factors relating to bond strength of concrete such as the chemical adhesion between the rebar and concrete, the frictional force between the rebar and concrete, and the interlock force resulting from the ribs of the rebar. Concrete cylinders were cast on 6 in.(152.4 mm.) x 12 in.(304.8 mm.) for 21 molds for each mixed design for 1, 3, 7, 14, 28, 56, and 90 day(s) test. Rebars No.4 were put at embedded length for 4 in. (10.16 cm.) and 12 in. (30.48 cm.) during casting concrete into cylinder molds. The pull-out test procedure used in this study basically followed the specification of ASTM C-234. The bearing plate was designed to accommodate the specimens. The pull-out test was performed in a universal material testing machine as shown in Figure 2.24. The average value to control the stroke rate is 0.8 mm/min (0.0312 in/min). During the test, the loading and the displacement values were recorded using a data acquisition system. The displacement was measured at the surface of the concrete automatically. However, the effective displacement was required for the analytical model by adjusting from displacement in steel bar. Moreover, pattern of failure for pull-out test is very important. Thus, failure pattern had to be recorded after testing. There are four patterns of failure mode such as shear pull-out failure, spitting failure, cone shape tensile failure, and splitting tensile failure. To determine only bond capacity of concrete and rebar without other effect, concrete cylinders have to collapse in pull-out failure mode. Therefore, to control failure mode for pull-out failure, steel bar was put into concrete at 4 inch embedded length.

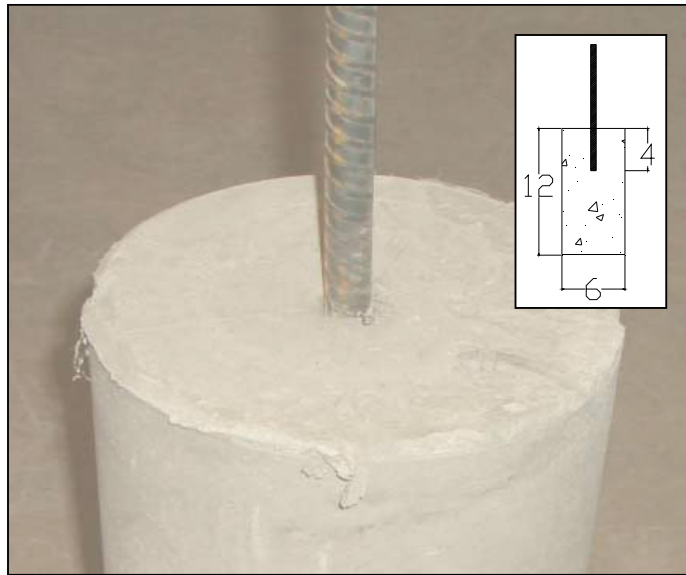


Figure 2.21 Pull out failure pattern

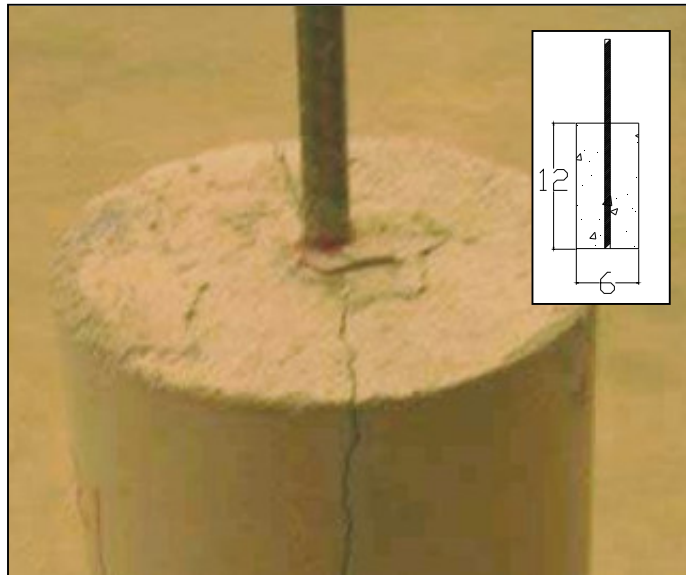


Figure 2.22 Splitting failure pattern

#### 2.3.4.1 Pull-out test set-up

Following ASTM C234, concrete cylinders with rebar were taken off from the plastic molds. Concrete cylinders were set up at the top of compression machine shown in Figure 2.21. Metal grips were used to grab the steel rod by measuring the length between concrete surface and steel grip to determine bond stress and displacement curve of concrete cylinders. The 60 kips tensile compression machine using hydraulic system is used for this test. Displacement sensor was attached to this machine to record displacement of cylinder specimens when the machine starts loading. Data of load and displacement were recorded through computer.

The loading rate on hydraulic machine should be controlled and adjusted by users. Graphs between load and displacement were plotted in the computer. Finally,  $P_y$ ,  $P_{max}$ , and initial stiffness were determined from graphs. However, displacements have to be converted to actual displacements from the following equation.

$$U_{desired} = U_{measured} - U_{offset} = U_{measured} - \frac{P * L_{offset}}{EA} \quad (2.9)$$

$P$  = Load from the graph

$L_{offset}$  = length between concrete surface and steel grip before loading starts

$E$  = modulus of elasticity of steel bar






$A$  = section area of steel bar



Figure 2.23 Pull-out test with universal material testing machine



Table 2.8 Failure mode for concrete cylinder

		<i>Embedment length</i>	<i>1day</i>		<i>3days</i>		<i>7days</i>		<i>14days</i>		<i>28days</i>		<i>56days</i>		<i>90days</i>	
			<i>Failure mode</i>		<i>Failure mode</i>		<i>Failure mode</i>		<i>Failure mode</i>		<i>Failure mode</i>		<i>Failure mode</i>		<i>Failure mode</i>	
			<i>Pull out</i>	<i>Splitting</i>	<i>Pull out</i>	<i>Splitting</i>	<i>Pull out</i>	<i>Splitting</i>	<i>Pull out</i>	<i>Splitting</i>	<i>Pull out</i>	<i>Splitting</i>	<i>Pull out</i>	<i>Splitting</i>	<i>Pull out</i>	<i>Splitting</i>
<i>Regular concrete</i>		4	x		x		x		x		x	x	x	x	x	x
<i>Regular concrete</i>		12		x		x		x		x		x		x		x
<i>Lightweight concrete</i>		4	x		x		x		x		x		x		x	
<i>Lightweight concrete</i>		12	x		x		x	x	x	x	x	x	x	x	x	x

From Table. 2.8, when the concrete becomes more mature, compressive strength of concrete also increases. For regular weight concrete, failure mode for pull-out test are pull-out failure for 4 in. (10.16 cm.) embedded length and splitting failure for 12 in. (30.48 cm.) embedded length. Ductile lightweight concrete had pull-out failure for both 4 in. (10.16 cm.) and 12 in. (30.48 cm.) embedded length while splitting failure occurred for some specimens with 12 in. (30.48 cm.) embedded length when concrete became more mature. Therefore, to determine pull out strength of the concrete, failure mode or tests are considered. Only ultimate loads from pull-out failure were collected to identify bond strength between concrete and rebar.

#### 2.3.4.2. Pull-out test result

##### *Bond strength and bond stiffness*

To determine the bond strength of concrete, failure modes of concrete cylinders is very important. Therefore, failure modes of concrete cylinders were recorded for analysis consideration. Considered failure mode to determine bond strength is pull-out failure mode. Only graph relationship between load and displacement for pull-out failure mode were used to calculate bond strength of concrete by the following equation.

$$Bond\ strength = \frac{P}{A_{surface}} = \frac{P}{\pi DL_{embedded}} \quad (2.10)$$

P = Load from the graph

D = Diameter of steel bar

L<sub>embedded</sub> = Embedded length of steel bar inserted in the concrete cylinder

Table 2.9 Bond strength for concrete mixed at Site 1 (Grand Prairie)

Site 1														
Mix date	1day		3days		7days		14days		28days		56days		90days	
	Bstr	weight	Bstr	weight	Bstr	weight	Bstr	weight	Bstr	weight	Bstr	weight	Bstr	weight
	psi	pcf	psi	pcf	psi	pcf	psi	pcf	psi	pcf	psi	pcf	psi	pcf
2/27/07	117.77	92.73	183.6	94.46	158.74	88.77	213.69	92.35	355	94.76	355	94.5	383	94.76
2/27/07	109.87	92.02	165.92	93.22	206	93.22	281	94.27	315	93.22	315	92.17	343	93.22
2/27/07	125.8	93.22	143.31	93.22	145.06	89.47	181.21	92.69	287	93.35	307	93.35	287	92.33
2/27/07	96.125	92.35	147.13	92.48	230.68	93.22	259.66	93.22	258	90.77	271	90.77	281	90.77
2/27/07	124.52	94.27	176.38	93.45	190.29	93.22	174	90.05	341	93.89	341	94.2	366	93.89
2/27/07	104.56	92.64	178.66	93.86	140.76	87.25	201.7	90.8	212.31	87.94	225	87.94	186	87.37
3/6/07	158.76	94.7	223.41	94.76	382.48	95.11	329.14	95.88	394.11	95.03	394.11	95.37	409	95.03
3/6/07	97.771	91.72	splitting	94.89	270.22	95.88	413	95.88	445.86	96.35	409	96.35	445.86	96.78
3/6/07	154	94.46	splitting	95.19	311	95.88	354	95.13	429.94	95.88	377	95.88	429.94	95.46
3/6/07	198.46	95.11	282	95.88	394.11	95.88	407	95.63	splitting	95.88	splitting	95.88	splitting	95.88
3/6/07	242.73	95.7	265	95.19	330.04	95.88	413.11	95.88	splitting	95.88	splitting	95.88	splitting	95.88
3/6/07	249.04	95.88	200	94.59	339	95.32	388.38	95.3	splitting	95.88	splitting	95.88	splitting	95.88
3/20/07	75.955	88.48	191.08	93.97	177	91	187	88.48	215.05	88.48	247.31	88.48	216	89.18
3/20/07	102.71	90.32	166.72	92.59	159.24	88.48	222.93	91.62	256.37	91.62	294.82	91.62	295	92.05
3/20/07	87.58	88.48	178.98	92.7	167	88.48	294.59	93.94	338.77	94.29	389.59	94.29	365	94.29
3/20/07	124.42	91.94	150.53	88.48	163	88.48	216	91.72	248.4	90.99	285.66	90.99	290	91.35
3/20/07	108.07	90.72	164.76	91.97	245	94.54	252.34	92.81	290.19	92.81	333.71	92.81	383.77	93.13
3/20/07	78.45	89.96	118	88.48	216.77	94.08	203.18	88.48	233.66	90.55	268.71	90.55	309.02	90.55
3/27/07	58.917	87.1	105.1	87.1	157	87.1	151.27	87.1	173.96	87.1	200.06	87.1	230.07	87.56
3/27/07	88.535	89.31	125.64	87.1	116.24	87.1	133.12	87.1	153.09	86.65	176.05	86.65	187	86.65
3/27/07	91.72	89.86	125.64	90.15	123.41	87.1	151.27	87.1	173.96	87.66	200.06	87.66	230.07	89.75
3/27/07	117.57	87.1	158.81	92.18	208.23	92.7	191.88	92.7	220.66	92.7	253.76	92.7	291.82	92.7
3/27/07	119.69	87.1	112	89	197.98	94.27	257.43	94.27	296.05	94.27	340.45	94.27	391.52	94.27
3/27/07	94.639	88.88	83	87.1	205.47	92.29	221.23	92.29	254.42	92.47	292.58	92.47	336.47	92.47

Table 2.10 Bond strength for concrete mixed at Site 2 (NewOrleans)

Site2														
Mix date	1day		3days		7days		14days		28days		56days		90days	
	Bstr	weight	Bstr	weight	Bstr	weight	Bstr	weight	Bstr	weight	Bstr	weight	Bstr	weight
	psi	pcf	psi	pcf	psi	pcf	psi	pcf	psi	pcf	psi	pcf	psi	pcf
3/29/07	NA	NA	187.74	87.33	377.2	100.49	546	101.96	584.22	101.96	590.06	101.96	595.96	101.96
3/29/07	NA	NA	242.9	95.44	394.9	101.54	536	101.74	573.52	101.74	579.26	101.74	585.05	101.74
3/29/07	NA	NA	273.9	94.8	429.3	103.45	splitting	101.74	splitting	101.74	splitting	101.74	splitting	101.74
3/29/07	NA	NA	318.47	101.33	291.93	91.2	splitting	101.74	splitting	101.74	splitting	101.74	splitting	101.74
3/29/07	NA	NA	323.3	97.45	splitting	91.2	splitting	101.74	splitting	101.74	splitting	101.74	splitting	101.74
3/29/07	NA	NA	254.78	91.3	splitting	91.2	splitting	101.74	splitting	101.74	splitting	101.74	splitting	101.74
3/30/07	NA	NA	176.75	89.86	249.52	89.86	267	88.56	285.69	88.12	316	88.12	291.43	88.51
3/30/07	NA	NA	191.08	89.87	230.89	89.42	294.59	90.532	291	89.64	318.36	89.86	321.54	89.64
3/30/07	NA	NA	191.08	89.87	363.1	94.8	332	91.532	355.24	89.81	339	89.81	362.38	90.03
3/30/07	NA	NA	254.78	90.98	297.7	91.43	283	88.964	302.81	89.28	344	89.28	308.9	89.45
3/30/07	NA	NA	260.08	91.2	304.8	91.88	294.59	90.532	315.21	92.15	360	92.15	321.54	92.53
3/30/07	NA	NA	233.55	90.08	370	96.69	348	91.3	372.36	92.53	376.08	92.77	379.84	92.26
4/3/07	NA	NA	210.19	89.64	242	88.108	296	89.64	316.72	90.16	340	90.16	323.09	90.33
4/3/07	NA	NA	183.12	87.88	224	87.08	204	87.54	218.28	87.88	322	87.88	270	87.88
4/3/07	NA	NA	205.41	91.64	244.16	88.617	357	91.64	381.99	91.64	385.81	91.46	389.67	92
4/3/07	NA	NA	185.77	87.86	307.86	92.692	214.97	87.86	230.02	87.46	275	87.46	322	87.46
4/3/07	NA	NA	269.4	93.3	splitting	92.692	splitting	87.86	splitting	87.46	splitting	87.46	splitting	87.46
4/3/07	NA	NA	244.16	88.92	splitting	92.692	splitting	87.86	splitting	87.46	splitting	87.46	splitting	87.46
4/4/07	NA	NA	252.87	94.36	297.77	93.81	361	93.81	386.27	93.81	406	93.81	394.03	94.13
4/4/07	NA	NA	238.85	91.16	278.66	90.655	334	90.655	357.38	90.655	313	90.87	364.56	90.96
4/4/07	NA	NA	388.69	103.39	631.21	105.42	398.09	105.42	425.96	105.42	430.21	105.42	434.52	105.42
4/4/07	NA	NA	242	91.67	525.27	103.39	334.39	103.39	357.8	103.39	361.38	103.39	364.99	103.39
4/4/07	NA	NA	237.05	91.67	440.23	97.97	557.32	97.97	596.34	97.97	602.3	97.97	608.32	97.97
4/4/07	NA	NA	splitting	91.67	splitting	97.97	398.09	104.56	425.96	104.56	430.21	104.56	434.52	104.56

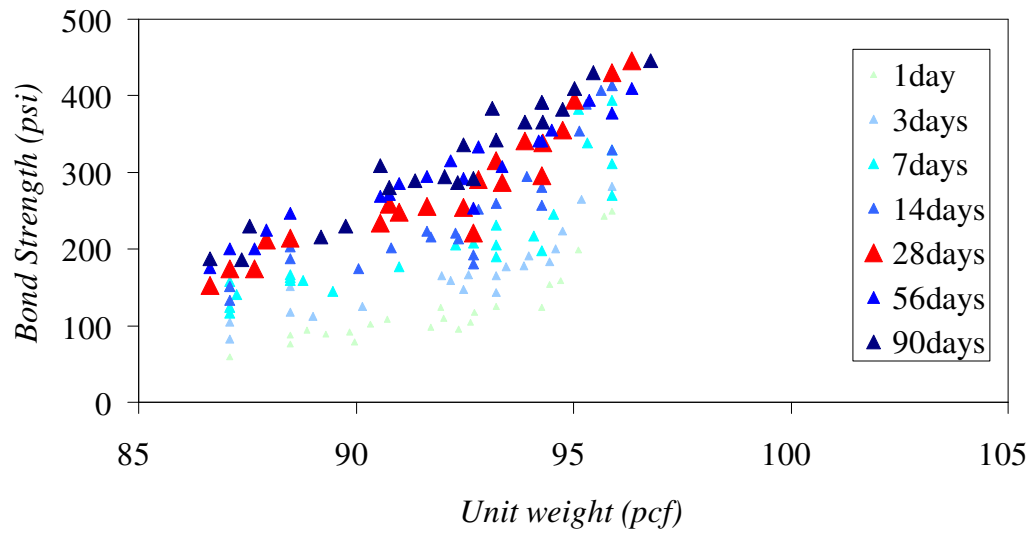


Figure 2.24 Graph relationship between bond strength and unit weight for concrete mixed at Site 1

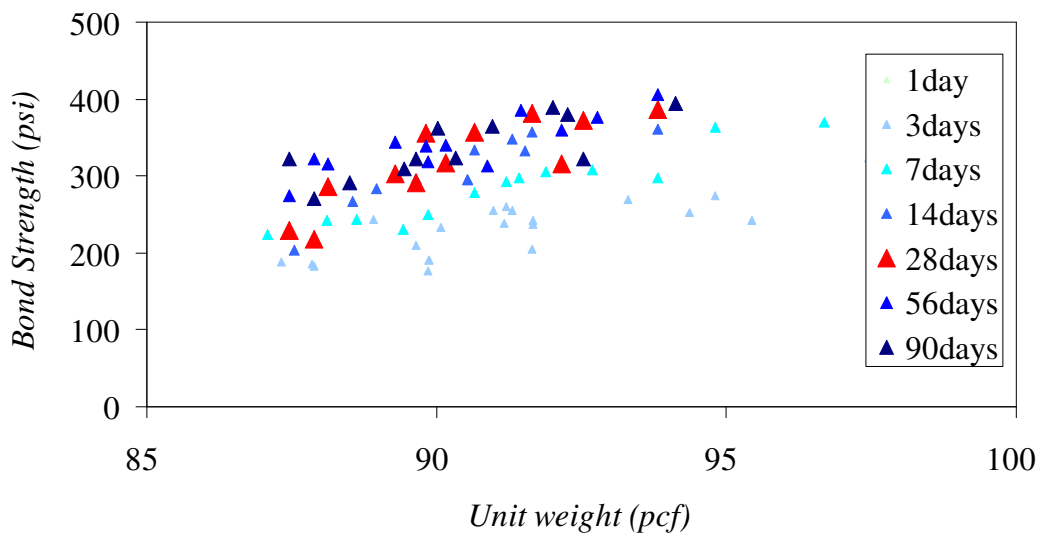


Figure 2.25 Graph relationship between bond strength and unit weight for concrete mixed at Site 2

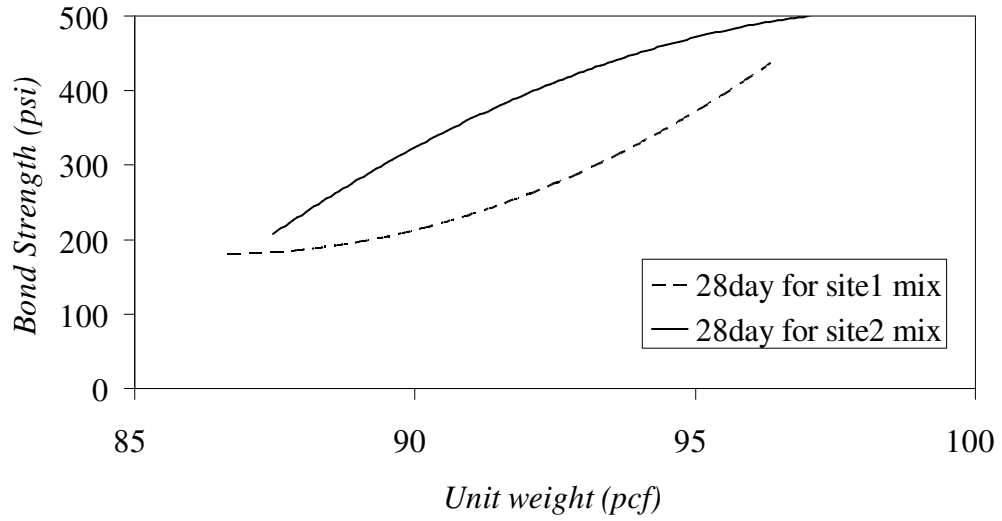


Figure 2.26 Graph relationship between bond strength and unit weight on the 28<sup>th</sup> day by comparing concrete mixed at Site 1 and Site 2

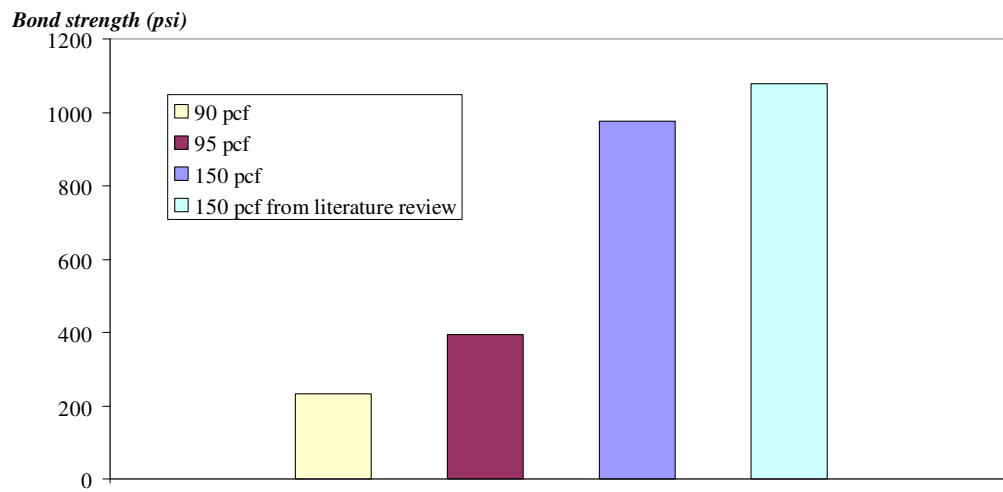


Figure 2.27 Comparison of bond strength for concrete unit weight of 90, 95, and 150 pcf

From the result, bond strength of ductile lightweight concrete from site 1 and Site 2 are different at unit weight around 88 pcf to 93 pcf. Concrete mixed at Site 2 has bond strength higher than concrete mixed at site 1.

Bond strength of concrete on the 28<sup>th</sup> day and unit weight of concrete for Site 1 are related by the following equation

$$\text{Bond Strength} = 2.6612w^2 - 460.62w + 20112 \quad (2.11)$$

Bond strength of concrete on the 28<sup>th</sup> day and unit weight of concrete for Site 2 are related by the following equation

$$\text{Bond Strength} = -3.4393w^2 + 679.34w - 32996 \quad (2.12)$$

Bond strength = bond strength of concrete on the 28<sup>th</sup> day (psi)

$w$  = unit weight of concrete (pcf)

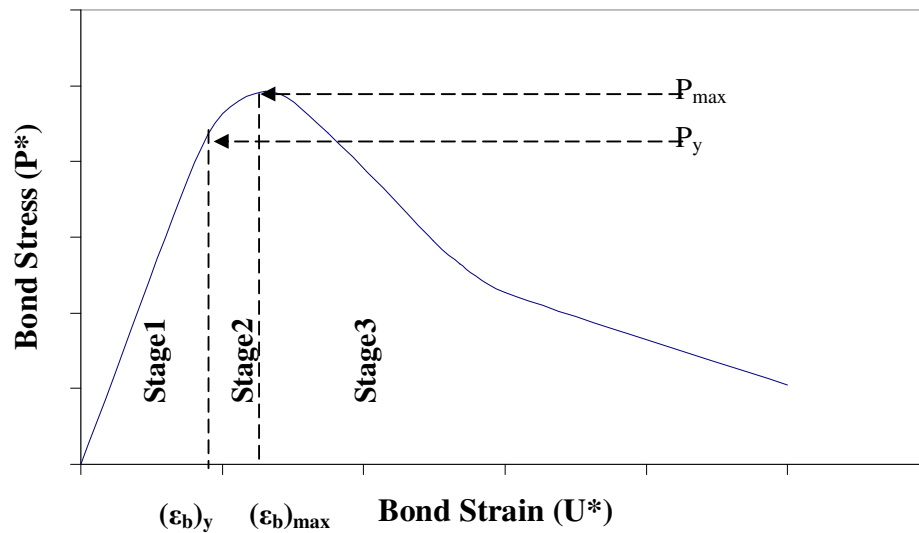


Figure 2.28 Typical load-displacement curve

A typical pull-out load-displacement curve is shown in Figure 2.28. From the curve, in the first stage, load and displacement have a linear relationship. Initial bond stiffness can be determined from the slope of the bond stress and displacement.

After first stage, the load-displacement curve becomes nonlinear and reaches the second stage at bond stress  $P_y$ . From the pull-out force vs. displacement curve, the turning point,  $P_{max}$  can be found at the extreme value of  $P^*$  where the slope of the  $P^* - U^*$  curve equal to zero.

In the third stage, the curve declines after passing the maximum load. The interface failure propagates further after the maximum load and the entire rebar slips after complete debonding.

Bond stiffness of concrete is determined from the initial slope of the load and displacement of concrete cylinders in the first stage of the graph under pull-out failure mode.



Table 2.11 Bond stiffness for concrete mixed at Site 1 (Grand Prairie)

Site 1														
Mix date	1day		3days		7days		14days		28days		56days		90days	
	BS	weight	BS	weight	BS	weight	BS	weight	BS	weight	BS	weight	BS	weight
	psi	pcf	psi	pcf	psi	pcf	psi	pcf	psi	pcf	psi	pcf	psi	pcf
2/27/07	4210	92.73	6320	94.46	4401	88.77	11450	93.22	14690	94.76	15000	94.93	14690	95.07
2/27/07	4750	92.02	6570	93.22	5974	93.22	6370	93.22	12660	93.22	12660	93.22	14680	92.86
2/27/07	4430	91.08	6320	93.22	4402	89.47	10890	93.22	14040	93.35	14040	93.35	14040	93.35
2/27/07	3327	92.35	7000	92.48	9130	93.22	8374	93.22	11462	92.00	11462	92.00	11462	92.00
2/27/07	4827	94.27	5510	93.22	7744	93.22	8770	90.05	14250	93.89	14250	93.89	14680	93.89
2/27/07	3662	92.64	6320	93.86	7048	91.10	9236	90.80	9274	88.31	9274	88.31	9274	88.31
3/6/07	7197	94.7	6111	94.76	11340	95.11	13897	95.88	16360	95.03	16360	95.03	16360	95.03
3/6/07	4159	91.72	splitting	94.76	9955	95.88	12310	93.75	16400	95.88	16090	95.88	18090	96.2
3/6/07	4130	90.84	splitting	94.76	11653	95.88	splitting	93.75	18860	95.88	17820	96.54	17820	95.48
3/6/07	6214	95.11	10771	95.88	13982	95.88	16899	95.63	splitting	95.88	splitting	96.54	splitting	95.48
3/6/07	6848	95.7	8000	95.19	13601	95.88	15470	95.57	splitting	95.88	splitting	96.54	splitting	95.48
3/6/07	8555	95.88	7780	94.59	15235	95.32	12936	95.3	splitting	95.88	splitting	96.54	splitting	95.48
3/20/07	3350	88.48	5130	93.97	6664	91.00	10268	92.25	11295	92.25	12424	92.25	13667	92.25
3/20/07	4810	90.32	4791	92.59	7301	88.48	11029	91.62	12132	90.61	13345	91.62	14680	91.62
3/20/07	4463	88.48	4857	92.70	6664	88.48	11149	93.94	12264	93.94	13490	93.94	14839	93.94
3/20/07	4043	91.94	6140	88.48	6430	90.60	12025	93.86	13228	93.86	14550	93.86	16005	94.07
3/20/07	3730	90.72	6467	91.97	9180	94.54	14974	94.73	16471	94.73	18119	94.73	19930	94.73
3/20/07	4160	89.96	7729	88.48	10455	94.08	7739	88.48	8512.9	88.48	9364.2	88.48	10301	88.48
3/27/07	4762	91.54	6214	89.10	6115	91.43	8400	89.67	9240	89.67	10164	89.67	11180	89.67
3/27/07	3780	89.31	5400	89.10	6483	87.93	9940	91.74	10934	91.74	12027	91.74	13230	91.74
3/27/07	3190	89.86	7815	90.15	5890	91.15	11840	93.36	13024	93.36	14326	93.36	15759	93.36
3/27/07	4210	92.91	4970	92.18	8960	92.70	10303	92.78	11333	92.78	12467	92.78	13713	92.78
3/27/07	5935	92.23	7616	89.00	11830	94.27	13459	94.53	14805	94.53	16285	94.53	17914	94.53
3/27/07	4043	88.88	5130	88.63	9127	92.29	13211	93.78	14532	93.78	15985	93.78	17584	93.78

Table 2.12 Bond stiffness for concrete mixed at Site 2 (New Orleans)

Site2														
Mix date	1day		3days		7days		14days		28days		56days		90days	
	BS	weight	BS	weight	BS	weight	BS	weight	BS	weight	BS	weight	BS	weight
	psi	pcf	psi	pcf	psi	pcf	psi	pcf	psi	pcf	psi	pcf	psi	pcf
3/29/07	NA	NA	4400	87.33	9760	100.49	9810	93.35	15600	93.62	15230	94.05	16950	94.11
3/29/07	NA	NA	5490	95.44	10370	101.54	12400	101.74	16120	101.74	20956	101.74	27243	101.74
3/29/07	NA	NA	7000	99.72	11230	103.45	splitting	101.74	splitting	101.74	splitting	101.74	splitting	101.74
3/29/07	NA	NA	8510	101.33	7360	91.2	splitting	101.74	splitting	101.74	splitting	101.74	splitting	101.74
3/29/07	NA	NA	6950	97.45	splitting	91.2	splitting	101.74	splitting	101.74	splitting	101.74	splitting	101.74
3/29/07	NA	NA	6440	91.3	splitting	91.2	splitting	101.74	splitting	101.74	splitting	101.74	splitting	101.74
3/30/07	NA	NA	5270	89.86	6630	89.86	8260	88.964	10738	87.81	11730	89.05	16000	96.98
3/30/07	NA	NA	5204	89.87	7050	90.04	8470	90.26	11011	90.532	12840	90.32	14370	90.532
3/30/07	NA	NA	5204	89.87	9330	95.48	8160	91.532	12780	93.27	13790	91.76	14430	92.27
3/30/07	NA	NA	5360	90.98	7080	91.43	9020	91.205	11726	91.66	13080	91.32	14310	91.54
3/30/07	NA	NA	8390	91.2	7120	91.88	8350	90.09	10855	90	14112	90	12350	90
3/30/07	NA	NA	5790	90.08	10840	98.38	8350	90.09	10855	90	14112	90	12350	90
4/3/07	NA	NA	3932	89.64	7259	88.108	7984.9	87.56	10380	88.41	11240	88.108	15360	96.39
4/3/07	NA	NA	3767	87.88	7688	89.41	8456.8	89.72	10994	89.41	14292	89.41	11550	89.21
4/3/07	NA	NA	3818	91.64	6740	88.617	7414	88.617	9638.2	88	12530	88.34	11180	88.73
4/3/07	NA	NA	4100	87.86	8050	92.692	8855	92.692	13940	92.692	14965	92.692	15000	93.05
4/3/07	NA	NA	6090	93.3	splitting	92.692	splitting	92.692	splitting	92.692	splitting	92.692	splitting	93.05
4/3/07	NA	NA	5230	88.92	splitting	92.692	splitting	92.692	splitting	92.692	splitting	92.692	splitting	93.05
4/4/07	NA	NA	7885	98.29	10580	96.96	11638	98.803	15129	98.803	19668	98.803	25569	98.803
4/4/07	NA	NA	5895	91.16	8089	90.655	8897.9	90.96	11567	90.655	13570	90.98	12840	90.655
4/4/07	NA	NA	9720	103.39	13090	105.42	14399	105.42	18719	105.42	24334	105.42	31635	105.42
4/4/07	NA	NA	5270	91.67	11820	103.39	13002	103.39	16903	103.39	21973	103.39	28565	103.39
4/4/07	NA	NA	splitting	91.67	splitting	103.39	11286	96.04	15850	95.15	17080	94.84	15540	95.5

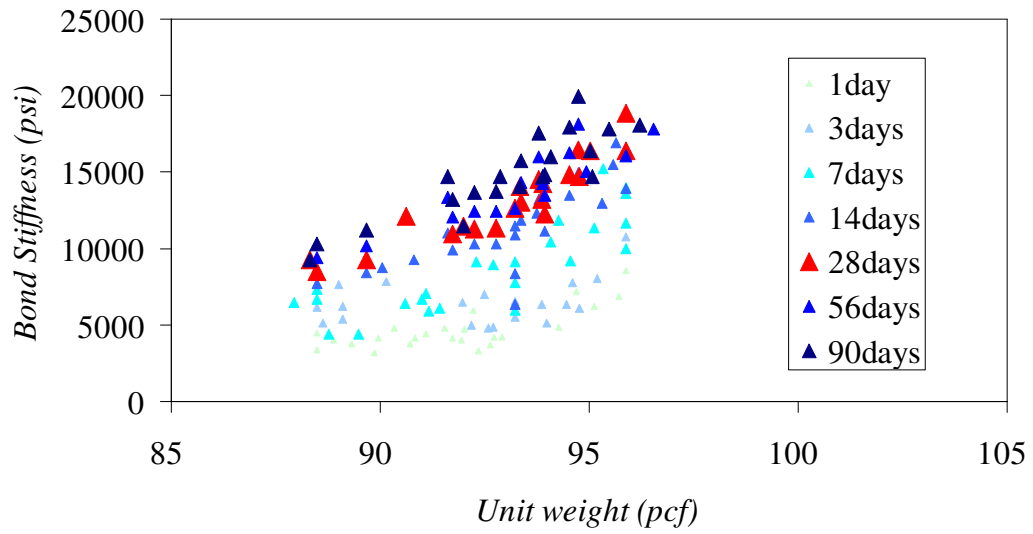


Figure 2.29 Graph relationship between bond stiffness and unit weight for concrete mixed at Site 1

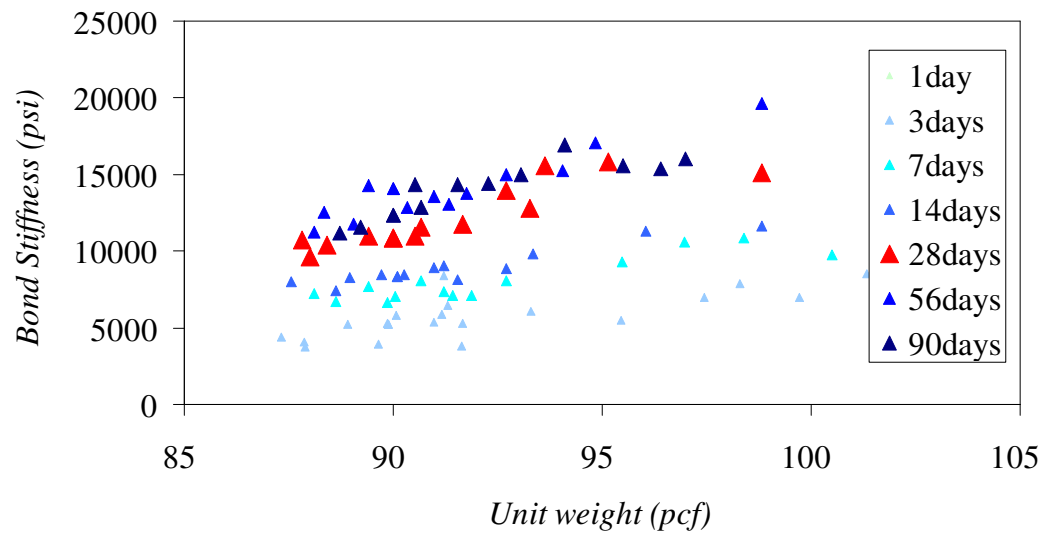


Figure 2.30 Graph relationship between bond stiffness and unit weight for concrete mixed at Site 2

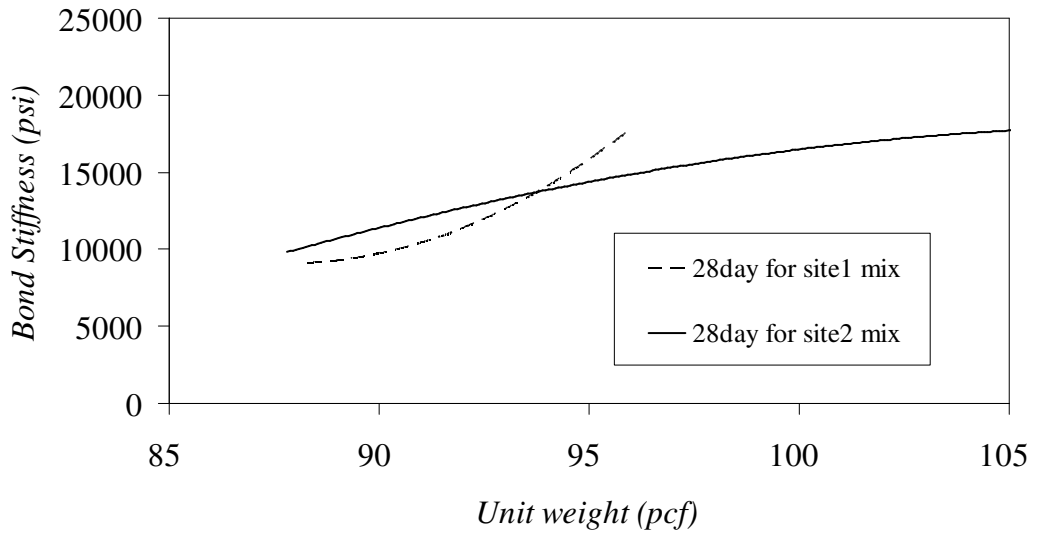


Figure 2.31 Graph relationship between bond stiffness and unit weight on the 28<sup>th</sup> day by comparing concrete mixed at Site 1 and Site 2

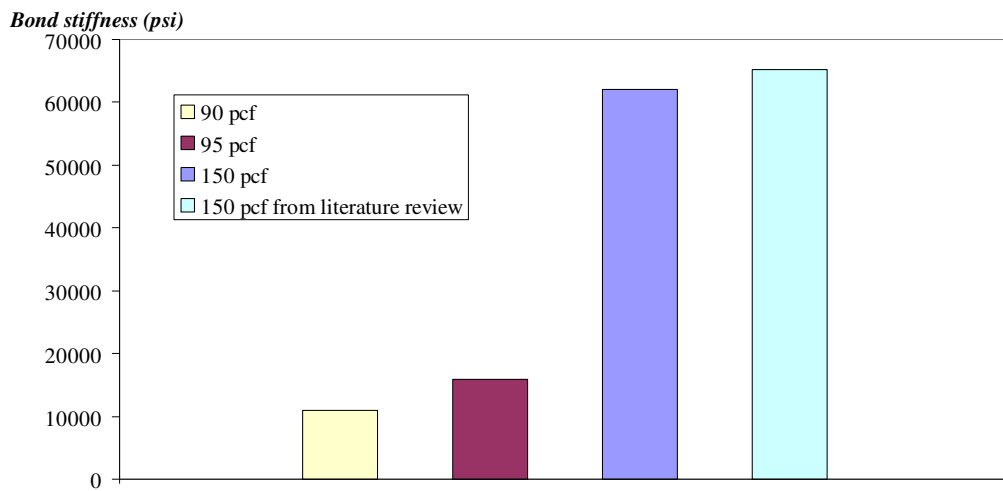


Figure 2.32 Comparison of Bond stiffness for concrete unit weight of 90, 95, and 150 pcf

From the result, bond stiffness of ductile lightweight concrete from Site 1 and Site 2 are very similar.

Bond stiffness of concrete on the 28<sup>th</sup> day and unit weight of concrete for Site 1 are related by the following equation

$$\text{Bond Stiffness} = 129.99w^2 - 22829w + 1000000 \quad (2.13)$$

Bond stiffness of concrete on the 28<sup>th</sup> day and unit weight of concrete for Site 2 are related by the following equation

$$\text{Bond Stiffness} = -102.73w^2 + 20539w - 1000000 \quad (2.14)$$

Bond stiffness = bond stiffness of concrete on the 28<sup>th</sup> day (psi)

$w$  = unit weight of concrete (pcf)

## CHAPTER 3

### FULL-SCALE TEST

#### 3.1 Introduction

To determine the structural behavior of ductile lightweight components under loading condition, 124 full-scale tests were conducted in this project including ductile lightweight concrete beams with and without reinforcement, and ductile lightweight concrete panels with window and door openings. For full-scale beam tests, reinforcement details, test setup, test instrument and test procedures are shown in Figure. 3.4. Moreover, the failure patterns of the beams with and without reinforcement were investigated and the stiffness of the beams were determined from load-deformation plots. Comparisons between beams made from regular concrete and ductile lightweight concrete were made. In addition, ductile lightweight concrete panels with window and door openings were investigated for crack patterns.

#### 3.2 Full-scale beam tests

##### *3.2.1 Full-scale beam tests*

To observe the real behavior of structural element made from ductile lightweight concrete as compared with those made from regular concrete, full-scale big beams were constructed both with and without reinforcement. Therefore, 8 in.(20.32 cm.) x 20 in.(50.8 cm.) x 96 in.(243.84 cm.) beams with and without reinforcement were casted for each concrete type.

The reinforcements are shown in Figure 3.1, which was designed based on 150 psf live load. Third point loading was chosen for this experiment by installing displacement sensors at the bottom of the beams at mid span. In addition, load cells are attached to the top of the beams and connected to the data acquisition system equipment to collect the load-deformation data.

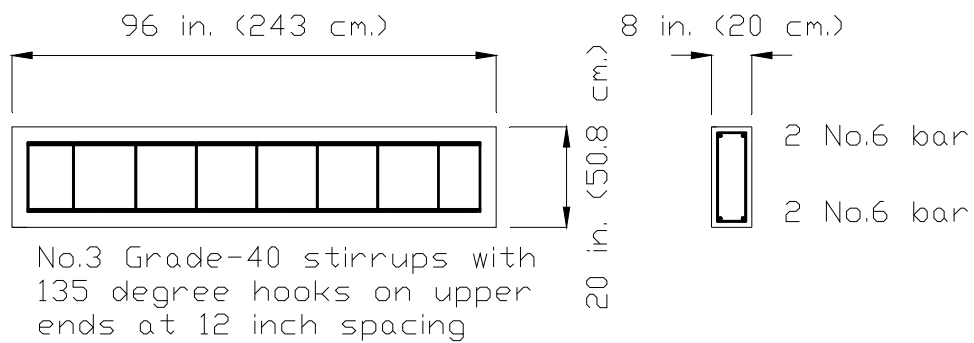


Figure 3.1 Reinforcement detail for big beam tests



Figure 3.2 Casting for beams with and without reinforcement.

### 3.2.2 *Full-scale beam test set-up*

The concrete beams were set-up by third point load method for flexural tests. Two steel rods were set at the top of the concrete beams at one third of the beam length from each steel supports. Then, the steel beam was installed above the steel rods. Load cell was used to collect the load data history during the tests at the top of the steel beam shown in Figure 3.3, while displacement sensors were applied for gathering the displacement data history at the middle of the bottom of the beams as shown in Figure 3.4. Both load cells and displacement sensors were connected to the data acquisition system to keep data simultaneously, so graphs between load and displacement were plotted by basing on the same time history. Moreover, the types of failure cracks were recorded to investigate the causes of failures.



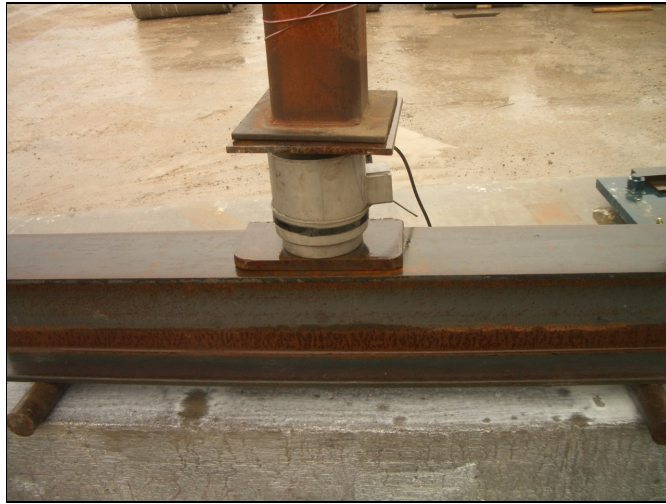


Figure 3.3 Load cell set-up at the middle of the steel beam above concrete beam



Figure 3.4 Displacement sensor attached to the middle under the beam with wooden protection after concrete beams were failed

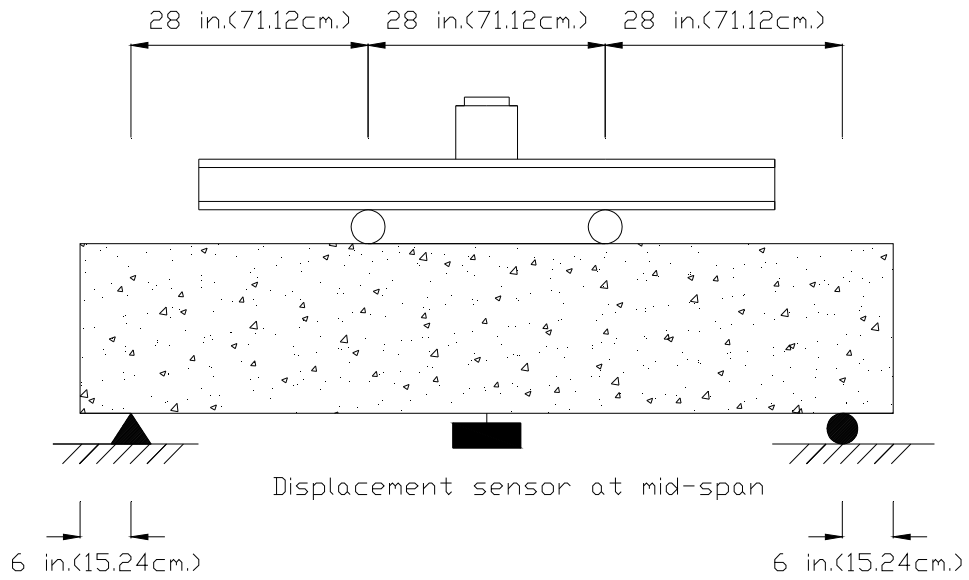


Figure 3.5 Detail for beam test set-up



Figure 3.6 Set up position for loading and displacement sensor

### 3.2.3 Result for beam tests without reinforcement

From the tests, both concrete beams made from regular weight concrete and ductile lightweight concrete have the same failure mode. The beams were collapsed by splitting cracks in the middle of each beam as shown in the Figure 3.7.



(a)



(b)



(c)



(d)

Figure 3.7 Failure mode for big beam tests without reinforcement compare concrete beams made from regular weight concrete and ductile lightweight concrete; Figure 3.7 (a) and (c) failure mode for Regular weight concrete (150 pcf(2400 kg/m<sup>3</sup>)), Figure 3.7 (b) and (d) failure mode for Ductile lightweight concrete (90 pcf(1450 kg/m<sup>3</sup>))

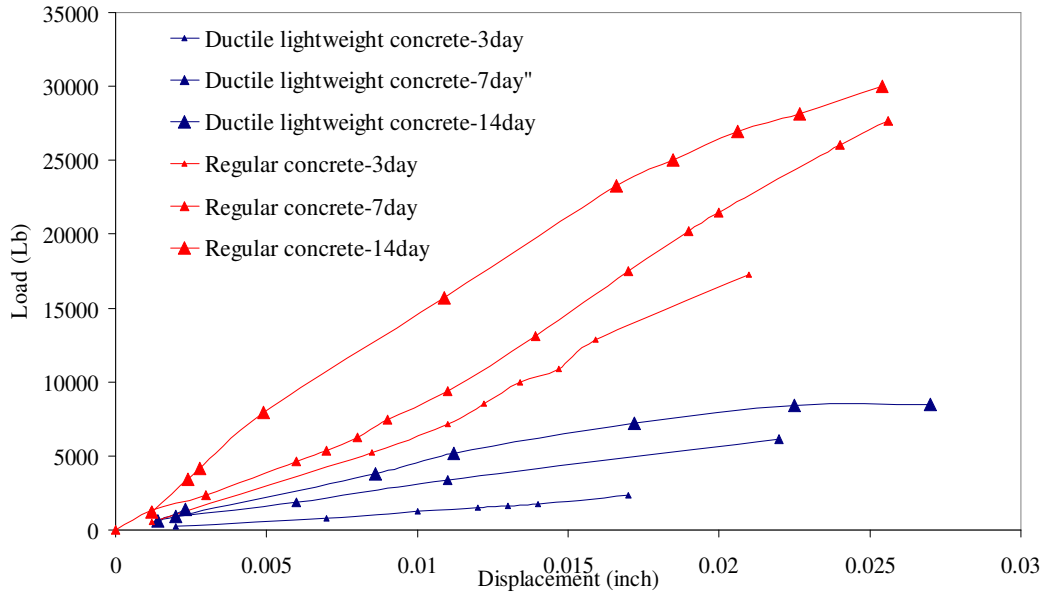


Figure 3.8 Graph relationship between load and displacement compare concrete beams without reinforcement made from regular weight concrete and ductile lightweight concrete

Table 3.1 Mechanical properties for regular and lightweight concrete beams without reinforcement

A	Stiffness		Modulus of rupture				f <sub>c</sub>				α			Maximum deflection (inch)		
	(1)	(2)	(1)	(3)	(4)	(3)	(5)	(6)	(5)	(7)	(8)	(7)	(9)	(10)	(9)	
G	150	90	—	150	90	—	150	90	—	150	90	—	150	90	—	
E	pcf	pcf	(2)	pcf	pcf	(4)	pcf	pcf	(6)	pcf	pcf	(8)	pcf	pcf	(10)	
3	339,530	118,211	2.87	454	182	2.49	5,105	812	6.29	6.35	6.37	1	0.02	0.06	0.29	
7	443,567	154,433	2.87	726	291*A	2.49	5,765	917	6.29	9.56	9.6	1	0.03	0.032*B	0.8	
14	452,762	175,698	2.58	788	220	3.58	6,287	1,077	5.84	9.94	6.69	1.49	0.01	0.012	1.08	

Remark: \*A: Modulus of rupture should decent as concrete becomes more mature.

\*B: Maximum deflection should decrease as concrete becomes more mature.

The above table summarized the mechanical properties of concrete beams without reinforcement comparing between regular weight concrete (150pcf(2400 kg/m<sup>3</sup>)) and ductile lightweight concrete (90pcf(1450 kg/m<sup>3</sup>)). The table showed the mechanical properties for each type of concrete and demonstrated the ratio between regular weight concrete and ductile lightweight concrete properties. From Figure 3.7, the type of failure cracks is due to the splitting failure cracks from the moment at the middle of the beam span. The beams for both types of concrete failed suddenly after the cracks at the middle. Moreover, secondary crack could not be found during the tests.

### 3.2.4 Result for beam tests with reinforcement

From the tests, both concrete beams made from regular weight concrete and ductile lightweight concrete have the same failure mode. The beams were collapsed by 45 degree shear cracks at the supports of the beam as shown in the Figure 3.9. Moreover, small cracks were found during loading of the beams from the center and spread to surrounding areas.



(a)

(b)



(c)

(d)

Figure 3.9 Failure mode for big beam tests with reinforcement compare concrete beams made from regular weight concrete and ductile lightweight concrete; Figure 3.9 (a) and (c) failure mode for Regular weight concrete (150pcf(2400 kg/m<sup>3</sup>)), Figure 3.9 (b) and (d) failure mode for Ductile lightweight concrete (90pcf(1450 kg/m<sup>3</sup>))

### 3.2.5 Reinforced concrete beam test designation

The tests were conducted by wall panel with window and door openings by applying the concentration load at the middle of the walls. The test designations were defined as: RB\_ H-L-T\_ W-A where designations are:

RB – Reinforced concrete beam

H-L-T – Dimension of the beam in inch (cm) (height, span length, and thickness)

W-A – Unit weight of concrete in pcf ( $\text{kg/m}^3$ ) and Age in day

For example RB\_20-96-8\_ 90-1(RB\_51-244-20\_1440-1), identifies a reinforced concrete beam test with the dimensions of: Height = 20 in. (51 cm.), Span length = 96 in. (244 cm.) and Thickness = 8 in. (20 cm.) with unit weight = 90 pcf ( $1440 \text{ kg/m}^3$ ) at age of 1 day.

Table 3.2 Summary of Test Results for 96 in. (244 cm.) length and 20 in. (50.2 cm.) reinforced concrete beams mixed on 2/8/07

Event No.	Event	Test/ Load in kip (kN)					
		RB-20-96-8_150-3 (RB-51-244-20_2400-3)	RB-20-96-8_150-3 (RB-51-244-20_2400-3)	RB-20-96-8_150-7 (RB-51-244-20_2400-7)	RB-20-96-8_150-7 (RB-51-244-20_2400-7)	RB-20-96-8_150-14 (RB-51-244-20_2400-14)	RB-20-96-8_150-14 (RB-51-244-20_2400-14)
1.	First non-measurable crack detected at the middle of the beams	15 (67)	10 (45)	24 (106)	25 (112)	36 (160)	10 (45)
2.	Initial flexural crack at the middle of the wall	28 (124)	35 (156)	35 (156)	40 (178)	42 (187)	25 (112)
3.	Flexural crack detected around the middle of the beams	34 (153)	42 (187)	46 (205)	42 (187)	52 (232)	34 (153)
4.	First shear crack initiated at the Loading end.	51 (229)	54 (242)	65 (290)	61 (271)	75 (334)	42 (187)
5.	Ultimate load	66 (296)	61 (271)	81 (363)	75 (336)	94 (423)	51 (230)



Table 3.3 Summary of Test Results for 96 in. (244 cm.) length and 20 in. (50.2 cm.) reinforced concrete beams mixed on 2/20/07

Event No.	Event	Test/ Load in kip (kN)					
		RB-20-96-8_106-3 (RB-51-244-20_1700-3)	RB-20-96-8_106-3 (RB-51-244-20_1700-3)	RB-20-96-8_106-7 (RB-51-244-20_1700-7)	RB-20-96-8_106-7 (RB-51-244-20_1700-7)	RB-20-96-8_106-14 (RB-51-244-20_1700-14)	RB-20-96-8_106-14 (RB-51-244-20_1700-14)
1.	First non-measurable crack detected at the middle of the beams	8 (36)	10 (45)	8 (36)	10 (45)	8 (36)	10 (45)
2.	Initial flexural crack at the middle of the wall	13 (58)	14 (63)	13 (58)	12 (54)	15 (67)	16 (72)
3.	Flexural crack detected around the middle of the beams	-	-	15 (67)	15 (67)	18 (81)	22 (98)
4.	First shear crack initiated at the Loading end.	15 (67)	16 (72)	16 (72)	18 (81)	24 (106)	28 (125)
5.	Ultimate load	15 (67)	16 (72)	19 (85)	18 (81)	28 (125)	33 (147)

Table 3.4 Summary of Test Results for 96 in. (244 cm.) length and 20 in. (50.2 cm.) reinforced concrete beams mixed on 2/27/07

Event No.	Event	Test/ Load in kip (kN)					
		RB-20-96-8_93-3 (RB-51-244-20_1488-3)	RB-20-96-8_93-3 (RB-51-244-20_1488-3)	RB-20-96-8_93-3 (RB-51-244-20_1488-7)	RB-20-96-8_93-3 (RB-51-244-20_1488-7)	RB-20-96-8_93-3 (RB-51-244-20_1488-14)	RB-20-96-8_93-3 (RB-51-244-20_1488-14)
1.	First non-measurable crack detected at the middle of the beams	8 (36)	10 (45)	8 (36)	10 (45)	10 (45)	10 (45)
2.	Initial flexural crack at the middle of the wall	13 (58)	12 (54)	13 (58)	12 (54)	15 (68)	10 (45)
3.	Flexural crack detected around the middle of the beams	-	-	-	13 (58)	18 (81)	13 (58)
4.	First shear crack initiated at the Loading end.	14 (63)	12 (54)	15 (67)	15 (67)	22 (98)	14 (63)
5.	Ultimate load	14 (63)	12 (54)	15 (67)	15 (67)	22 (98)	15 (67)

Table 3.5 Summary of Test Results for 96 in. (244 cm.) length and 20 in. (50.2 cm.) reinforced concrete beams mixed on 3/6/07

Event No.	Event	Test/ Load in kip (kN)			
		RB-20-96-8_96-3 (RB-51-244-20_1540-3)	RB-20-96-8_96-3 (RB-51-244-20_1540-3)	RB-20-96-8_96-14 (RB-51-244-20_1540-14)	RB-20-96-8_96-14 (RB-51-244-20_1540-14)
1.	First non-measurable crack detected at the middle of the beams	10 (36)	10 (45)	13 (36)	13 (45)
2.	Initial flexural crack at the middle of the wall	14 (58)	14 (63)	18 (63)	15 (67)
3.	Flexural crack detected around the middle of the beams	15 (67)	15 (67)	22 (98)	16 (72)
4.	First shear crack initiated at the Loading end.	18 (63)	18 (63)	28 (125)	22 (98)
5.	Ultimate load	18 (63)	24 (54)	35 (67)	23 (67)

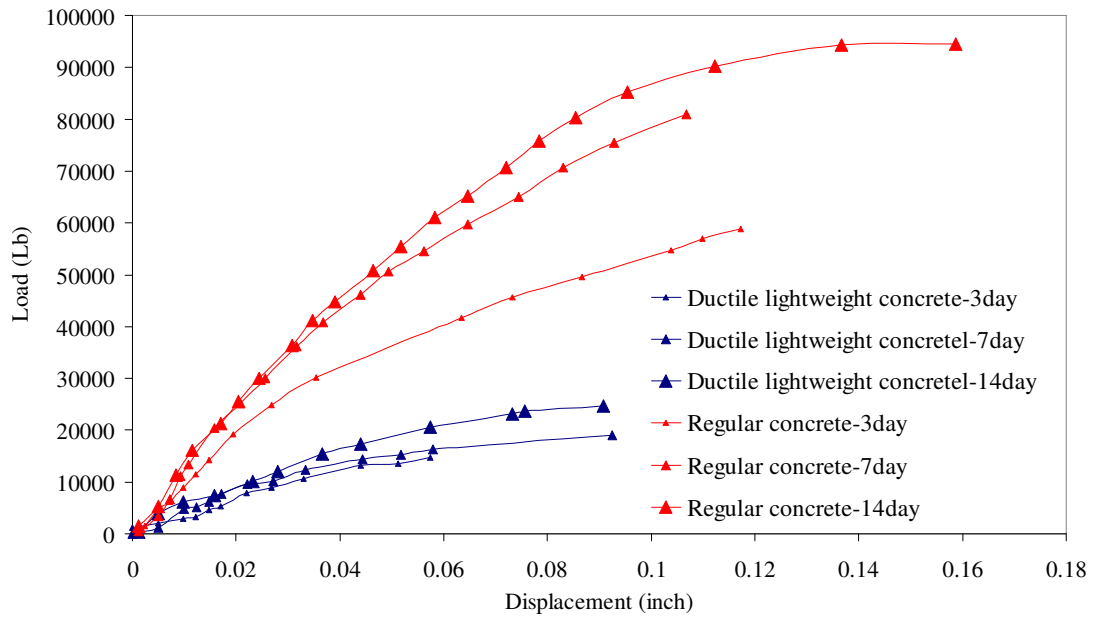


Figure 3.10 Graph relationship between load and displacement compare concrete beams with reinforcement made from regular weight concrete and ductile lightweight concrete for unit weight 93.3 pcf

Table 3.6 Mechanical properties for regular and lightweight concrete for 93.3 pcf unit weight beams with reinforcement

A	Stiffness (lb/in)			Maximum deflection (inch)		
	(1)	(2)	(1)	(3)	(4)	(3)
G	150	93.3	—	150	93.3	—
E	pcf	pcf	(2)	pcf	pcf	(4)
3	883,019	455,554	1.93834101	0.0781	0.0916	0.85262009
7	1,000,000	520,327	1.92186836	0.0162	0.0855	0.18947368
14	1,000,000	532,454	1.87809651	0.1587	0.0842	1.8847981

The table 3.2 shows the mechanical properties for stiffness and deflection from regular weight concrete beams and ductile lightweight concrete beams with reinforcement. Ratios between properties between those two types of concrete were determined to show the difference of structural properties. Moreover, the failure cracks from reinforced concrete beams are different from the failure cracks from non-reinforced concrete beams. Reinforced beams were failed by the 45 degree shear cracks at the supports, while non-reinforced concrete beams were broken by the splitting tensile cracks at the middle of the beams. In addition, secondary cracks could be observed during the tests.

### 3.3 Full-scale panel tests

Four concrete panels with openings were fabricated to determine the behavior of pre-cast concrete structural elements under concentrate load at mid panel. In this experiment, there are two patterns of wall opening such as door opening and window opening. Detail drawings of concrete panels are shown in Figures 3.12 and 3.13. The tests are set up by placing the load at the middle of the panels at the top by using a hydraulic machine. Numerical values of actual load on the top of the panels were sent to a monitor through the data acquisition system equipment. Moreover, displacement sensor was installed at the middle span of opening. The installations of the load cell and displacement sensor are shown in Figure 3.11. Hence, both loading numerical data and displacement numerical data were collected simultaneously in the computer for records. During tests, loads were applied to concrete panels at every 2 kip increment. Concrete panels were also observed carefully at every increment.

#### *3.3.1 Full-scale panel tests set-up*

The wall panels were set up by installing the load cell at the top of the panels in the middle of the walls. Displacement sensors were installed at the bottom of the middle of the wall opening as shown in Figure 3.11. Both the load and displacement data were collected through the data acquisition system simultaneously.



(a)



(b)

Figure 3.11 Installation of load cell at the top of the concrete panel and displacement sensor at the opening; (a) load cell installation, (b) displacement sensor set up

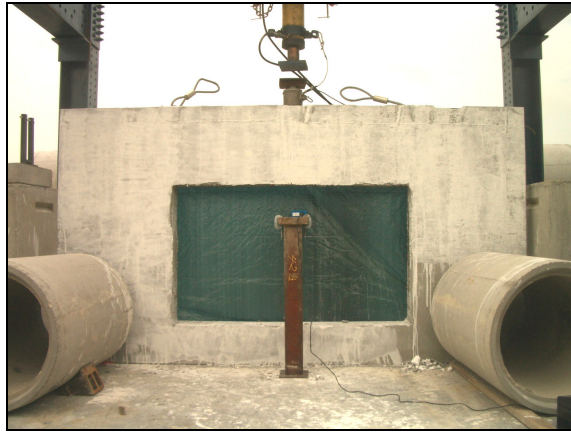


Figure 3.12 Set up equipment for wall with window opening test



Figure 3.13 Set up equipment for wall with door opening test



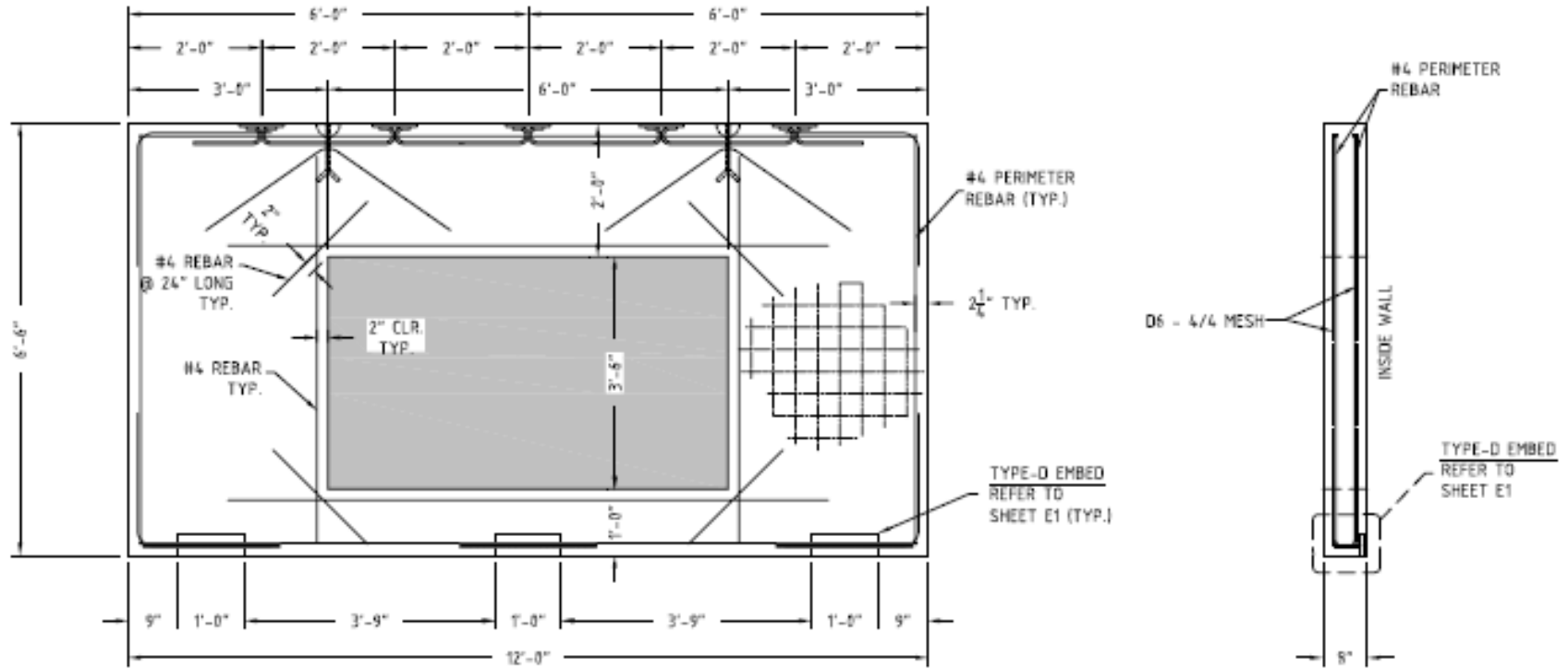


Figure 3.14 Detail drawing for concrete panel with window opening

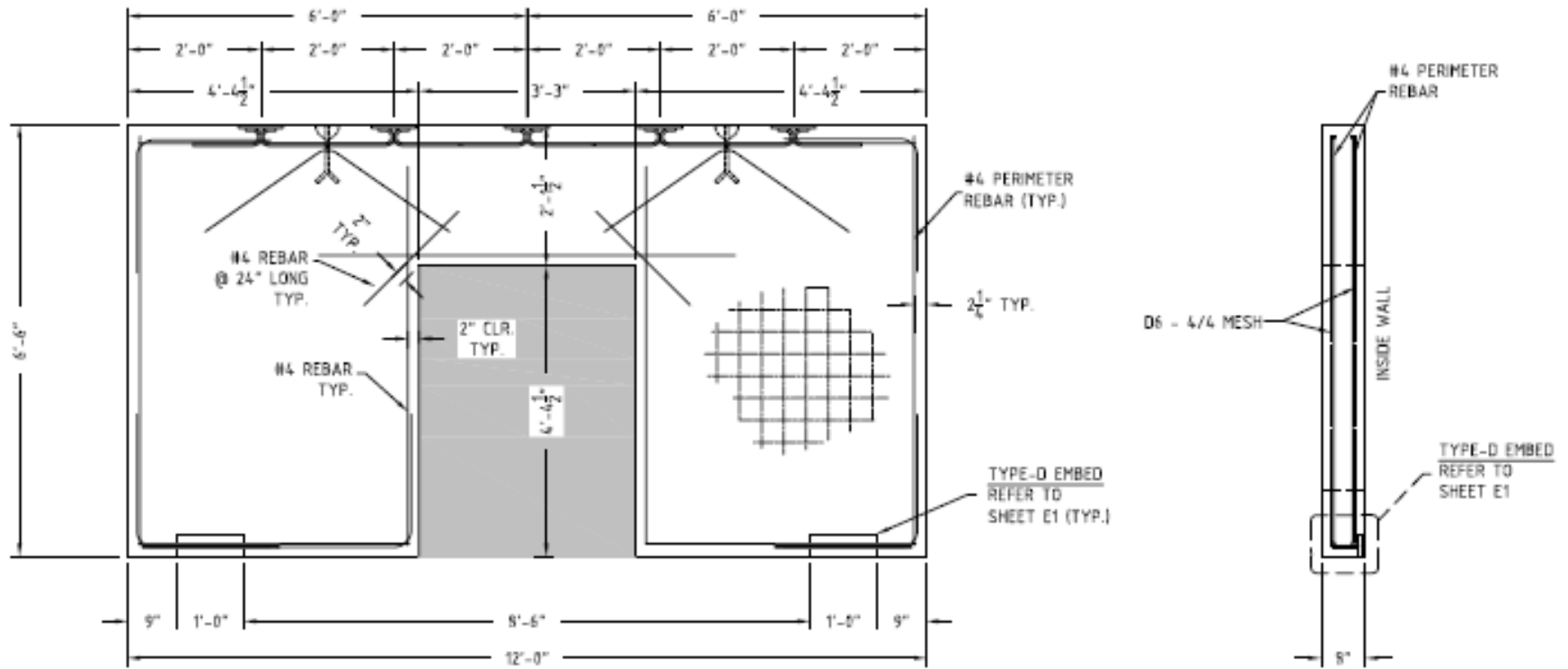


Figure 3.15 Detail drawing for concrete panel with door opening

### 3.3.2 Wall panel test designation

The tests were conducted by wall panels with window and door openings by applying the concentration load at the middle of the walls. The test designations were defined as: PW or PD\_ H-L-T\_OH-OL where designations are:

PW – Wall panel with window opening

PD – Wall panel with door opening

H-L-T – Dimension of the wall in inch (cm) (height, span length, and thickness)

OH-OH – Dimension of the wall opening in inch (cm) (height, and span length)

For example PW\_78-144-8\_42-72(PW\_199-366-20\_107-183), identifies a wall panel test with window opening with the dimensions of: Height = 78 in. (199 cm.), Span length = 144 in. (366 cm.) and Thickness = 8 in. (20 cm.) with opening height = 42 in. (107 cm.) and opening span length = 72 in. (183 cm.)

### 3.3.3 Result for concrete panel tests

Table 3.7 Summary of Test Results for 78 in. (199 cm.) length and 144 in. (366 cm.) wall panel

Event No.	Event	Test/ Load in kip (kN)			
		PW-78-144-8_42-72 (PW-199-366-20_107-	PW-78-144-8_42-72 (PW-199-366-20_107-	PD-78-144-8_39-52.5 (PW-199-366-20_99-	PD-78-144-8_39-52.5 (PW-199-366-20_99-
1.	First non-measurable crack detected on the corner and at the middle of opening	20 (89)	24 (107)	28 (124)	20 (89)
2.	Crack for negative moment at the top of the wall	28 (124)	35 (156)	32 (143)	34 (151)
3.	Initial flexural crack at the middle of the wall	30 (134)	34 (151)	44 (195)	46 (204)
4.	Flexural crack extend around the wall span	44 (195)	60 (267)	66 (294)	62 (276)
5.	Wall start to lost stiffness	50 (223)	62 (276)	70 (312)	68 (302)
6.	First serviceability shear crack detected	98 (436)	100 (448)	110 (493)	122 (543)
7	Ultimate load* /failure	100 (448)	116 (515)	123 (548)	140 (622)



Figure 3.16 Wall panel with window opening after test

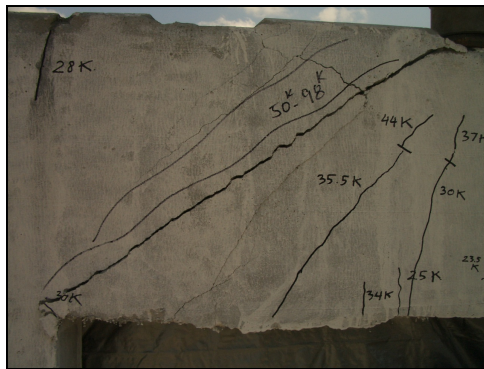
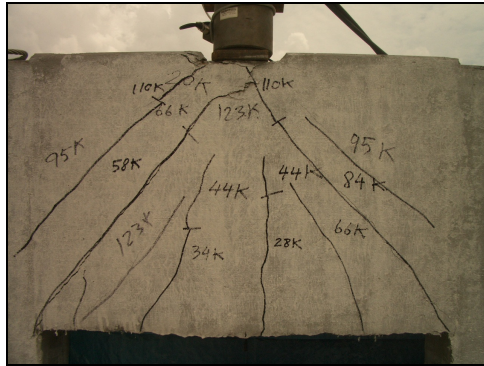
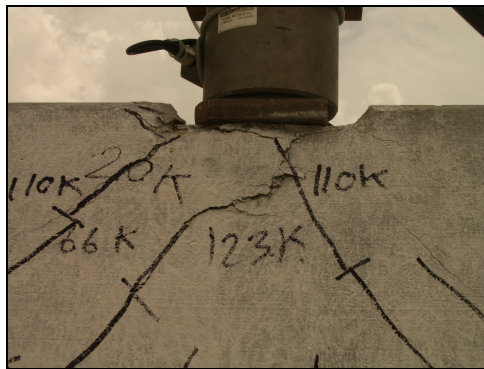


Figure 3.17 Big crack 45 degree at the corner of the window opening occur at failure load

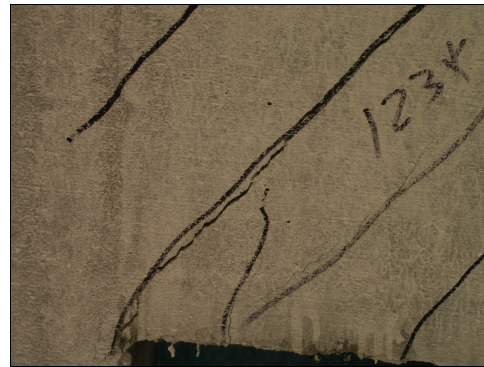
As the result from the experiments, concrete panel with window opening had non-measurable crack at 20 kips (89 kN) and 24 kips (107 kN). Cracks for negative moment at the top of the wall was detected at 28 kips (124 kN) and 35 kips (156 kN). Initial flexural crack at the middle of the wall were observed at 30 kips (134 kN) and 34 kips (151 kN). Flexural crack extend around the wall span when applied a load of 44 kips (195 kN) and 60 kips (267 kN). Finally, ultimate load for the test is 100 kips (448 kN) and 116 kips (515 kN). The detailed events of the test are shown in Appendix. C.



(a)



(b)



(c)

Figure 3.18 Wall panel with door opening after test.

As the result from experiments, concrete panels with door opening reached the ultimate load at 123 kip (548 kN) and 140 kip (622 kN). The detailed events of the test are shown in Appendix. C.

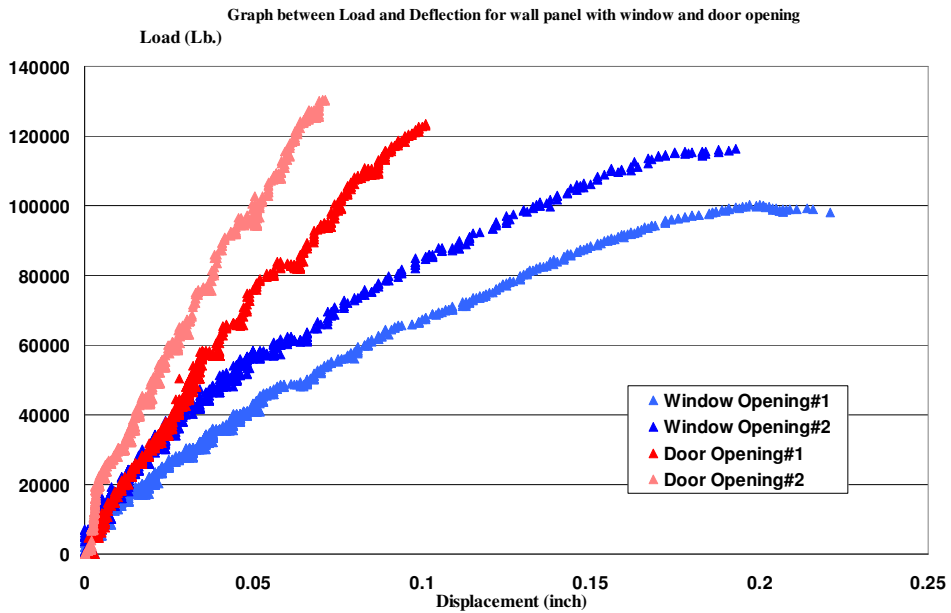


Figure 3.19 Graph load and displacement compare concrete panel with door and window openings

### 3.3.3 Compare result for concrete panel with door opening tests and window opening.

Load and displacement curves are made to determine stiffness of concrete panel with door and window openings. From the result, concrete panel with door opening has more stiffness than concrete panel with window opening. On the contrary, concrete wall with window opening is more ductile than concrete wall with door opening because concrete panel with door opening has an opening span length which is shorter than the opening span length of concrete panel with window opening.

CHAPTER 4  
FINITE ELEMENT MODELING AND ANALYSIS

4.1 Introduction

Finite element modeling and analysis is conducted to simulate the behavior of structural wall element during loading conditions. The three-dimensional finite element models of the concrete wall panels were performed by using the computer program, ABAQUS version 6.6-3. The optimum mesh with regard to the element type was selected and coupled nonlinear analysis was performed by static non-linear analysis. The models include 3-D solid and 3-D shell elements having geometric and material non-linearity. In addition, properties of concrete such as tension stiffening, shear retention, and failure ratio were applied to the models to incorporate the smeared crack algorithm. The reinforcement was modeled as rebar elements embedded in the concrete solid element. The geometric dimensions of the models are presented in Figures 3.15, and 3.16 of Chapter 3. Predicted crack patterns of concrete panel models were compared to the crack patterns from experiments. Finally, the load and displacement graphs from ABAQUS for both the concrete panels with the door and window openings were compared to the load and the displacement relationship from the full scale experimental tests.



## 4.2 FEM model

The finite element models are developed to simulate the structural behaviors of the ductile concrete panels developed in this study. The FEM model parameters are based on the material tests conducted in Chapter 2. The structural wall panels tested with and without opening are modeled by using three dimensional FEM. To simulate the behavior up to failure; material, contact, and geometric nonlinear algorithms are incorporated.

Concrete panels were simulated by ABAQUS program based on the reinforcement details from the drawings. The tested material properties of the ductile concrete were applied which included compressive strength and modulus of elasticity, and parameter  $\alpha$  which related compressive to tensile strength. Concrete elements of panels were modeled using solid element and the reinforcement were modeled by using the rebar element. Three dimensional solid and thick shell elements were used to predict the behavior.

## 4.3 Elements

### *Solid Element*

Solid elements used are volume elements which consisted of a single homogeneous material. Hexahedral elements were chosen for this model which yield accurate results for non-linear analysis involving contact, plasticity, and large deformations.

### *Thick Shell Element*

The 8-noded quadrilateral in-plane general purpose continuum shell with reduced integration (SC8R) and finite membrane strains were used. The rebar elements were simulated by using thin shell element. The perfect bond between the rebar and the concrete was assumed for the models. During meshing, the shell element was defined as sweep mesh for model behavior.

### *Brick Element*

A separate model with reduced integration 8-noded linear brick elements were used for predicting the cracking strain at various load levels. This is due to the fact that thick shell elements only show the inside and the outside surfaces of the top bottom walls in the visualization mode for depicting stress and strain values. These elements have a limitation of predicting shear force and bending moment due to having only translational degree of freedom, whereas this is not the case with shell elements which have rotational degree of freedom. The type of element used for the concrete model is shown in Figure. 4.1.

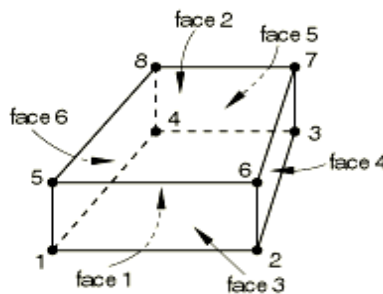


Figure 4.1 8-node linear brick, reduced integration (C3D8R)  
(Re: ABAQUS (2006) Version 6.6)

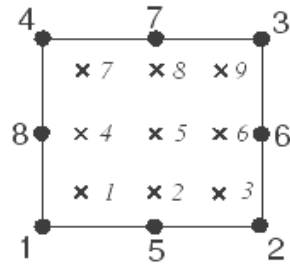


Figure 4.2 The 8-noded quadrilateral in-plane general purpose continuum shell, reduced integration, (SC8R), (Re: ABAQUS (2006) Version 6.6)

### *Embedded Element*

This technique can constrain the translational degree-of-freedom of the embedded node(s) at desired locations on the embedded element by the host element. The rebar elements are modeled as embedded region in concrete using constraints in interaction module, and making the concrete the “host”.

### *Concrete element*

Concrete element for the panel model is simulated by using the solid element. The material properties of concrete is obtained from the lab tests which are: modulus of elasticity; compressive strength; Poisson’s ratio; and the tensile strength coefficient,  $\alpha$ . For concrete, a density of 1450 kg/m<sup>3</sup> (90 pcf), Modulus of Elasticity of 13790 MPa (2000 ksi), Poisson’s ratio 0.17, and a total strain of 0.003 were used.

### *Smearred crack*

To represent the discontinuous micro crack due to the brittle behavior of concrete, smeared crack model was used. The information with regard to the cracking stress of the developed concrete was obtained from the experimental results of Chapter 2 which has a following form:

$$f_t = \alpha \sqrt{f'_c} \quad (4.1)$$

The value of  $\alpha$  for different concrete unit weight is obtained and plotted in Figure 5.3. For this analysis,  $\alpha = 7.5$  is used which is also recommended by the AISE for normal weight concrete.

### *Tension stiffening*

Because concrete loses strength through a softening mechanism and the effect of damage, tension stiffening (refer ABAQUS (2006) version 6.6) is required to model the concrete smeared cracking. Smeared crack is determined by post-failure stress-strain relationship. Tension stiffening is defined as the plastic strain at which the cracking stresses cause the tensile strength of the concrete reduce to zero.

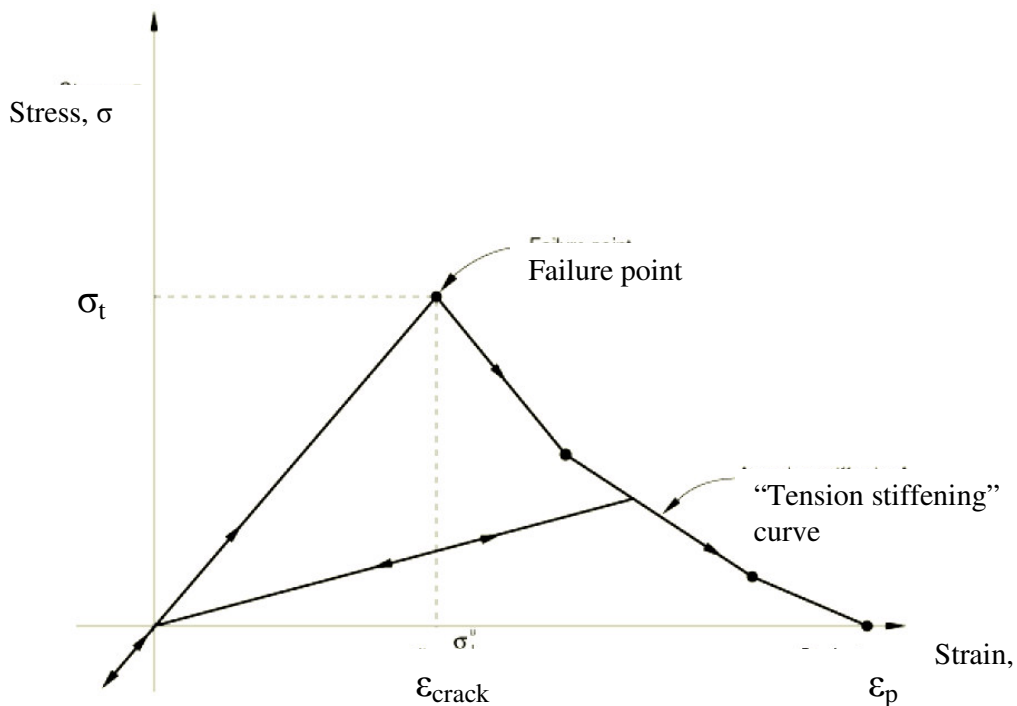


Figure 4.3 Tension stiffening model (Re: ABAQUS (2006) Version 6.6)

Several factors such as the density of reinforcement, the model of the bond between the rebar and the concrete, the relative size of the concrete aggregate compared to the rebar diameter, and the mesh size are related to the estimate of the tension stiffening effect.

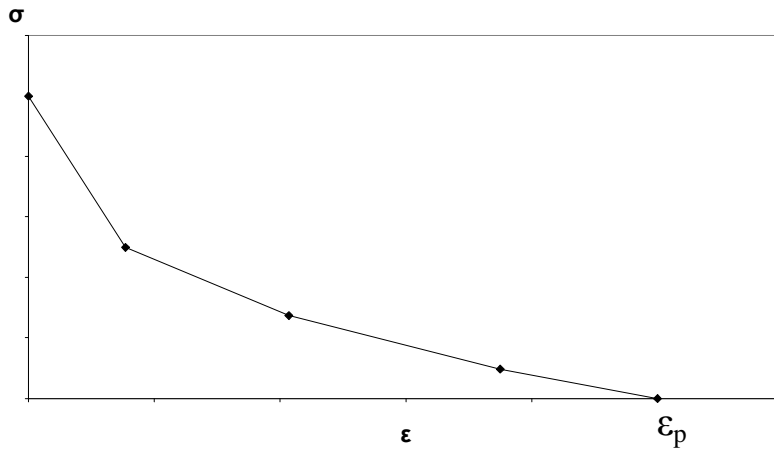


Figure 4.4 Post-failure stress-strain relation (Re: ABAQUS (2006) Version 6.6)

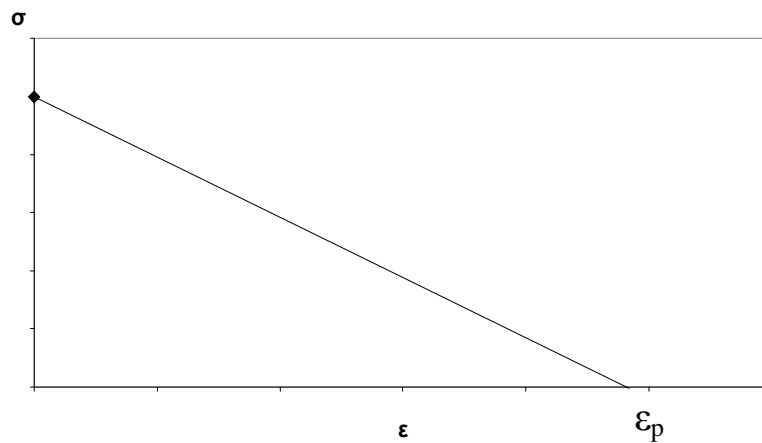


Figure 4.5 Post-failure stress-strain relation applied for model

Figures 4.4 and 4.5 present typical tensile stiffening concrete models which are used based on the type of problems. In Figure 4.4, multi linear type stress-strain behavior is modeled, while, in Figure 4.5, the idealized bi-linear are most suitable for crack model which is the case in this study. Thus, the post-failure stress-strain relationship of Figure 4.5 is used in this study. Since the tension stiffening model (refer to Figure 4.3) depends on the cracking strain and the concrete modulus of elasticity, the experimental results of this study was used to identify the parameter that

most accurately defines the behavior of the developed ductile concrete. Since the plot of tensile strength coefficient,  $\alpha$ , versus the concrete unit weight of Figure 5.3 (refer to Chapter5) shows the value of  $\alpha$  varies between  $\alpha = 6$  and  $\alpha = 8$ , the value of  $\alpha = 7.5$  was selected. Thus the following equations are used to determine tensile strength and the corresponding cracking strain along with the modulus of elasticity:

$$f_t = 7.5\sqrt{f'_c} \quad (4.2)$$

$$E = 57000\sqrt{f'_c} \quad (4.3)$$

$$\varepsilon = \frac{f_t}{E} = \frac{7.5\sqrt{f'_c}}{57000\sqrt{f'_c}} = 0.000132 \quad (4.4)$$

The study conducted by Garg (2006) and Abolmaali and Garg (2007) indicated that for the stress carrying capacity in the smeared crack models will diminish to zero at strain corresponding to  $10\varepsilon_{\text{crack}}$ . Thus, the mathematical model representing the tensionstiffening crack model for this study using  $\varepsilon_p = 10\varepsilon_{\text{crack}}$ .

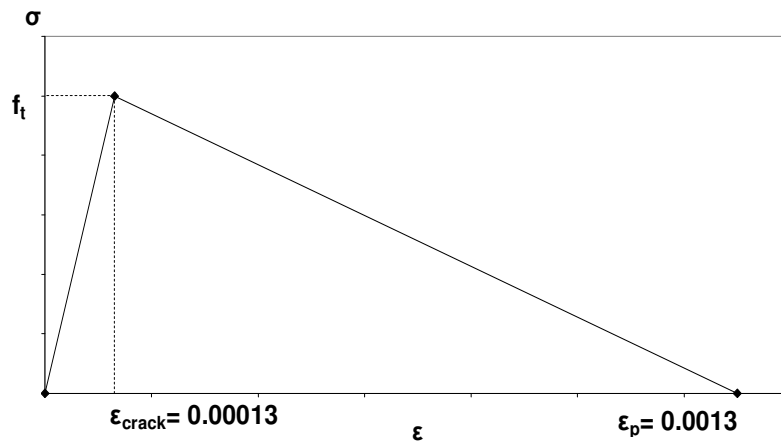


Figure 4.6 Tension stiffening model used for this study

### *Shear retention*

The initiation of cracks in concrete causes a reduction in the shear stiffness which is specified during modeling by a reduction in the shear modulus as a function of the opening strain across the crack. If the solution algorithm does not incorporate for this reduced modulus, a stiffer solution due to higher shear modulus is obtained. Also, this reduced shear modulus will also have an effect when the normal stresses across a crack become compressive. In the solution algorithm, the shear modulus is defined as  $\rho G$ , where  $G$  is the elastic shear modulus of the un-cracked concrete and  $\rho$  is a multiplying reduction factor. The shear retention model assumes that the shear stiffness of open cracks reduces linearly to zero as the crack opening increases. This phenomenon is presented by equation 4.5 as follows:

$$\rho = (1 - \varepsilon / \varepsilon_{\max}) \text{ for } \varepsilon < \varepsilon_{\max}, \rho = 0 \text{ for } \varepsilon \geq \varepsilon_{\max} \quad (4.5)$$

where  $\varepsilon$  is the direct strain across the crack and  $\varepsilon_{\max}$  is a user-specified value in the ABAQUS software.

### *Failure ratio*

To define the concrete smeared crack model the following ratios is defined

1. The ratio of the ultimate biaxial compressive stress to the uniaxial compressive ultimate stress. A suggested value of 1.16 was used (Garg (2006)).

2. The absolute value of the ratio of uniaxial tensile stress at failure to the uniaxial compressive stress at failure. A value of 0.085 was used in this study as recommended by Garg (2006).

3. The ratio of the magnitude of a principal component of plastic strain at ultimate stress in biaxial compression to the plastic strain at ultimate stress in uniaxial compression was set at 1.28 (Garg (2006)).

4. the ratio of the tensile principal stress value at cracking in plane stress, when the other nonzero principal stress component is at the ultimate compressive stress value, to the tensile cracking stress under uniaxial tension was set to be 0.333 (Garg (2006)).

#### *Modified Riks Algorithm*

The modified Riks method (refer ABAQUS (2006) version 6.6) is used which is an algorithm that allows effective solution and obtains nonlinear static equilibrium solutions for unstable problems. During the cracking of concrete, a local region softens while the adjoining material unloads elastically. These local effects may be accompanied by a sudden change in load keeping displacement constant or a sudden change in displacement keeping load constant (Figure 4.7).

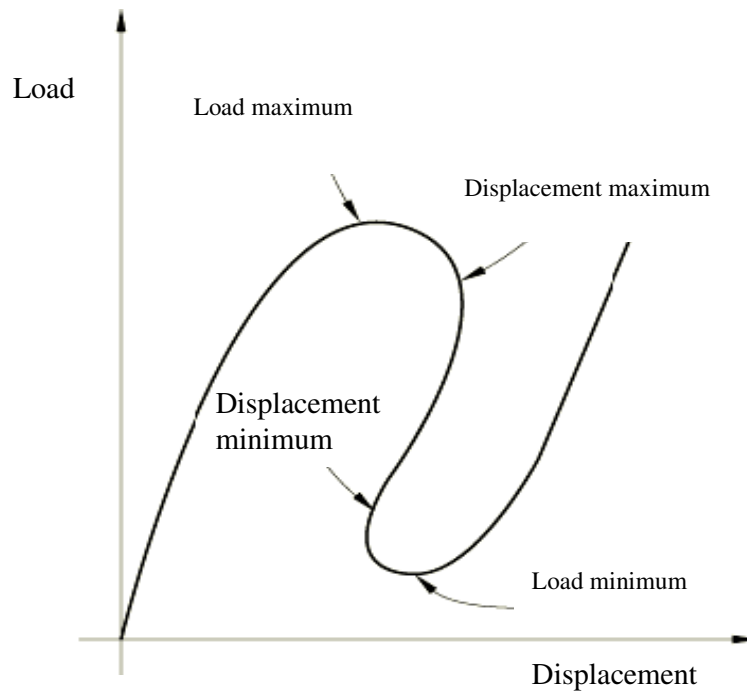


Figure 4.7 Typical Unstable Static Response (Re: ABAQUS (2006) Version 6.6)



The concrete models for window and door openings are shown in Figures 4.8 and 4.9.

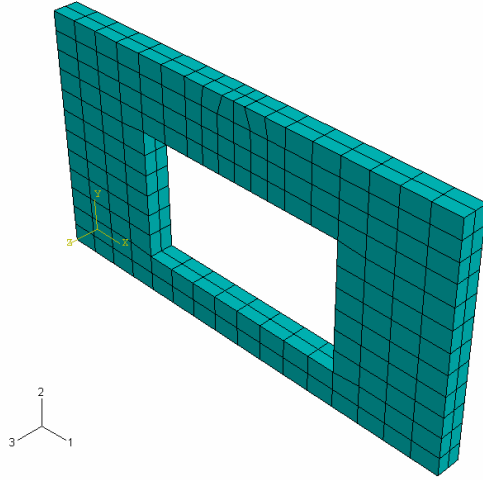


Figure 4.8 Finite element models for concrete element for window opening model

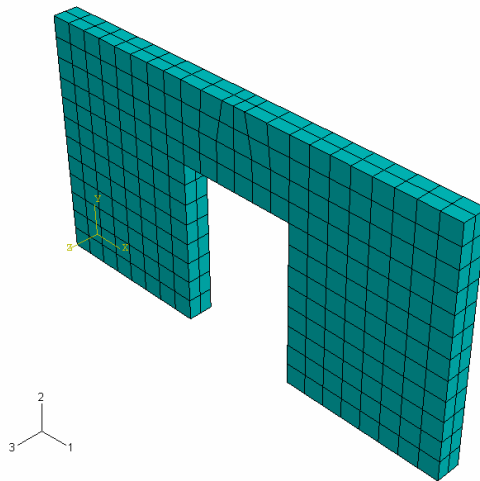


Figure 4.9 Finite element models for concrete element for door opening model

### *Rebar element and interaction step*

The steel welded wire mesh representing the reinforcement inside the concrete panels is modeled by using the two dimensional shell elements. The bond between concrete and welded wire mesh was assumed to be totally constrained even after crack occurred. This was due for simplicity and reduction in the computer run time. This simplified assumption did not affect the true behavior as observed during the experimental tests significantly. The author recommends more detail investigation to justify this observation.

The equivalent thickness of the rebar elements was calculated from the wire mesh D6 (nominal area 0.06 in.<sup>2</sup>) by 4 inch center to center spacing. The volume of the welded wire mesh per 1 ft<sup>2</sup> was determined by the following equation.

$$V = nA_w l \quad (4.6)$$

Where V= volume of welded wire mesh per 1 ft<sup>2</sup> (in<sup>3</sup>)

n= number of the welded wire mesh per 1 ft<sup>2</sup>

A<sub>w</sub>= nominal area of the welded wire (in<sup>2</sup>)

l= length of the welded wire mesh per 1 ft (in.)

Thus, volume of the of welded wire mesh per 1 ft<sup>2</sup> is equal to 4.32 in.<sup>3</sup> by using n = 6 bars, A = 0.06 in<sup>2</sup>, and l = 12 in. Finally, the equivalent thickness of the shell element was identify by the following equation.

$$t = \frac{V}{A} \quad (4.7)$$

Where t= the equivalent thickness of the rebar element (in)

A= area of the rebar shell element per 1 ft<sup>2</sup> (in<sup>2</sup>)

The equivalent thickness was 0.03 in. by using  $A = 144 \text{ in}^2$  and  $V$  from the previous equation.

The material's properties of steel was used as follows: a density 7850 kg/m<sup>3</sup> (490.0 pcf), Modulus of Elasticity 200,000 MPa (29000 ksi), Poisson's ratio 0.3 were used.

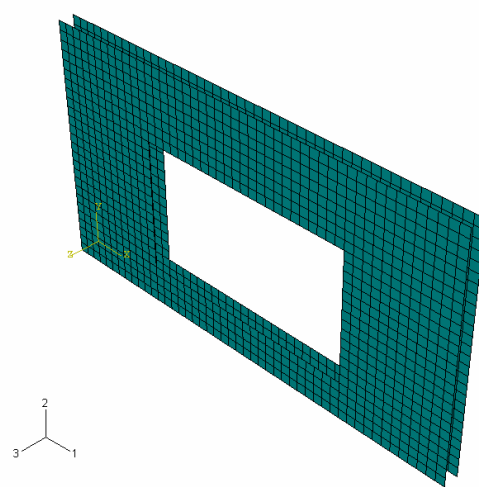


Figure 4.10 Finite element models for rebar element for window opening model

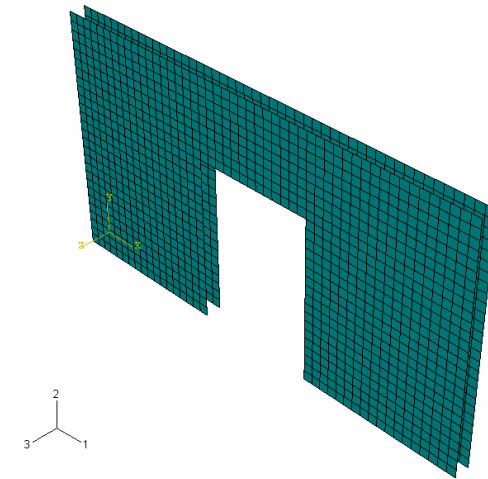


Figure 4.11 Finite element models for rebar element for door opening model

*Assembly step*

In assembly step, the concrete and rebar elements were assembled into one element as shown in Figures 4.12 and 4.13, for the panels with both opening configurations.

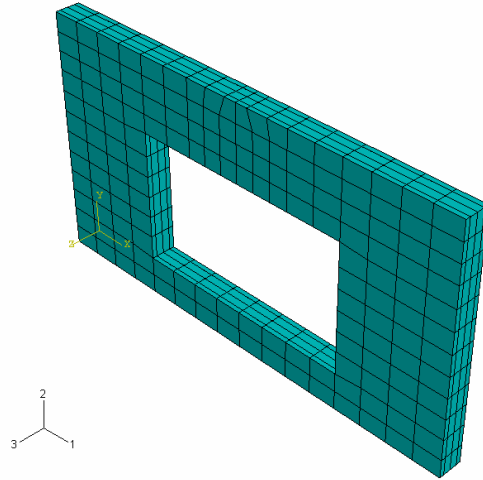


Figure 4.12 Finite element models for assembled element for window opening with 2636 nodes and 2128 elements

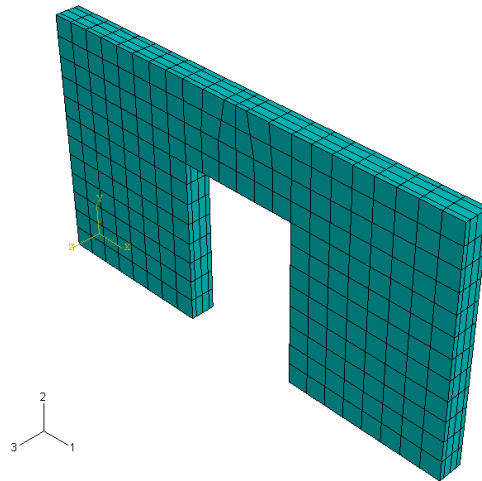


Figure 4.13 Finite element models for assembled element for door opening with 3145 nodes and 2610 elements

Finally, “static riks” step was used for the nonlinear automatic incremental solution in ABAQUS in which the geometric nonlinearity known as “Nlgeom” was selected.

*Load and boundary condition step*

The load was placed at the middle of the panels (same as the experiments). The boundary condition was defined such that the translational degree of freedom was constrained at the bottom of the panel as shown in Figures 4.14, 4.15.

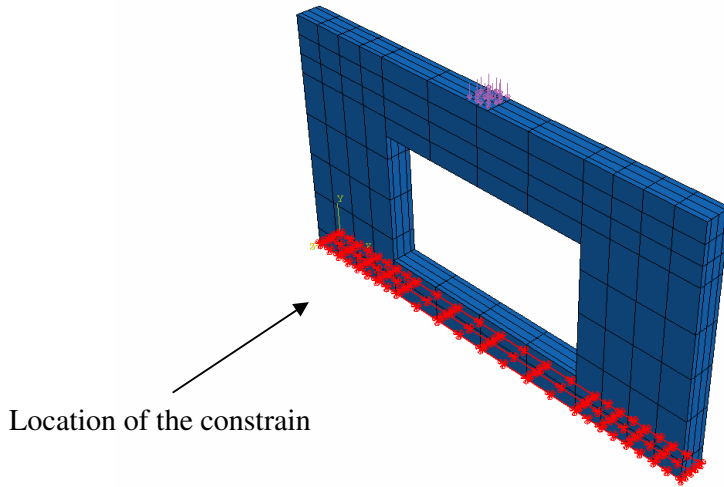


Figure 4.14 Finite element models for assembled element for door opening

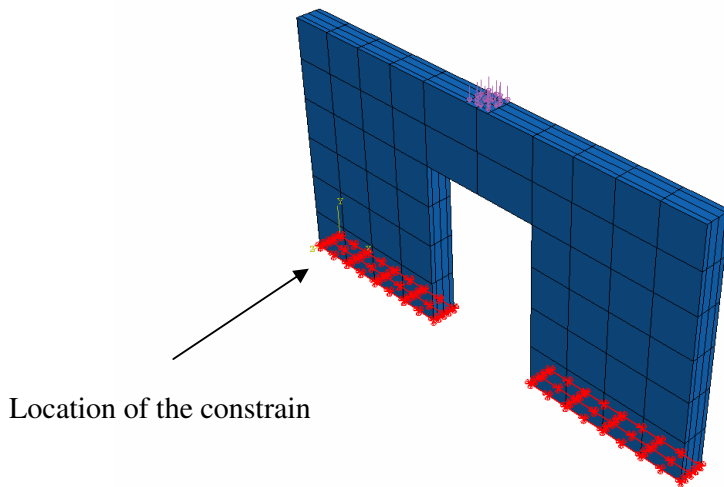


Figure 4.15 Finite element models for assembled element for door opening

*Seed and mesh step*

The appropriate size of seed was applied to panel model before structural analysis step. Hex pattern for mesh step was chosen for this model.

#### 4.4 Result for FEM model

Analysis results were shown by Van Mises stress. The rainbow color spectrums show the intensity of stress on the concrete panel with window opening as shown in Figure 4.16. S11, S22, and S33 are also shown in Figures 4.17, 4.18, and 4.19.

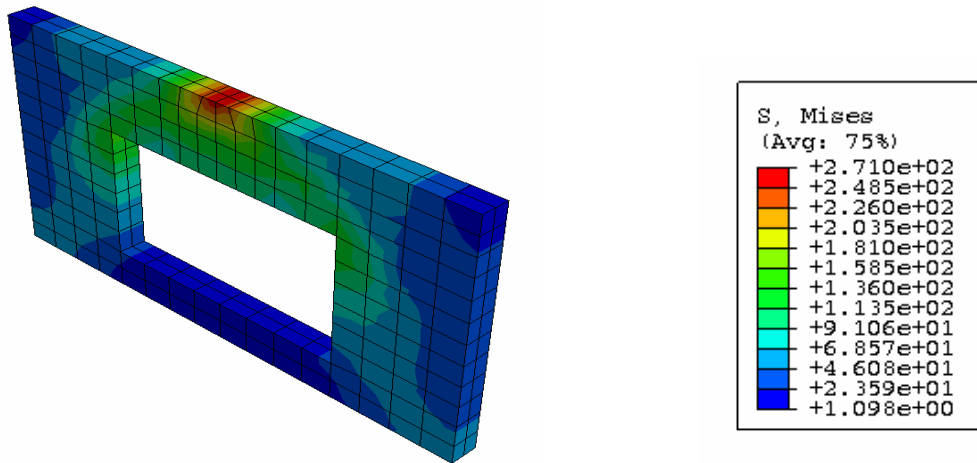


Figure 4.16 Van Mises stress for concrete panel with window opening

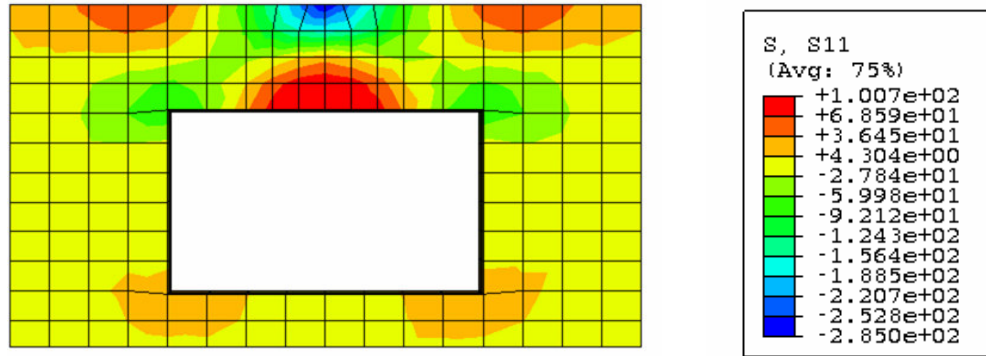


Figure 4.17 S11 for concrete panel with window opening

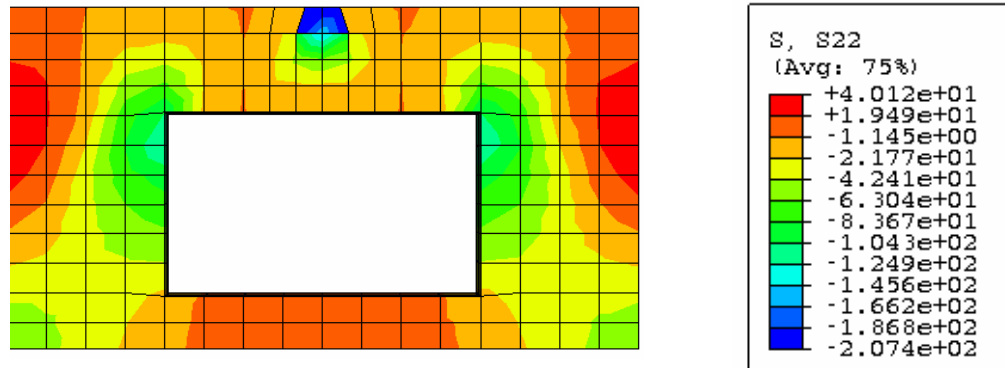


Figure 4.18 S22 for concrete panel with window opening

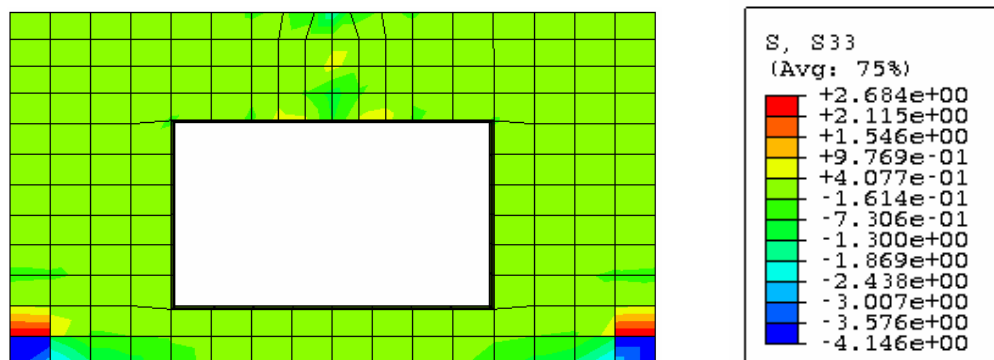


Figure 4.19 S33 for concrete panel with window opening

Analysis results were shown by Van Mises stress. The rainbow color spectrums show the intensity of stress on the concrete panel with door opening as shown in Figure 4.20. S11, S22, and S33 are also shown in Figures 4.21, 4.22, and 4.23.

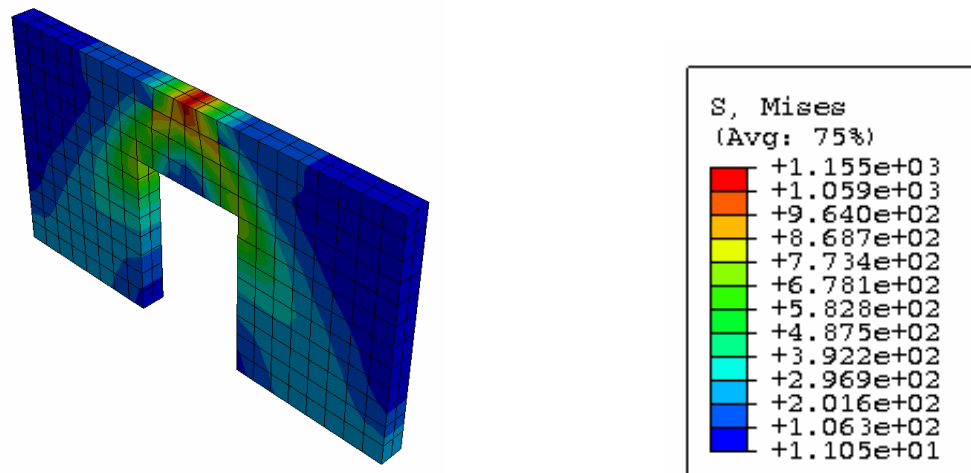


Figure 4.20 Van Mises stress for concrete panel with door opening



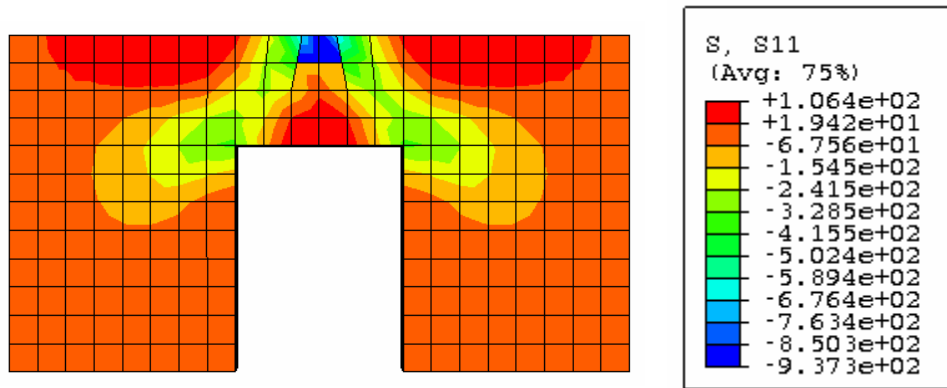


Figure 4.21 S11 for concrete panel with door opening

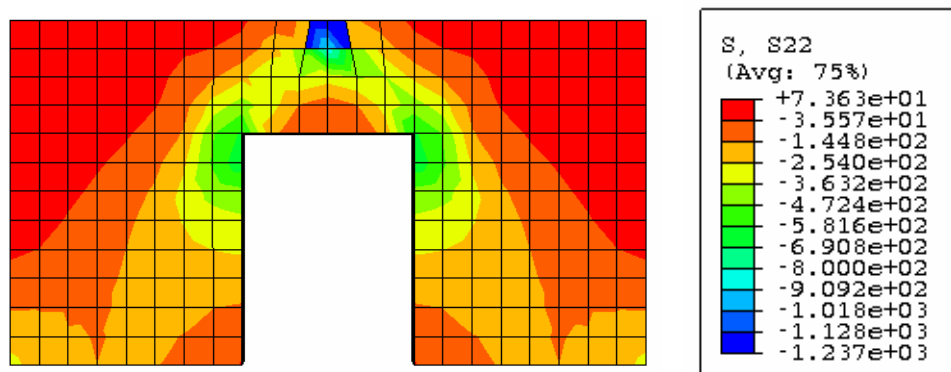


Figure 4.22 S22 for concrete panel with door opening

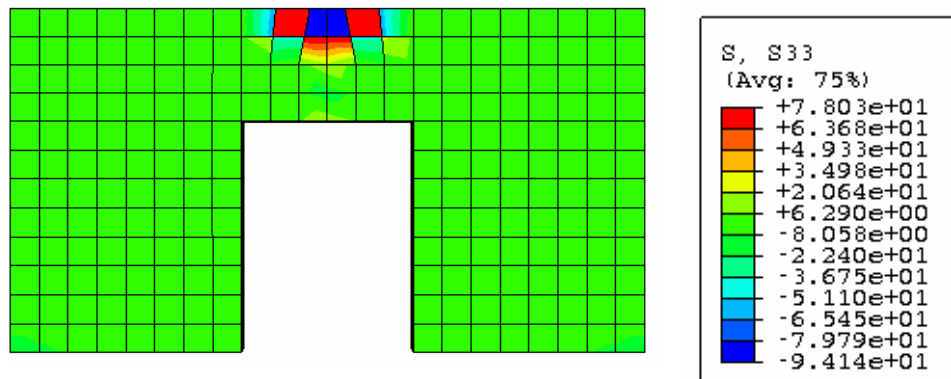


Figure 4.23 S33 for concrete panel with door opening

According to the results from FEM model, the maximum stresses occurred at the area around load and high stresses at the corners of window and door opening. The intensity of the stress has shown trend that it travels from the corners of the opening to location of the load by 45 degree pattern as shown in Figure 4.16 and 4.20.

### *First crack for concrete panel*

In order to verify the FEM model and the analysis algorithm, the crack load and patterns from the experimental test results are compared with the FEM. Since the load at which the first crack initiated for the panels with window and door openings were 20 kip (89 kN) and 28 kip (124 kN), respectively. The strain values above cracking strain ( $\epsilon_{\text{crack}}$ ) were identified for the same load level from FEM. It was specified that for strain values greater than  $\epsilon_{\text{crack}} = 0.00013$ . The elements are shown with different contour colors. Figures 4.25 and 4.28 show the comparisons between the FEM and experimental crack patterns for both panels under investigation.

Also, crack patterns for the both panels at failure which were 116 kip (515 kN) and 140 kip (622 kN) for the panels with the window and door openings, respectively, were compared with cracking strains from FEM results for both failure loads. The results are presented in Figures 4.25 and 4.28.

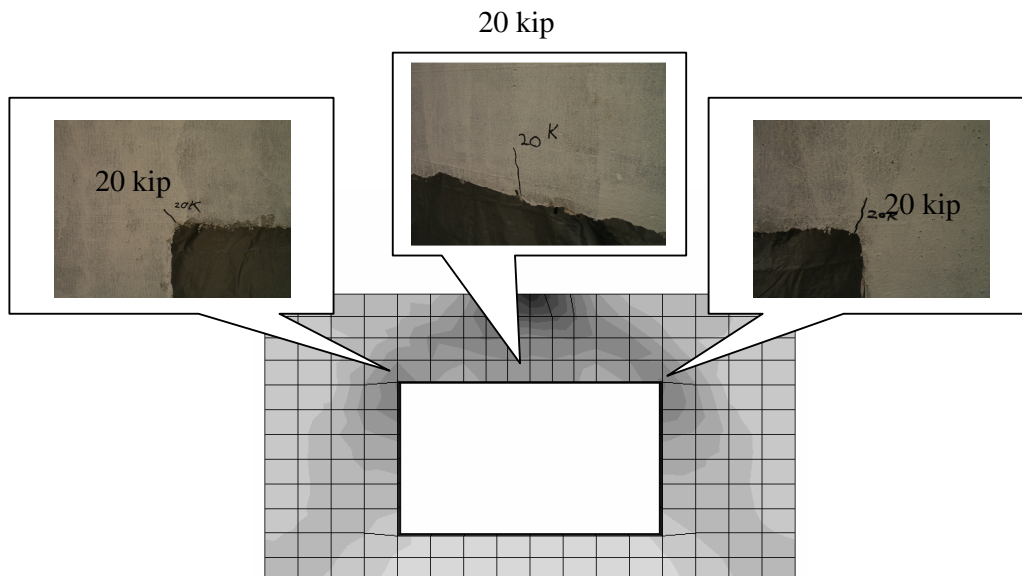


Figure 4.24 The first cracks of the panel with window opening by FEM model

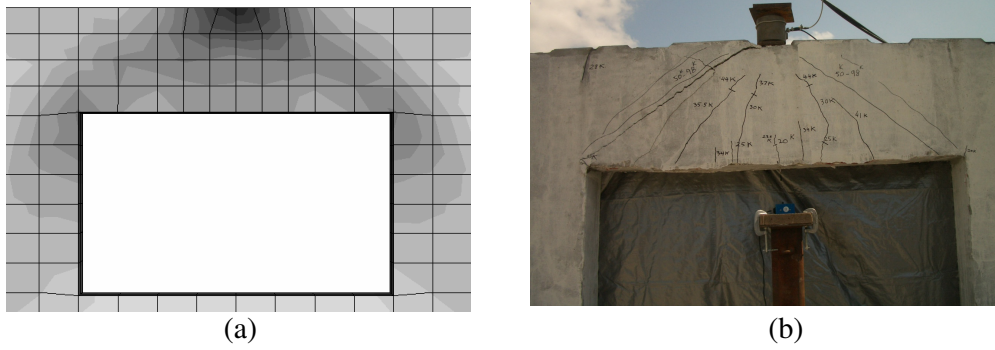


Figure 4.25 The failure cracks of the panel with window opening by FEM model:  
 (a) failure crack from FEM and (b) failure crack from experiment

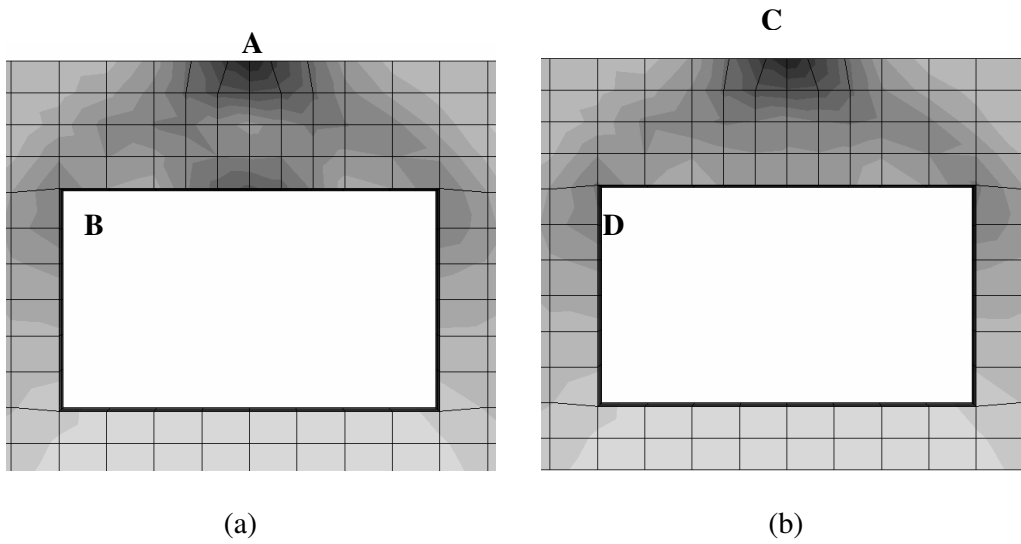


Figure 4.26 The cracks of the panel with window opening by FEM model:  
 (a) at 20 kip load and (b) at 120 kip load

Strain at A = 0.000021

Strain at B = 0.0000165

Strain at C = 0.00015

Strain at D = 0.00008

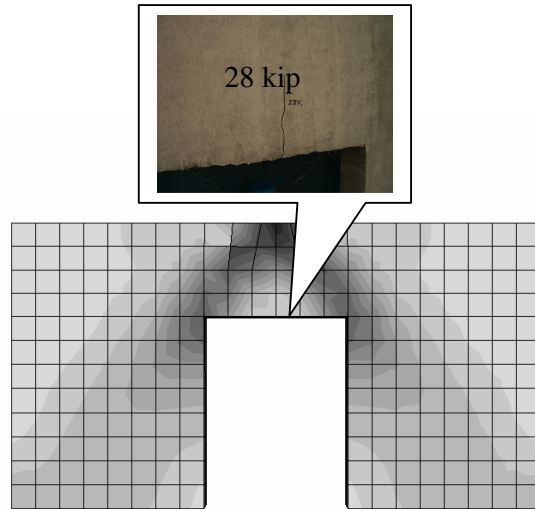


Figure 4.27 The first cracks of the panel with door opening by FEM model

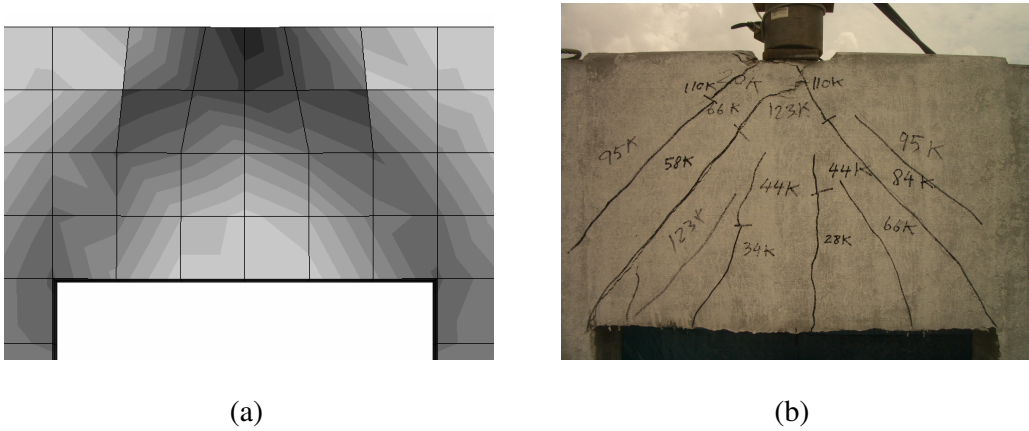


Figure 4.28 The failure cracks of the panel with door opening by FEM model:  
 (a) failure crack from FEM and (b) failure crack from experiment

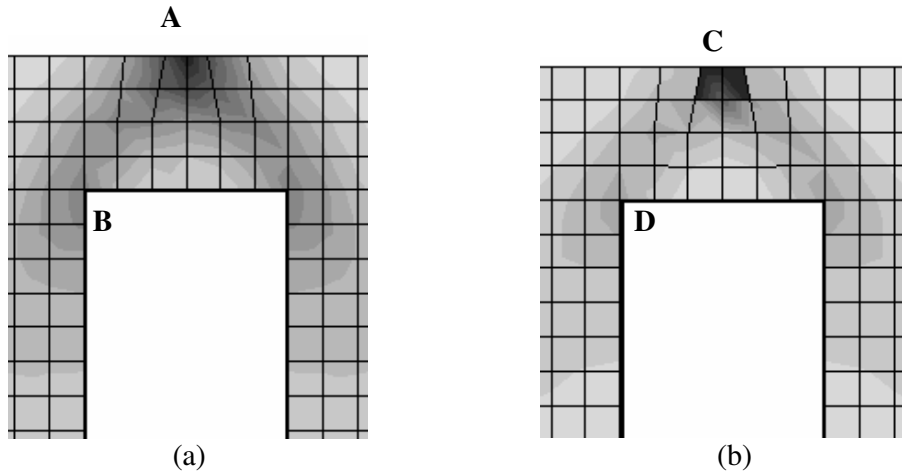


Figure 4.29 The cracks of the panel with window opening by FEM model:  
 (a) at 28 kip load and (b) at 140 kip load

Strain at A = 0.0003

Strain at B = 0.000143

Strain at C = 0.0056

Strain at D = 0.0008

The comparison between experiments and FEM for load and displacement are shown in Figures 4.30 and 4.31. As it can be seen close correlation between the experimental results and the FEM is obtained for test1 and the relatively close correlation is observed between the FEM and test2 for both panel types. It seems like the test2 specimens for both panels had higher compressive strength as compared to the test1 specimens. Core samples were not taken from the test specimens after test. Thus, the author cannot verify this point.

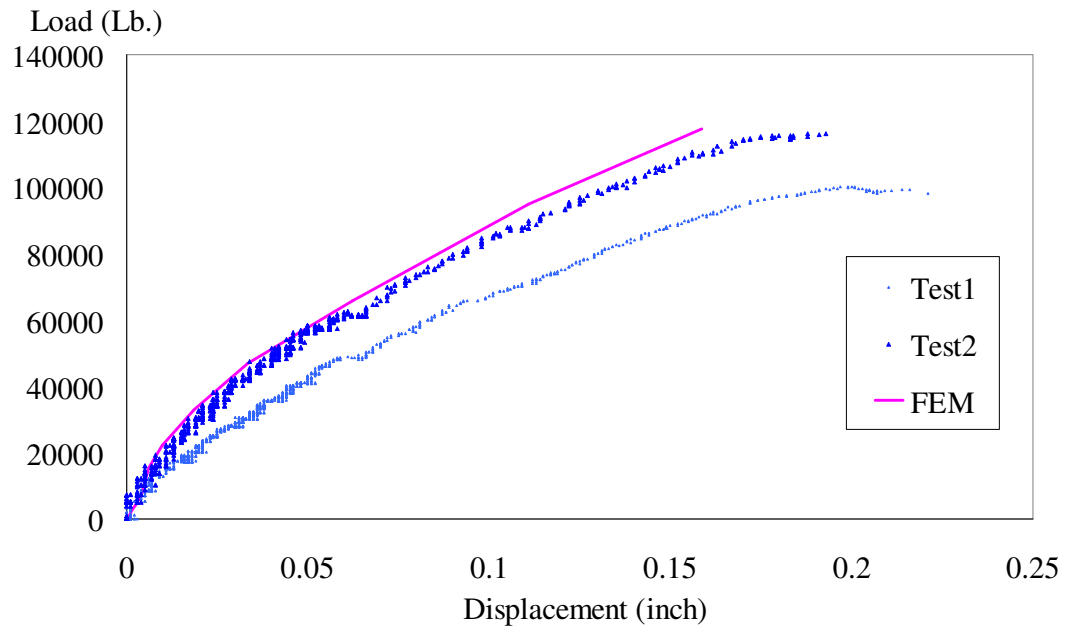


Figure 4.30 Comparison of FEM with experiment for concrete panel with window opening

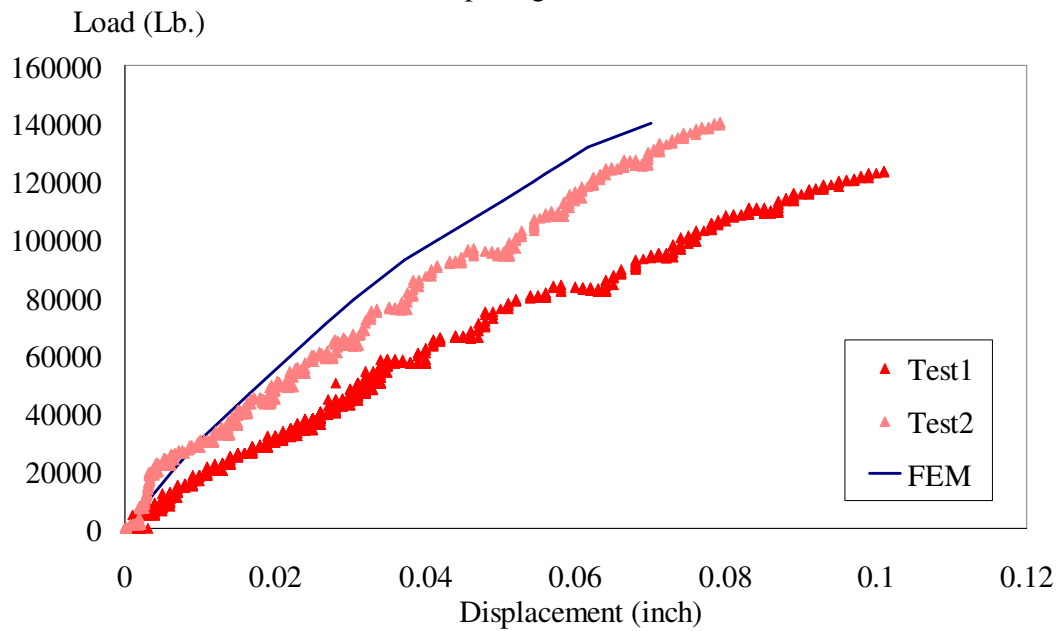


Figure 4.31 Comparison of FEM with experiment for concrete panel with door opening

## CHAPTER 5

### SUMMARY, CONCLUSION, AND RECOMMENDATION

#### 5.1 Summary

This study developed a ductile concrete for precast wall systems which are capable of resisting high wind in excess of 500 mph. The developed concrete mix design consists of sand, cement, glass fiber, and a foaming agent to produce lightweight concrete in the range of 87 pcf (1392 kg/m<sup>3</sup>) to 90 pcf (1440 kg/m<sup>3</sup>).

A comprehensive testing program for evaluation of the developed concrete material was undertaken. The mix designs were prepared both in the laboratory and in the mix truck with drum capacity of 27 ft<sup>3</sup> (0.77 m<sup>3</sup>), and 177.6 ft<sup>3</sup> (5 m<sup>3</sup>), respectively. The large concrete batches using trucks were prepared at the Hanson plants in Grand Prairie, Texas and News Orleans, Louisiana.

The material test included: 188 compressive strength tests (ASTM C39); 166 Modulus of rupture tests (ASTM C78); and 310 Pull-out test (ASTM C234-86) for both sites. From each mix design, three specimens for 1, 3, 7, 14, 28, 56, and 90 day(s) were prepared and tested on the designated test day. The relationships between the concrete unit weight and each of the a aforementioned properties were obtained and recorded.

Two types of pull out test (ASTM C234-86) were conducted: (1) the steel bar (#4) was embedded at 4 in. (10.16 cm.) in the 6 in.(152.4 mm.) x 12 in.(304.8 mm.) cylinders and (2) the steel bar was embedded at 12 in.(304.8 mm.) in the 6in.(152.4 mm.) x 12 in.(304.8 mm.) cylinders. This was done to document both the

pull-out and fracture mode of the failure during the pull-out test. Full-scale beam tests with specimen sizes of 8 in.(20.32 cm.)x 20 in.(50.8 cm.) x 96 in.(243.8 cm.) were conducted with and without reinforcements. A total of 124 beams (95 without reinforcement and 29 with reinforcement) were tested in four-point bending. The crack patterns and failure loads were identified and recorded. Also, the behavior of the non-reinforced full-size test beams were compared with the ASTM C78 beams. The full-scale testing was continued by testing lightweight precast wall panel with two types of opening configurations: (1) window opening and (2) door opening. Four full-scale walls were tested by being subjected to a single concentrated load at the center of the panel and being loaded to failure. These wall panels were cast at the Hanson's News Orleans's site (Site 2) and were transported for testing to the University of Texas at Arlington structural field laboratory at the Hanson's Grand Prairie plant (site 1). The wall panels were loaded to failure in an incremental manner and the crack initiation and propagations were identified and recorded. Also the load-deformation plots were obtained.

Finally, a three dimensional nonlinear finite element model (FEM) of the wall panels were developed which included elements for the lightweight ductile concrete and the reinforcements. The material geometric and contact algorithms were coupled with the smeared crack model was incorporated in the analysis. The developed FEM is capable of predicting crack initiation and propagation which verified against the experimental tests. Also, the load-deformation plots from the experimental results were compared with those obtained from the FEM analysis, which showed very close correlations.



## 5.2 Conclusion

The conclusion of this study advances in the following forefronts:

- A mix design procedure to produce a lightweight concrete with the unit weight ranging from 87 pcf (1392 kg/m<sup>3</sup>) to 90 pcf (1440 kg/m<sup>3</sup>) is developed and tested. The mixed designs are repeatable in the two different mixing sites.
- The compressive strength test data based on ASTM C39 showed a direct relationship between the concrete unit weight and its compressive strength as shown in Figure 5.1. The data points used for this graph is obtained based on the average of the three specimens tested at 28 days for each mix design. This information for the lightweight concrete tested in the research, which was based on sand, cement, and a foaming agent (not lightweight aggregate) was not available prior to this research.

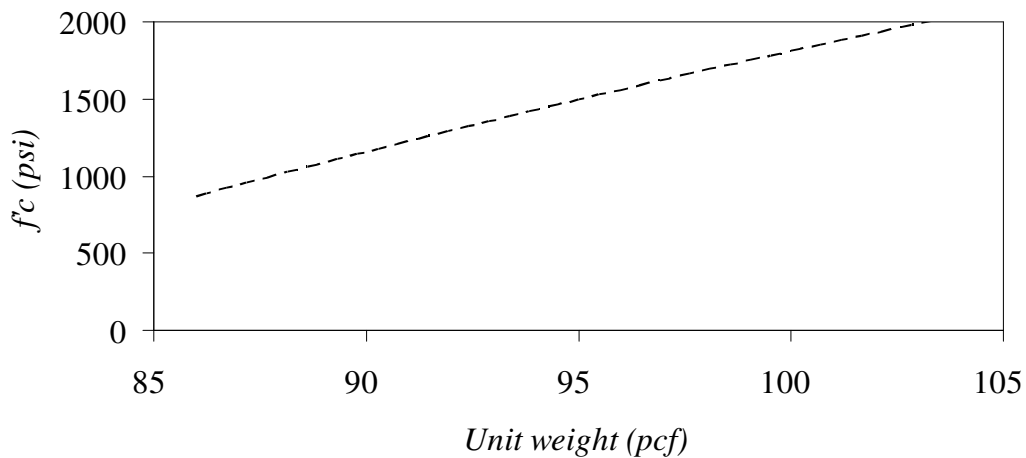


Figure 5.1 Graph relationship between compressive strength and unit weight for ductile lightweight concrete at 28 day

- The modulus of rupture test data based on the ASTM C78 is used to plot the concrete tensile strength versus the unit weight. This graph, which is shown in Figure 5.2, indicates that the concrete tensile strength increases with the unit weight. Again, this information, even though common to normal weight concrete, was not available prior to this research for a foam based concrete.

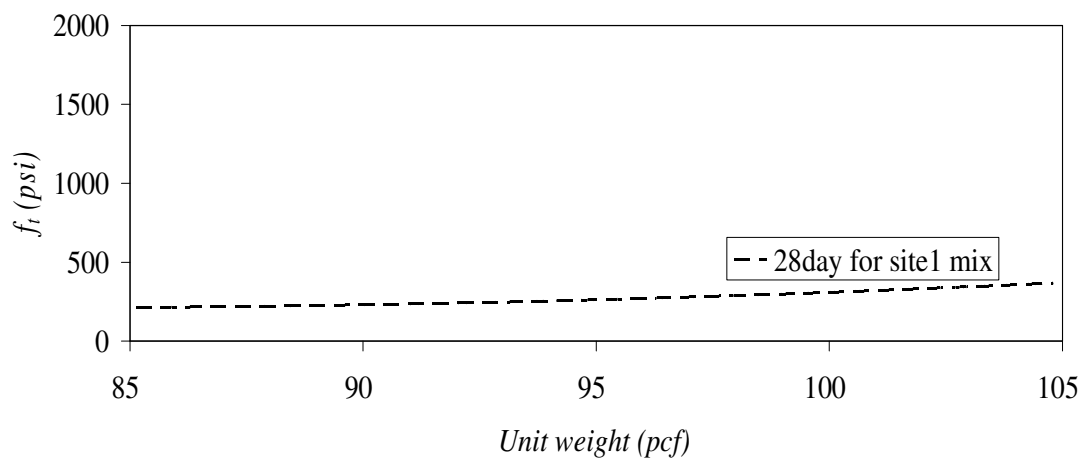


Figure 5.2 Graph relationship between modulus of rupture and unit weight for ductile lightweight concrete at 28 day

- The tensile strength factor,  $\alpha$ , from the following equation:

$$f_t = \alpha \sqrt{f'_c} \quad (5.1)$$

was plotted as a function of the concrete unit weight, which is shown in Figure 5.3. This plot indicates that the range of variation of  $\alpha$  is comparable with those reported by the American Concrete Institute (ACI) for the normal weight concrete.  $\alpha$  has range from 5.13 to 8.22.

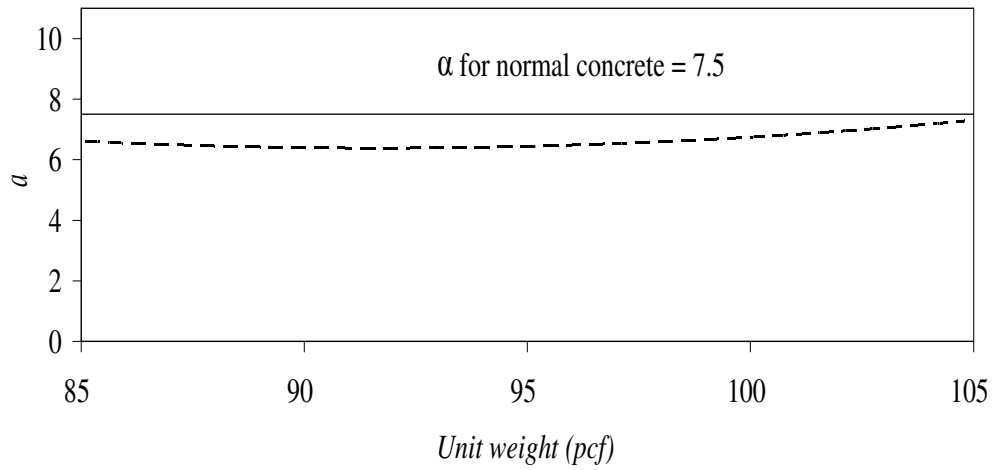


Figure 5.3 Graph relationship between alpha and unit weight for ductile lightweight concrete at 28 day

- The pull-out results are used to obtain the bond strength and stiffness plots as a function of concrete unit weight as shown in Figures 5.4 and 5.5, respectively. These figures show that bond strength and stiffness parameters increase with the increase of the concrete unit weight in a nonlinear function.

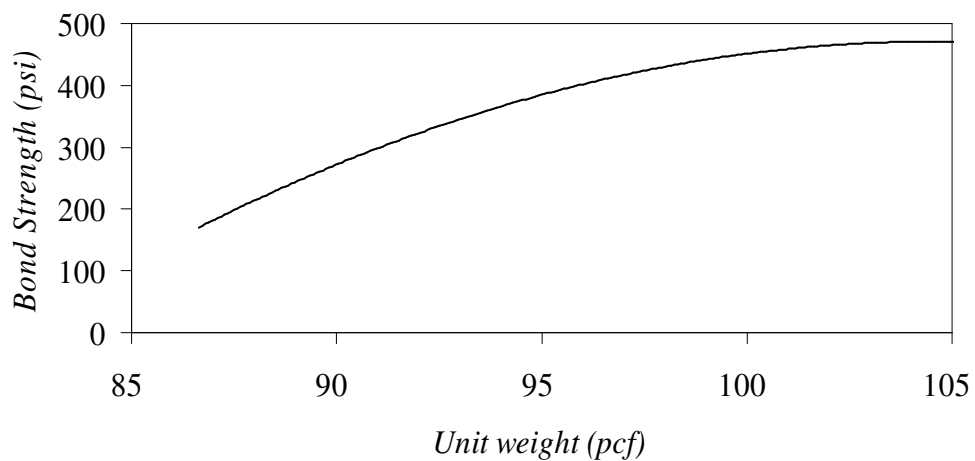


Figure 5.4 Graph relationship between bond strength and unit weight for ductile lightweight concrete at 28 day

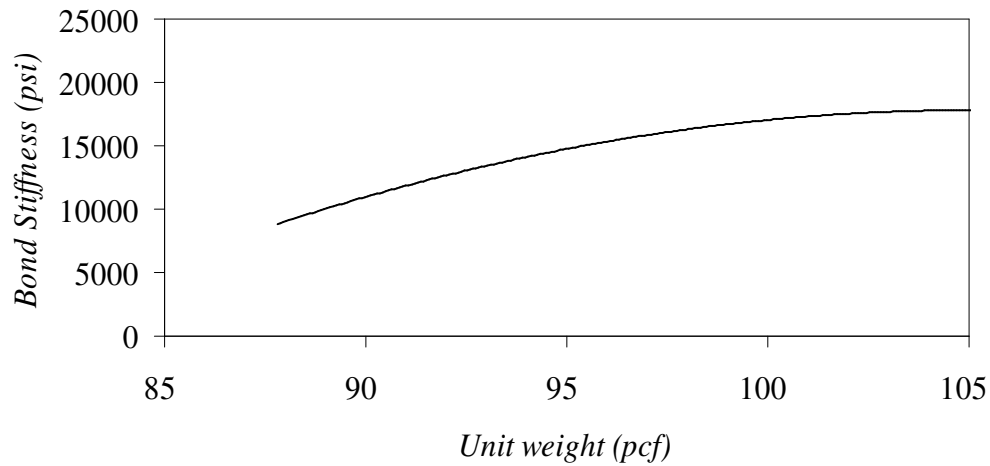


Figure 5.5 Graph relationship between bond stiffness and unit weight for ductile lightweight concrete at 28 day

- The full-scale beam tests without reinforcement showed similar failure pattern as these tested with normal weight concrete. The failure was sudden which means that even though the concrete was ductile with glass fiber, the ductility did not change the behavior as compared to normal weight concrete with the same crack pattern and locations.
- The full-scale beam tests for the ductile concrete with reinforcement showed similar crack patterns as compared with the normal weight concrete. This means that flexural cracks initiated at low load levels which then extended to the support and become shear cracks at the failure loads.

- The finite element models of the wall panel tests with window and door openings followed the experimental behavior very closely. Indeed, the location and the load level at which the crack initiated and propagated was predicted by the FEM accurately. Also, the load-deformation plots for the FEM and the experimental results were close.
- The experimental observations indicate that the behavior of the ductile concrete is similar to the normal weight concrete. Even though the developed ductile concrete has less strength and stiffness, the pattern of the behavior is similar to the normal weight concrete.

### 5.3 Recommendations

This study recommends the following future research studies to complement the work presented here:

- The ductile lightweight concrete should be developed and tested with different foaming agents.
- Variation of size of rebar should be investigated for pull-out test. Size of rebar might have an effect to bond strength of concrete and rebar.
- To verify structural behavior of reinforced concrete, full-scale reinforced concrete beam tests with different percentage of steel reinforcement should be investigated.

- Full-scale beam test with different  $a/d$  ratio as shown in Figure 5.6 should be conducted.

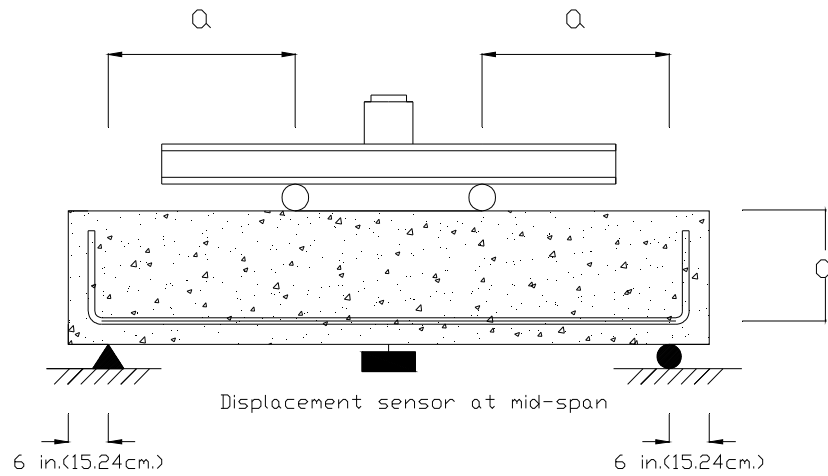


Figure 5.6 Full scale beam test with varied  $a/d$  ratio

- Because foaming agent is one of the ductile lightweight components, chemical reaction test should be investigated to identify that foaming agent does not have any effect to some chemical substances.
- Low frequency fully cyclic experimental tests could be conducted to identify the behavior of reinforced ductile lightweight concrete in earthquake induced ground acceleration.
- Long-term studies investigating the durability and creep of reinforced ductile light weight concrete should be conducted.

- Shrinkage characteristics of ductile lightweight concrete should be investigated for optimize of the fiber use.
- Some material properties should be investigated such as temperature effects on strength and elasticity of ductile lightweight concrete. The coefficient of linear expansion due to temperature is one of the most important material properties.

## APPENDIX A

PICTURES FOR MIX-DESIGN PANEL, BEAM, AND SPECIMEN CASTING





Figure A.1 Ready-mix for mixing concrete



Figure A.2 Launch fine aggregate into the truck



Figure A.3 Machine for mixing foaming agent



Figure A.4 Mixing foaming agent in the truck



Figure A.5 Mixing process for small batch



Figure A.6 Machine for mixing foaming agent



Figure A.7 Foaming agent (NEOPOR)



Figure A.8 Fine aggregate (sand)



Figure A.9 Weighting ingredient for mixing



Figure A.10 Weighting water for mixing process



Figure A.11 Mixing process



Figure A.12 Putting materials for concrete



Figure A.13 Take concrete from mixing drum



Figure A.14 Pouring concrete for test specimens



Figure A.15 Concrete specimens for compressive test



Figure A.16 Concrete specimens for pull-out test



Figure A.17 Concrete specimens for pull-out test



Figure A.18 Concrete specimens for pull-out test



Figure A.19 Formwork for full-scale beam



Figure A.20 Formwork for full-scale beam



Figure A.21 Checking beam dimension



Figure A.22 beam's covering



Figure A.23 Checking spacing for stirrup



Figure A.24 Checking spacing for stirrup





Figure A.25 Stand for concrete covering



Figure A.26 Stand for concrete covering



Figure A.27 Checking width of the beams



Figure A.28 Pouring concrete for full-scale beams



Figure A.29 Pouring concrete for full-scale beams



Figure A.30 Pouring concrete for full-scale beams



Figure A.31 Pouring concrete for full-scale beams



Figure A.32 Pouring concrete for full-scale beams

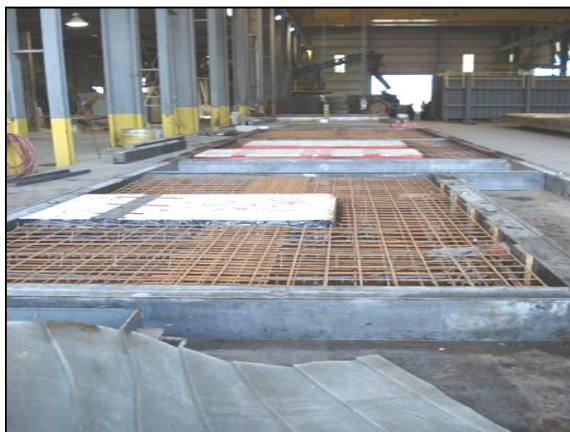


Figure A.33 Formwork for full-scale concrete panels



Figure A.34 Pouring for full-scale concrete panels



Figure A.35 Pouring for full-scale concrete panels

APPENDIX B

FULL-SCALE BEAM TEST

Table B.1 Summary of Full scale beam test for beams mixed on 10/18/06

Concrete mixed on 10/18/2006								
test date	age	Max load Lb (KN)	Max moment Lb-ft (KN-m)	$f_t$ psi(Mpa)	Concrete weight Lb/ft3(Kg/m <sup>3</sup> )	$f_c$ psi(Mpa)	$\alpha$	Location of failure crack
10/19/06	1	8888.412 (39.5)	10355 (14.03)	232 (1.60)	113.49 (1828.32)	1395 (9.61)	6.21	34 inch from support
10/19/06	1	8891.2732 (39.5)	10358 (14.14)	233 (1.60)	113.49 (1828.32)	1395 (9.61)	6.24	40 inch from support
10/21/06	3	12145.923 (54)	14150 (19.17)	318 (2.19)	113.49 (1828.32)	2049 (14.12)	7.03	36 inch from support
10/21/06	3	12761.087 (56.7)	14866 (20.14)	334 (2.30)	113.49 (1828.32)	2049 (14.12)	7.38	45 inch from support

Table B.2 Summary of Full scale beam test for beams mixed on 10/24/06

Concrete mixed on 10/24/2006								
test date	age	Max load Lb (KN)	Max moment Lb-ft (KN-m)	$f_t$ psi(Mpa)	Concrete weight Lb/ft3(Kg/m <sup>3</sup> )	$f_c$ psi(Mpa)	$\alpha$	Location of failure crack
10/25/2006	1	3862 (17.18)	4500 (6.09)	101.25 (0.96)	86.37 (1391)	529 (3.64)	4.40	41 inch from support
10/25/2006	1	4289 (19)	4997.5 (6.77)	112.4438 (0.77)	86.37 (1391)	529 (3.64)	4.89	35 inch from support
10/25/2006	1	1245 (5.54)	1451.25 (1.96)	32.65313 (0.22)	92.01 (1482)	613 (4.22)	1.32	35 inch from support

Table B.3 Summary of Full scale beam test for beams mixed on 10/26/06

Concrete mixed on 10/26/2006								
test date	age	Max load	Max moment	$f_t$	Concrete weight	$f_c$	$\alpha$	Location of failure crack
		Lb (KN)	Lb-ft (KN-m)	psi(Mpa)	Lb/ft <sup>3</sup> (Kg/m <sup>3</sup> )	psi(Mpa)		
10/27/2006	1	8404.5064 (37.38)	9791.25 (13.26)	220.3031 (1.52)	89.4 (1440)	924 (6.37)	7.25	41 inch from support
10/27/2006	1	9114.4492 (40.54)	10618.33333 (14.38)	238.9125 (1.64)	89.4 (1440)	924 (6.37)	7.86	44 inch from support
10/27/2006	1	8042.9185 (35.77)	9370 (12.69)	210.825 (1.45)	91.59 (1475)	718 (4.95)	7.87	35 inch from support
10/27/2006	1	8311.8741 (36.97)	9683.333333 (13.12)	217.875 (1.50)	91.59 (1475)	718 (4.95)	8.13	37 inch from support
10/29/2006	3	9638.412 (42.87)	11228.75 (15.21)	252.6469 (1.72)	89.4 (1440)	1486 (10.24)	6.55	41 inch from support
10/29/2006	3	9795.422 (43.57)	11411.66667 (15.46)	256.7625 (1.77)	89.4 (1440)	1486 (10.24)	6.66	42 inch from support
10/29/2006	3	8459.2275 (37.62)	9855 (13.36)	221.7375 (1.52)	91.59 (1475)	1362 (9.40)	6.01	34 inch from support
10/29/2006	3	8098.7124 (36.02)	9435 (12.78)	212.2875 (1.46)	91.59 (1475)	1362 (9.40)	5.75	35 inch from support

Table B.4 Summary of Full scale beam test for beams mixed on 10/27/06

Concrete mixed on 10/27/2006								
test date	age	Max load	Max moment	$f_t$	Concrete weight	$f_c$	$\alpha$	Location of failure crack
		Lb (KN)	Lb-ft (KN-m)	psi(Mpa)	Lb/ft <sup>3</sup> (Kg/m <sup>3</sup> )	psi(Mpa)		
10/30/2006	3	3136.2661 (13.95)	3653.75 (4.95)	82.20938 (0.56)	71.93 (1159)	447 (3.08)	3.8884	37 inch from support
10/30/2006	3	2789.6996 (12.40)	3250 (4.40)	73.125 (0.50)	71.93 (1159)	447 (3.08)	3.4587	32 inch from support
11/3/2006	7	1971.03 (8.76)	2296.25 (3.11)	51.66563 (0.35)	71.93 (1159)	549 (3.79)	2.205	42 inch from support
11/3/2006	7	2251.7883 (10.01)	2623.333333 (3.55)	59.025 (0.41)	71.93 (1159)	549 (3.79)	2.5191	41 inch from support

Table B.5 Summary of Full scale beam test for beams mixed on 11/2/06

Concrete mixed on 11/2/2006								
test date	age	Max load Lb (KN)	Max moment Lb-ft (KN-m)	$f_t$ psi(Mpa)	Concrete weight Lb/ft <sup>3</sup> (Kg/m <sup>3</sup> )	$f_c$ psi(Mpa)	$\alpha$	Location of failure crack
11/3/2006	1	5951.72 (26.47)	6933.75 (9.39)	156.01 (1.07)	80.68 (1300)	337.00 (2.32)	8.50	43 inch from support
11/3/2006	1	4825.46 (21.46)	5621.67 (7.61)	126.49 (0.87)	80.68 (1300)	337.00 (2.32)	6.89	37 inch from support
11/3/2006	1	4182.40 (18.6)	4872.50 (6.60)	109.63 (0.76)	78.07 (1257)	286.00 (1.97)	6.48	34 inch from support
11/3/2006	1	4128.76 (18.4)	4810.00 (6.51)	108.23 (0.75)	78.07 (1257)	286.00 (1.97)	6.40	34 inch from support
11/6/2006	3	10093.35 (44.9)	11758.75 (15.93)	264.57 (1.83)	80.68 (1300)	527.00 (3.63)	11.52	44 inch from support
11/6/2006	3	10254.29 (45.6)	11946.25 (16.18)	268.79 (1.86)	78.07 (1257)	561.00 (3.87)	11.35	38 inch from support
11/9/2006	7	7440.99 (33.1)	8668.75 (17.47)	195.05 (1.35)	80.68 (1300)	652.00 (4.49)	7.64	37 inch from support
11/9/2006	7	8284.33 (33.9)	9651.25 (13.01)	217.15 (1.5)	78.07 (1257)	641.00 (4.41)	8.58	33 inch from support
11/9/2006	7	7131.62 (31.7)	8308.33 (11.26)	186.94 (1.3)	78.07 (1257)	641.00 (4.41)	7.38	37 inch from support



Table B.6 Summary of Full scale beam test for beams mixed on 11/7/06

Concrete mixed on 11/7/2006								
test date	age	Max load Lb (KN)	Max moment Lb-ft (KN-m)	$f_t$ psi(Mpa)	Concrete weight Lb/ft <sup>3</sup> (Kg/m <sup>3</sup> )	$f_c$ psi(Mpa)	$\alpha$	Location of failure crack
11/8/2006	1	7680.26 (34.17)	8947.50 (12.12)	201.32 (1.388)	92.05 (1482)	723.00 (4.98)	7.49	41 inch from support
11/8/2006	1	6917.02 (30.77)	8058.33 (10.91)	181.31 (1.25)	92.05 (1482)	723.00 (4.98)	6.74	35 inch from support
11/10/2006	3	10579.40 (47.06)	12325.00 (16.70)	277.31 (1.91)	92.05 (1482)	1153.00 (7.94)	8.17	35 inch from support
11/10/2006	3	11316.17 (50.34)	13183.33 (17.86)	296.63 (2.05)	92.05 (1482)	1153.00 (7.94)	8.74	35 inch from support
11/14/2006	7	11663.09 (51.88)	13587.50 (18.41)	305.72 (2.10)	92.05 (1482)	1486.00 (10.24)	7.93	41 inch from support
11/14/2006	7	8042.92 (35.77)	9370.00 (12.69)	210.83 (1.46)	92.05 (1482)	1486.00 (10.24)	5.47	35 inch from support
12/5/2006	28	8565.45 (38.01)	9978.75 (13.51)	224.52 (1.55)	92.05 (1482)	1532.00 (10.56)	5.74	35 inch from support
12/5/2006	28	10562.23 (46.9)	12305.00 (16.67)	276.86 (1.90)	92.05 (1482)	1532.00 (10.56)	7.07	35 inch from support
1/2/2007	56	9370.17 (41.7)	10916.25 (14.79)	245.62 (1.70)	92.05 (1482)	1532.00 (10.56)	6.28	35 inch from support
1/2/2007	56	7237.48 (32.8)	8431.67 (11.43)	189.71 (1.30)	92.05 (1482)	1532.00 (10.56)	4.85	35 inch from support
2/5/2007	90	8726.39 (38.8)	10166.25 (13.78)	228.74 (1.58)	92.05 (1482)	1560.00 (10.75)	5.79	35 inch from support
2/5/2007	90	6595.14 (29.34)	7683.33 (10.42)	172.88 (1.20)	92.05 (1482)	1560.00 (10.75)	4.38	35 inch from support

Table B.6 Summary of Full scale beam test for beams mixed on 11/16/06

Concrete mixed on 11/16/2006								
test date	age	Max load Lb (KN)	Max moment Lb-ft (KN-m)	$f_t$ psi(Mpa)	Concrete weight Lb/ft <sup>3</sup> (Kg/m <sup>3</sup> )	$f_c$ psi(Mpa)	$\alpha$	Location of failure crack
1/1/1900	1	3973 (17.67)	5628.416667 (7.62)	126.6394 (0.87)	95.16 (1533)	675 (4.650)	4.8744	41 inch from support
1/1/1900	1	4650 (20.69)	6587.5 (8.92)	148.2188 (1.02)	95.16 (1533)	675 (4.65)	5.7049	35 inch from support
1/4/1900	3	11170 (40.69)	15824.16667 (21.44)	356.0438 (2.45)	95.16 (1533)	1456 (10)	9.3309	35 inch from support
1/4/1900	3	10082 (44.85)	14282.83333 (19.35)	321.3638 (2.21)	95.16 (1533)	1456 (10)	8.422	35 inch from support
1/13/1900	13	11000 (48.93)	15583.33333 (21.11)	350.625 (2.41)	95.16 (1533)	1739 (12)	8.408	41 inch from support
2/25/1900	56	6785 (30.18)	9612.083333 (13.01)	216.2719 (1.49)	95.16 (1533)	1750 (12)	5.1699	35 inch from support
2/25/1900	56	7647 (34.02)	10833.25 (14.67)	243.7481 (1.68)	95.16 (1533)	1750 (12)	5.8267	35 inch from support
3/30/1900	90	4797 (21.34)	6795.75 (9.2)	152.9044 (1.06)	95.16 (1533)	1775 (12.23)	3.6293	35 inch from support
3/30/1900	90	2848 (12.67)	4034.666667 (5.47)	90.78 (0.63)	95.16 (1533)	1775 (12.23)	2.1547	35 inch from support

Table B.7 Summary of Full scale beam test for beams mixed on 2/8/07

Concrete mixed on 2/8/2007								
test date	age	Max load Lb (KN)	Max moment Lb-ft (KN-m)	$f_t$ psi(Mpa)	Concrete weight Lb/ft3(Kg/m <sup>3</sup> )	$f_c$ psi(Mpa)	$\alpha$	Location of failure crack
2/11/2007	3	16041.979 (71.35)	18715.64217 (25.4)	421.1019 (2.9)	150 (2416)	5104.8949 (35.2)	5.8938	39 inch from support
2/11/2007	3	17278.861 (76.85)	20158.6707 (27.3)	453.5701 (3.1)	150 (2416)	5104.8949 (35.2)	6.3482	40 inch from support
2/15/2007	7	27661 (123)	32271.16667 (43.2)	726.1013 (5)	150 (2416)	5765.3879 (39.8)	9.5628	42 inch from support
2/22/2007	14	16041.979 (71)	18715.64217 (25.4)	421.1019 (2.9)	150 (2416)	6286.6204 (43.4)	5.311	46 inch from support
2/22/2007	14	30022 (133)	35025.66667 (47.5)	788.0775 (5.4)	150 (2416)	6286.6204 (43.4)	9.9394	44 inch from support

Table B.8 Summary of Full scale beam test for beams mixed on 2/20/07

Concrete mixed on 2/20/2007								
test date	age	Max load Lb (KN)	Max moment Lb-ft (KN-m)	$f_t$ psi(Mpa)	Concrete weight Lb/ft3(Kg/m <sup>3</sup> )	$f_c$ psi(Mpa)	$\alpha$	Location of failure crack
2/21/2007	1	5847 (26)	6821.5 (9.2)	153.4838 (1.05)	89.7 (1445)	367 (2.53)	8.0118	55 inch from support
2/21/2007	1	4835 (21.5)	5640.833333 (7.64)	126.91875 (0.87)	89.7 (1445)	367 (2.53)	6.6251	37 inch from support
2/27/2007	7	7657 (34)	8933.166667 (12.1)	200.9963 (1.37)	89.7 (1445)	861 (5.94)	6.8499	44 inch from support
3/6/2007	14	7769 (34.5)	9063.833333 (12.3)	203.9363 (1.4)	89.7 (1445)	820.44375 (5.65)	7.1198	46 inch from support

Table B.9 Summary of Full scale beam test for beams mixed on 2/27/07

Concrete mixed on 2/27/2007								
test date	age	Max load Lb (KN)	Max moment Lb-ft (KN-m)	$f_t$ psi(Mpa)	Concrete weight Lb/ft <sup>3</sup> (Kg/m <sup>3</sup> )	$f_c$ psi(Mpa)	$\alpha$	Location of failure crack
3/2/2007	3	3223 (14.33)	3760.166667 (5.09)	84.60375 (0.58)	93.22 (1500)	202 (1.39)	5.95	45 inch from support
3/2/2007	3	3073 (13.66)	3585.166667 (4.86)	80.66625 (0.55)	93.22 (1500)	202 (1.39)	5.68	36 inch from support
3/6/2007	7	2698 (12)	3147.666667 (4.23)	70.8225 (0.48)	93.22 (1500)	213 (1.46)	4.85	43 inch from support



Figure B.1 Beam cast on 10/18/06 for 1 day test; (a) before test, (b) after test



Figure B.2 Beam cast on 10/18/06 for 3 day test; (a) before test, (b) after test



Figure B.3 Beam cast on 10/24/06 for 1 day test; (a) before test, (b) after test



Figure B.4 Beam cast on 10/24/06 for 1 day test; (a) before test, (b) after test



Figure B.5 Beam cast on 10/24/06 for 1 day test; (a) before test, (b) after test



Figure B.6 Beam for 1<sup>st</sup> batch concrete cast on 10/26/06 for 1 day test; (a) before test, (b) after test



Figure B.7 Beam for 1<sup>st</sup> batch concrete cast on 10/26/06 for 1 day test;  
(a) before test, (b) after test

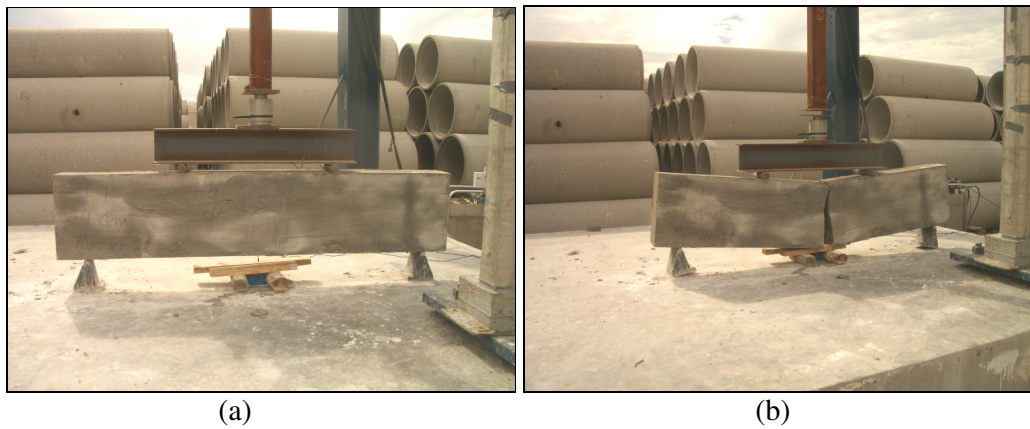


Figure B.8 Beam for 1<sup>st</sup> batch concrete cast on 10/26/06 for 3 day test;  
(a) before test, (b) after test

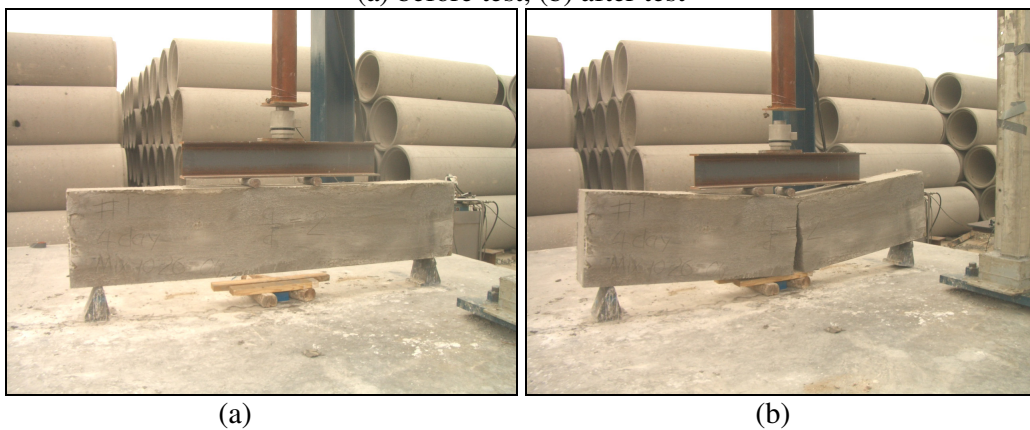


Figure B.9 Beam for 1<sup>st</sup> batch concrete cast on 10/26/06 for 3 day test;  
(a) before test, (b) after test



Figure B.10 Beam for 2<sup>nd</sup> batch concrete cast on 10/26/06 for 1 day test;  
 (a) before test, (b) after test



Figure B.11 Beam for 2<sup>nd</sup> batch concrete cast on 10/26/06 for 1 day test;  
 (a) before test, (b) after test

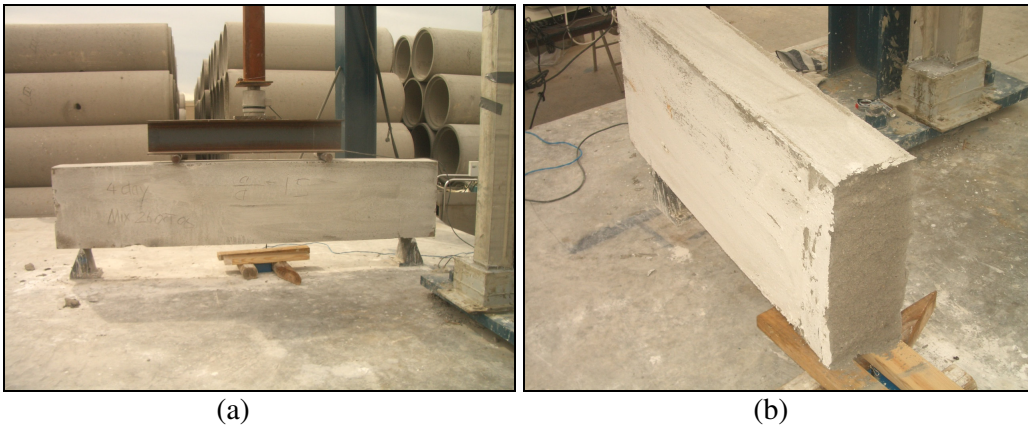


Figure B.12 Beam for 2<sup>nd</sup> batch concrete cast on 10/26/06 for 3 day test;  
 (a) before test, (b) after test



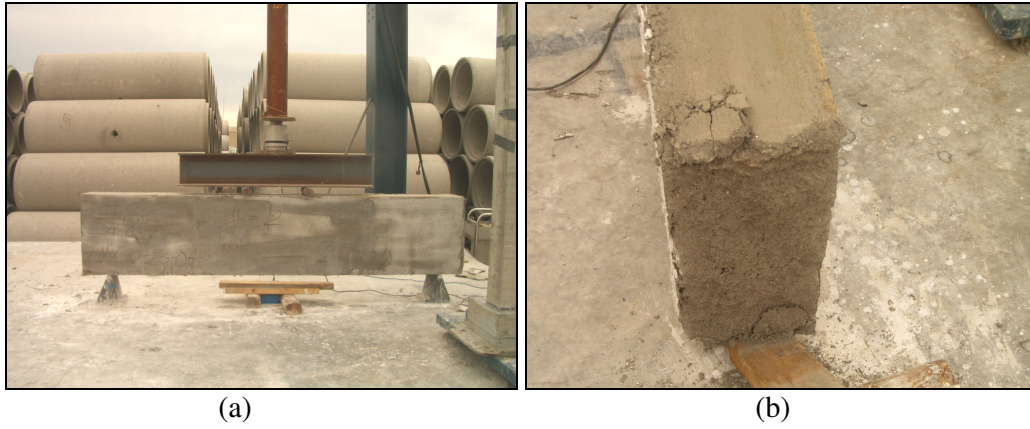


Figure B.13 Beam for 2<sup>nd</sup> batch concrete cast on 10/26/06 for 3 day test;  
 (a) before test, (b) after test



Figure B.14 Beam for concrete cast on 10/27/06 for 3 day test;  
 (a) before test, (b) after test



Figure B.15 Beam for concrete cast on 10/27/06 for 3 day test;  
 (a) before test, (b) after test

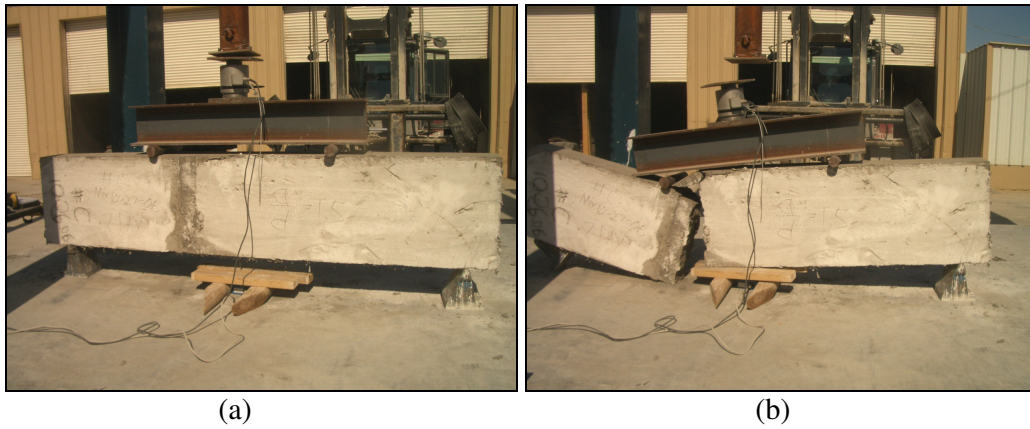


Figure B.16 Beam for concrete cast on 10/27/06 for 7 day test;  
(a) before test, (b) after test



Figure B.17 Beam for 1<sup>st</sup> batch concrete for concrete cast on 10/31/06 for 3 day test;  
(a) before test, (b) after test



Figure B.18 Beam for 1<sup>st</sup> batch concrete for concrete cast on 10/31/06 for 3 day test;  
(a) before test, (b) after test



Figure B.19 Beam for 2<sup>nd</sup> batch concrete cast on 10/31/06 for 3 day test;  
 (a) before test, (b) after test

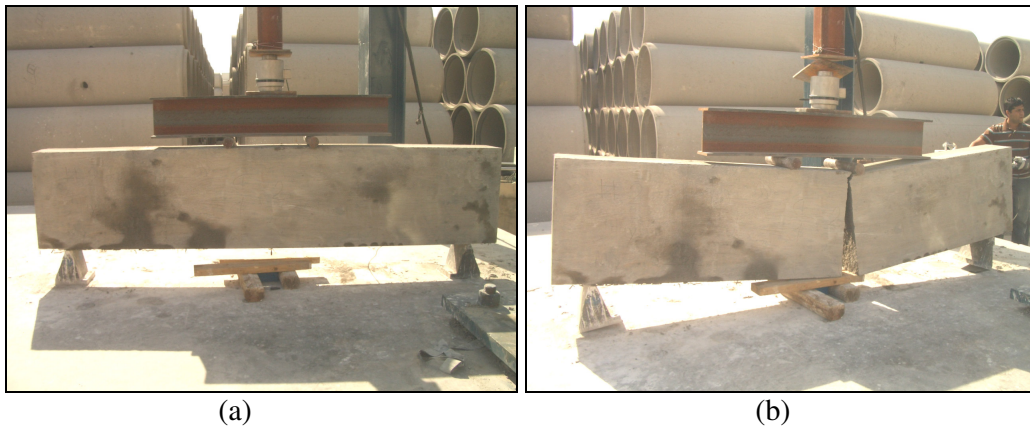


Figure B.20 Beam for 2<sup>nd</sup> batch concrete cast on 10/31/06 for 3 day test;  
 (a) before test, (b) after test

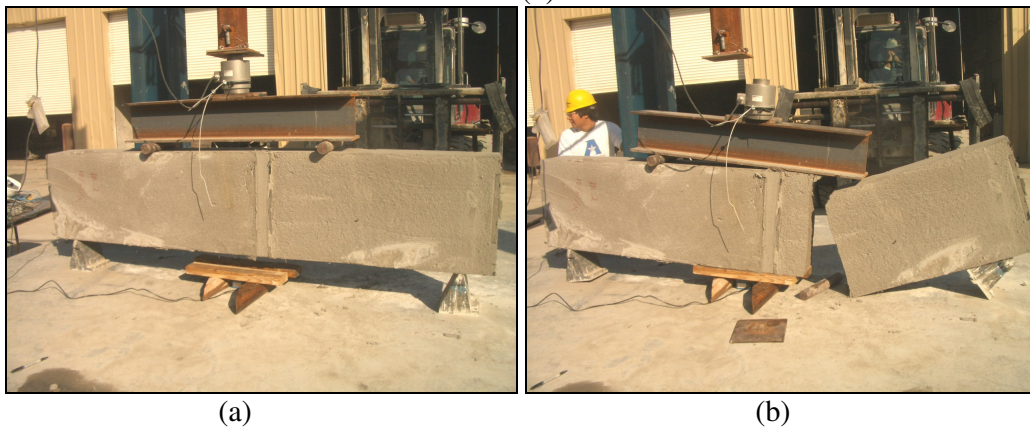


Figure B.21 Beam for 2<sup>nd</sup> batch concrete cast on 10/31/06 for 7 day test;  
 (a) before test, (b) after test



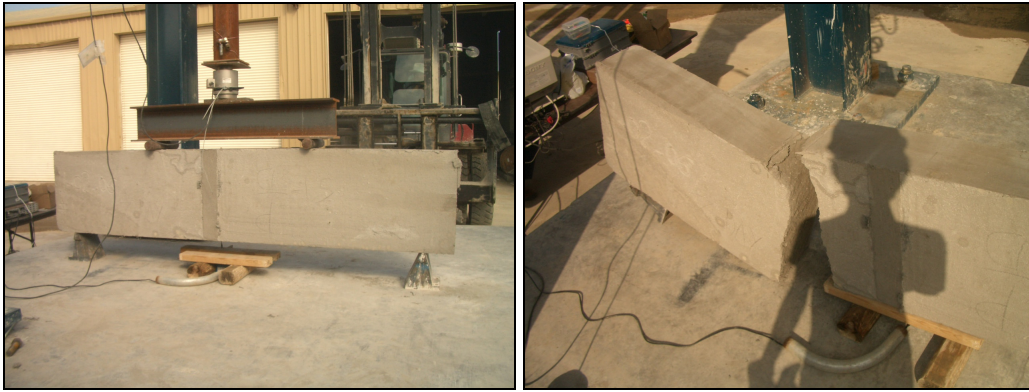
Figure B.22 Beam for 2<sup>nd</sup> batch concrete cast on 10/31/06 for 7 day test;  
(a) before test, (b) after test



Figure B.23 Beam for 1<sup>st</sup> batch concrete cast on 11/2/06 for 1 day test;  
(a) before test, (b) after test



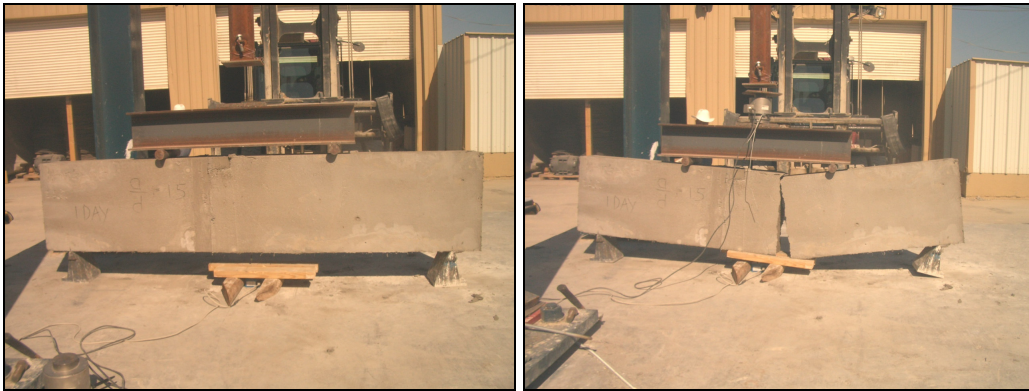
Figure B.24 Beam for 1<sup>st</sup> batch concrete cast on 11/2/06 for 1 day test;  
(a) before test, (b) after test



(a)

(b)

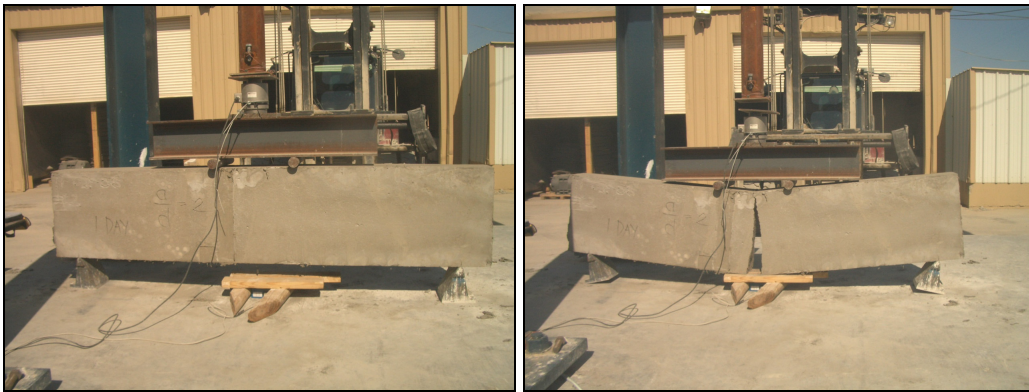
Figure B.25 Beam for 1<sup>st</sup> batch concrete cast on 11/2/06 for 7 day test;  
(a) before test, (b) after test



(a)

(b)

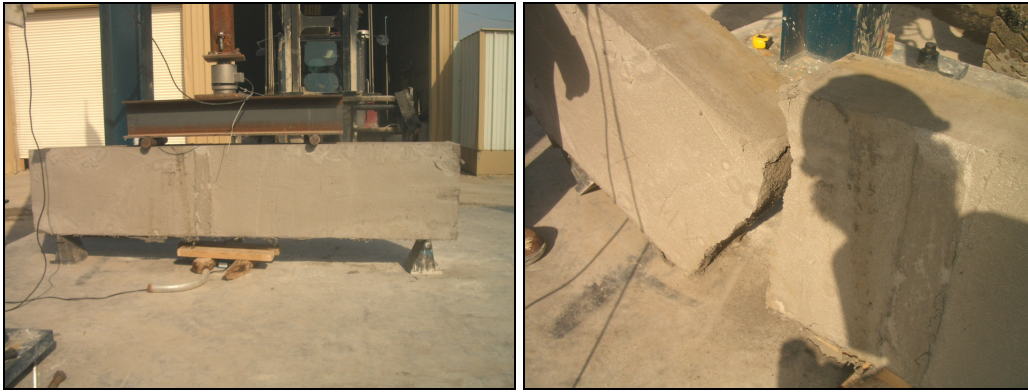
Figure B.26 Beam for 2<sup>nd</sup> batch concrete cast on 11/2/06 for 1 day test;  
(a) before test, (b) after test



(a)

(b)

Figure B.27 Beam for 2<sup>nd</sup> batch concrete cast on 11/2/06 for 1 day test;  
(a) before test, (b) after test



(a)

(b)

Figure B.28 Beam for 2<sup>nd</sup> batch concrete cast on 11/2/06 for 7 day test;  
(a) before test, (b) after test



(a)

(b)

Figure B.29 Beam for 2<sup>nd</sup> batch concrete cast on 11/2/06 for 7 day test;  
(a) before test, (b) after test



(a)

(b)

Figure B.30 Beam cast on 11/7/06 for 1 day test;  
(a) before test, (b) after test

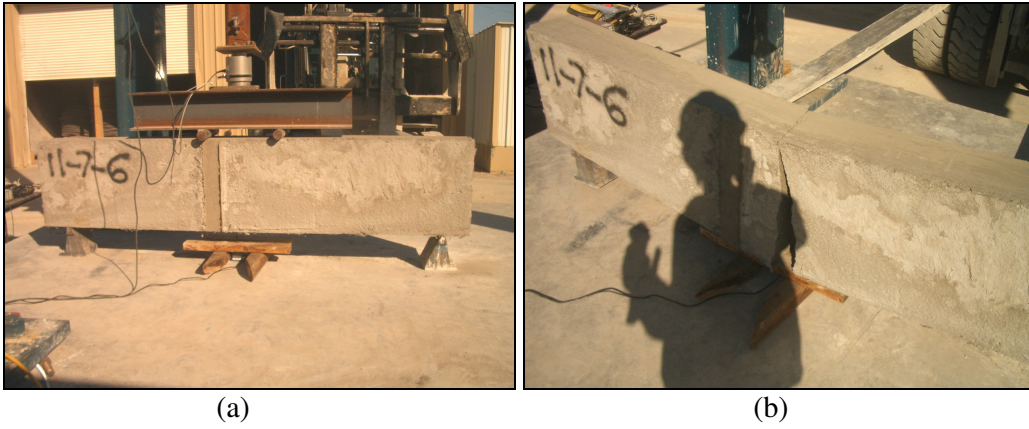


Figure B.31 Beam cast on 11/7/06 for 1 day test; (a) before test, (b) after test



Figure B.32 Beam cast on 11/7/06 for 3 day test; (a) before test, (b) after test



Figure B.33 Beam cast on 11/7/06 for 3 day test; (a) before test, (b) after test



(a)

(b)

Figure B.34 Beam cast on 11/7/06 for 7 day test; (a) before test, (b) after test



(a)

(b)

Figure B.35 Beam cast on 11/7/06 for 7 day test; (a) before test, (b) after test



(a)

(b)

Figure B.36 Beam cast on 11/7/06 for 56 day test; (a) before test, (b) after test





(a)

(b)

Figure B.37 Beam cast on 11/7/06 for 56 day test; (a) before test, (b) after test



(a)

(b)

Figure B.38 Beam for 1<sup>st</sup> batch concrete cast on 11/16/06 for 1 day test; (a) before test, (b) after test



(a)

(b)

Figure B.39 Beam for 1<sup>st</sup> batch concrete cast on 11/16/06 for 1 day test; (a) before test, (b) after test

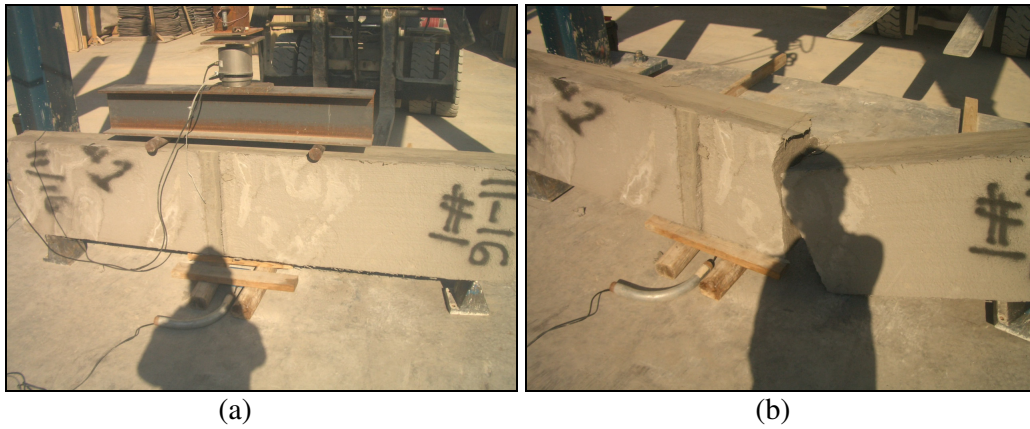


Figure B.40 Beam for 1<sup>st</sup> batch concrete cast on 11/16/06 for 3 day test;  
 (a) before test, (b) after test



Figure B.41 Beam for 1<sup>st</sup> batch concrete cast on 11/16/06 for 3 day test;  
 (a) before test, (b) after test

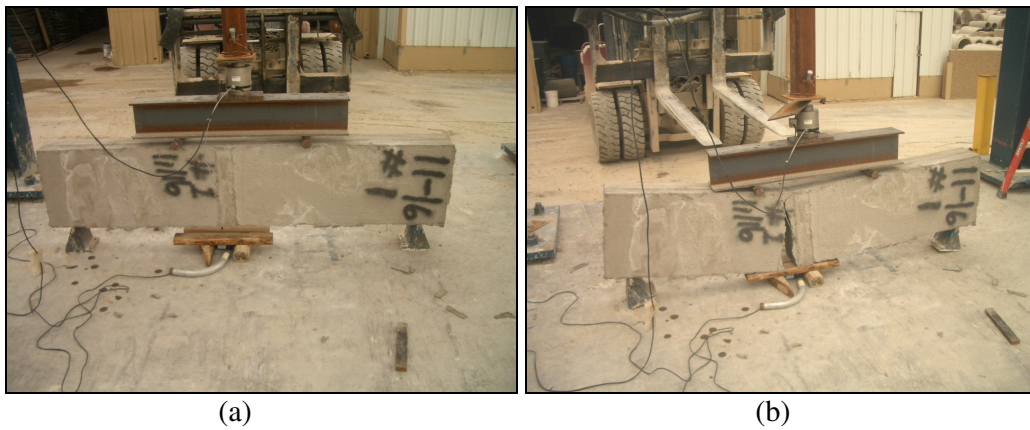


Figure B.42 Beam for 1<sup>st</sup> batch concrete cast on 11/16/06 for 14 day test;  
 (a) before test, (b) after test



(a)

(b)

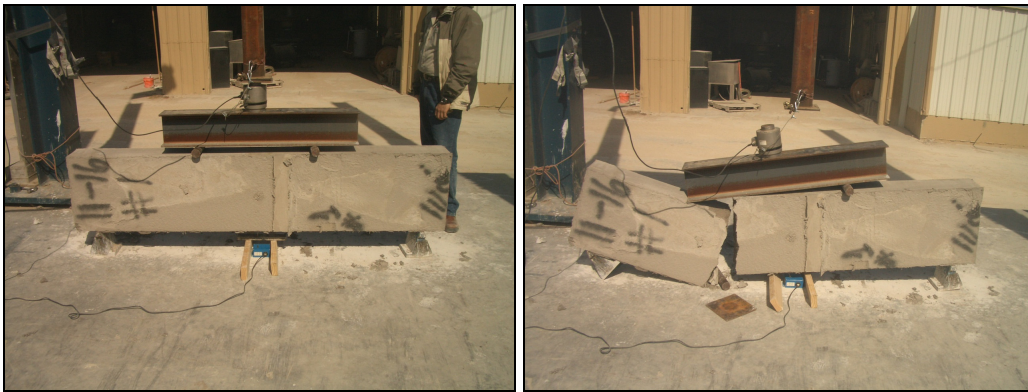
Figure B.43 Beam for 1<sup>st</sup> batch concrete cast on 11/16/06 for 56 day test;  
(a) before test, (b) after test



(a)

(b)

Figure B.44 Beam for 1<sup>st</sup> batch concrete cast on 11/16/06 for 56 day test;  
(a) before test, (b) after test



(a)

(b)

Figure B.45 Beam for 1<sup>st</sup> batch concrete cast on 11/16/06 for 90 day test;  
(a) before test, (b) after test

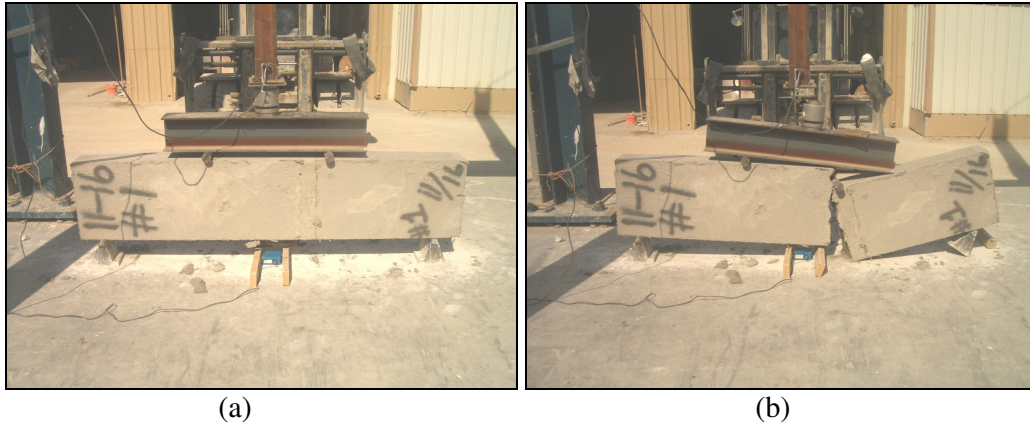


Figure B.46 Beam for 1<sup>st</sup> batch concrete cast on 11/16/06 for 90 day test;  
 (a) before test, (b) after test

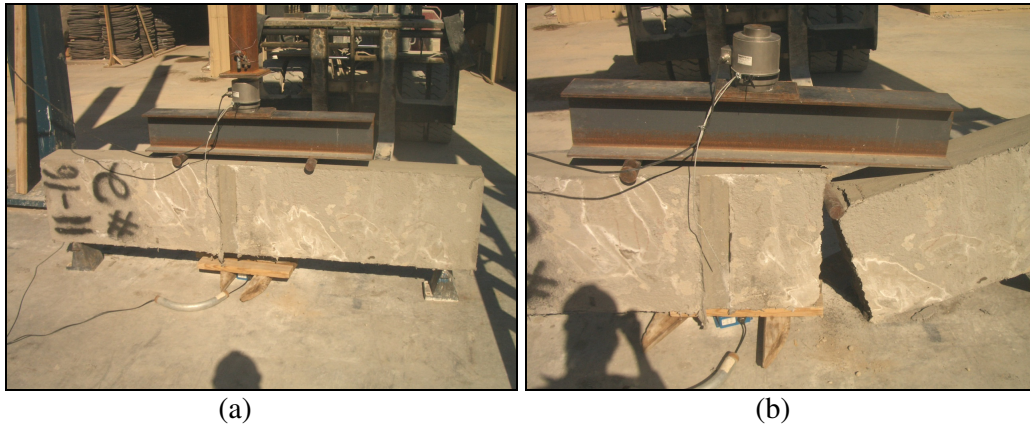


Figure B.47 Beam for 2<sup>nd</sup> batch concrete cast on 11/16/06 for 1 day test;  
 (a) before test, (b) after test

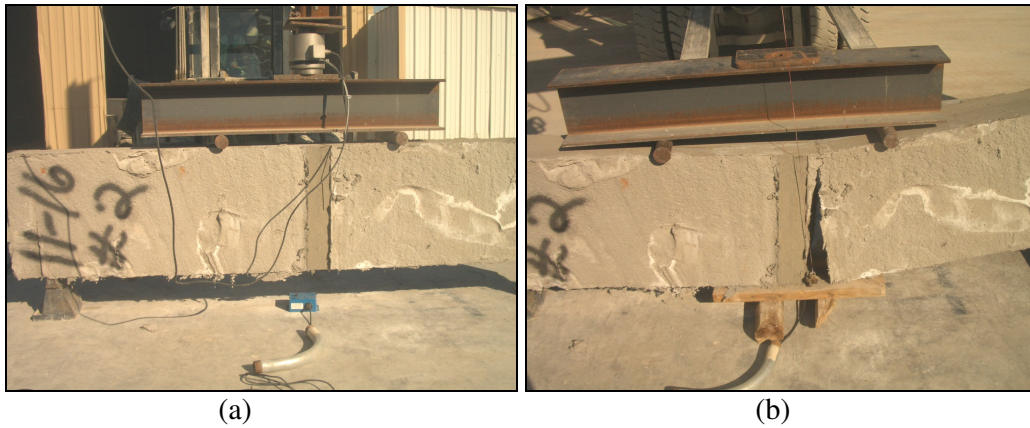


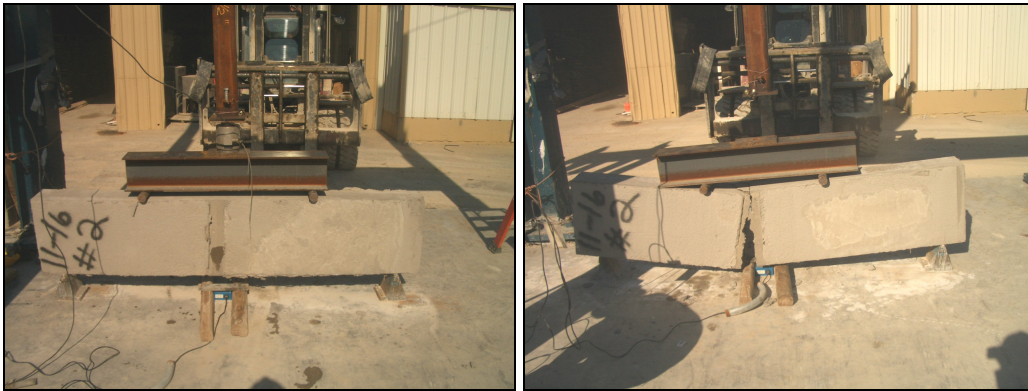
Figure B.48 Beam for 2<sup>nd</sup> batch concrete cast on 11/16/06 for 3 day test;  
 (a) before test, (b) after test



(a)

(b)

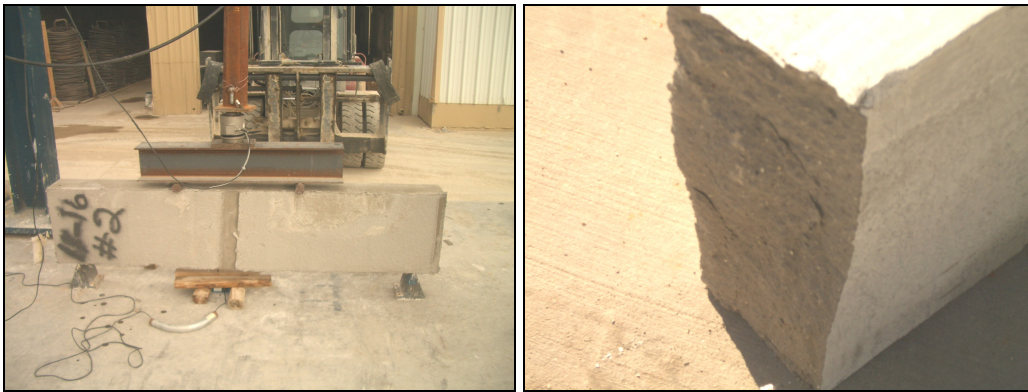
Figure B.49 Beam for 2<sup>nd</sup> batch concrete cast on 11/16/06 for 3 day test;  
 (a) before test, (b) after test



(a)

(b)

Figure B.50 Beam for 2<sup>nd</sup> batch concrete cast on 11/16/06 for 14 day test;  
 (a) before test, (b) after test



(a)

(b)

Figure B.51 Beam for 2<sup>nd</sup> batch concrete cast on 11/16/06 for 56 day test;  
 (a) before test, (b) after test

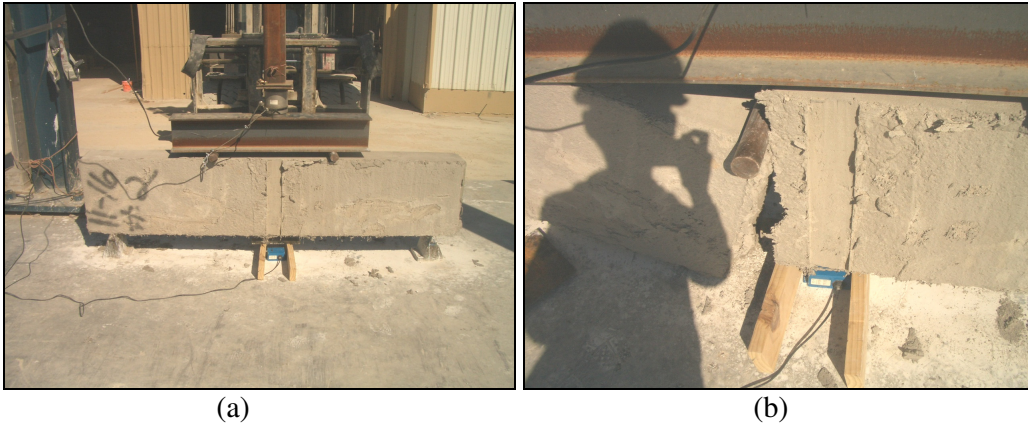


Figure B.52 Beam for 2<sup>nd</sup> batch concrete cast on 11/16/06 for 90 day test;  
(a) before test, (b) after test



Figure B.53 Beam for 2<sup>nd</sup> batch concrete cast on 11/16/06 for 90 day test;  
(a) before test, (b) after test

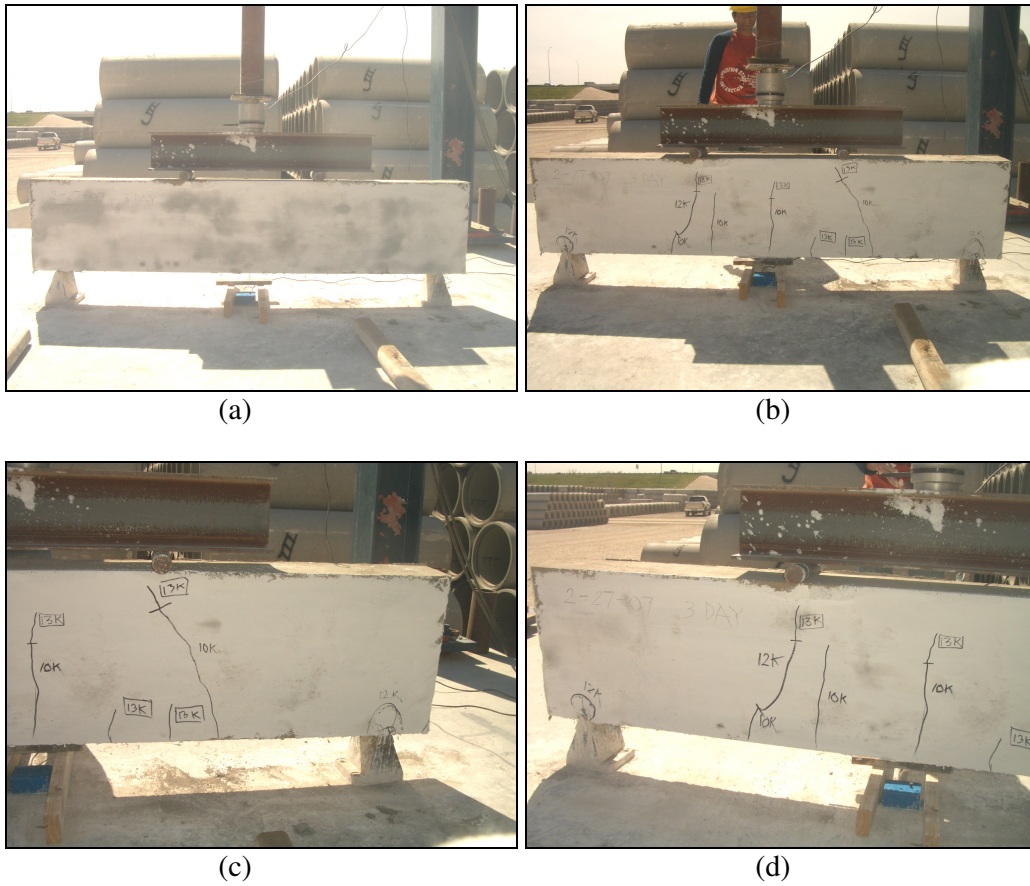


Figure B.54 Ductile lightweight concrete beam with reinforcement cast on 2/27/07 for 3 day test; (a) before test, (b), (c), and (d) cracks on the beam after test

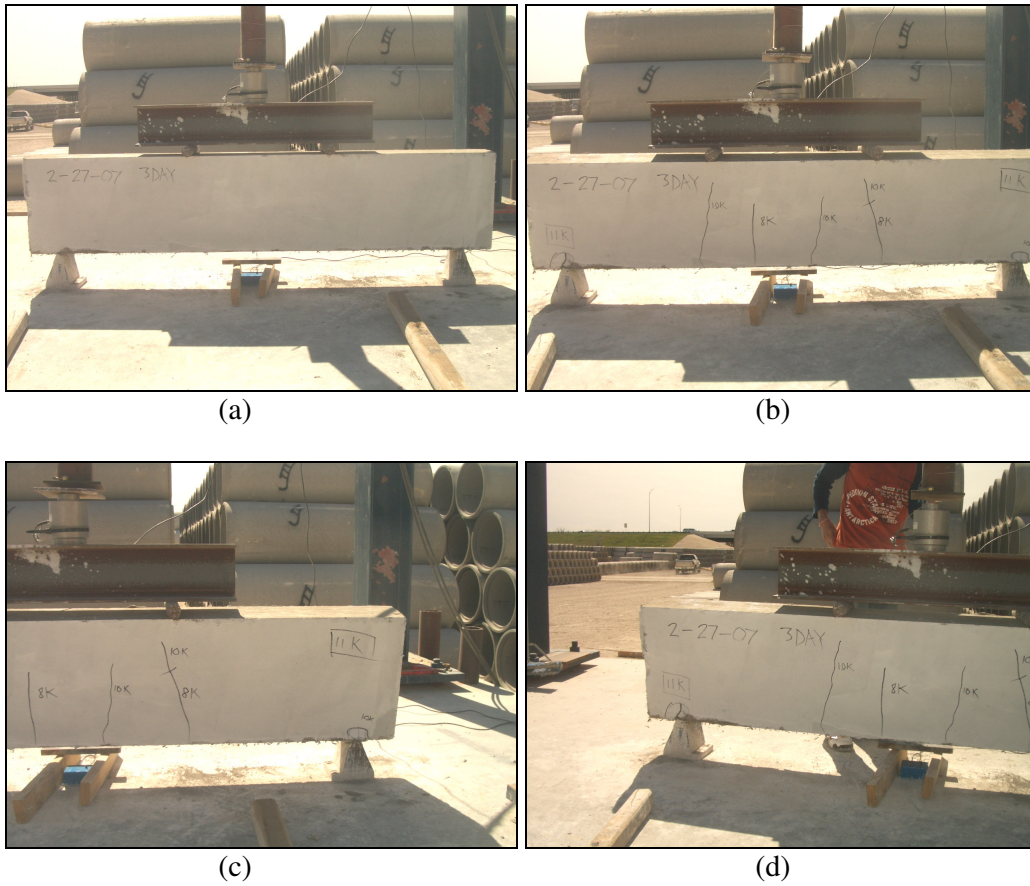


Figure B.55 Ductile lightweight concrete beam with reinforcement cast on 2/27/07 for 3 day test; (a) before test, (b), (c), and (d) cracks on the beam after test



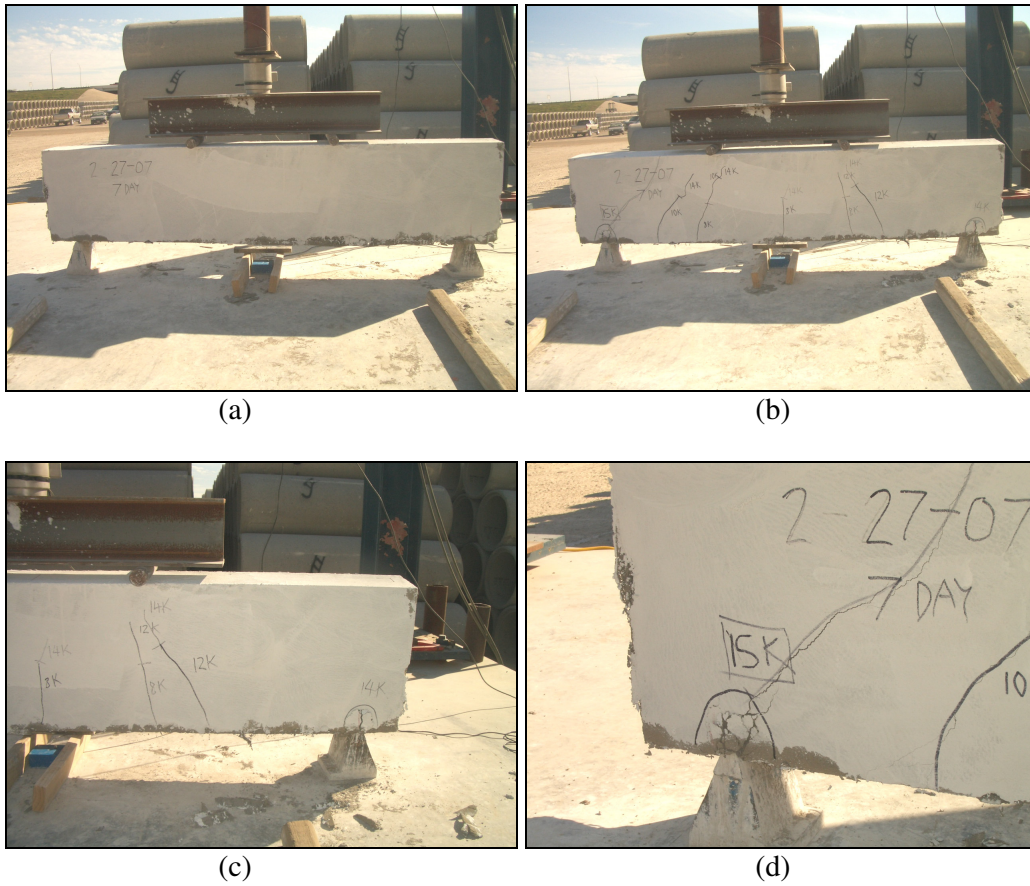


Figure B.56 Ductile lightweight concrete beam with reinforcement cast on 2/27/07 for 7 day test; (a) before test, (b), (c), and (d) cracks on the beam after test

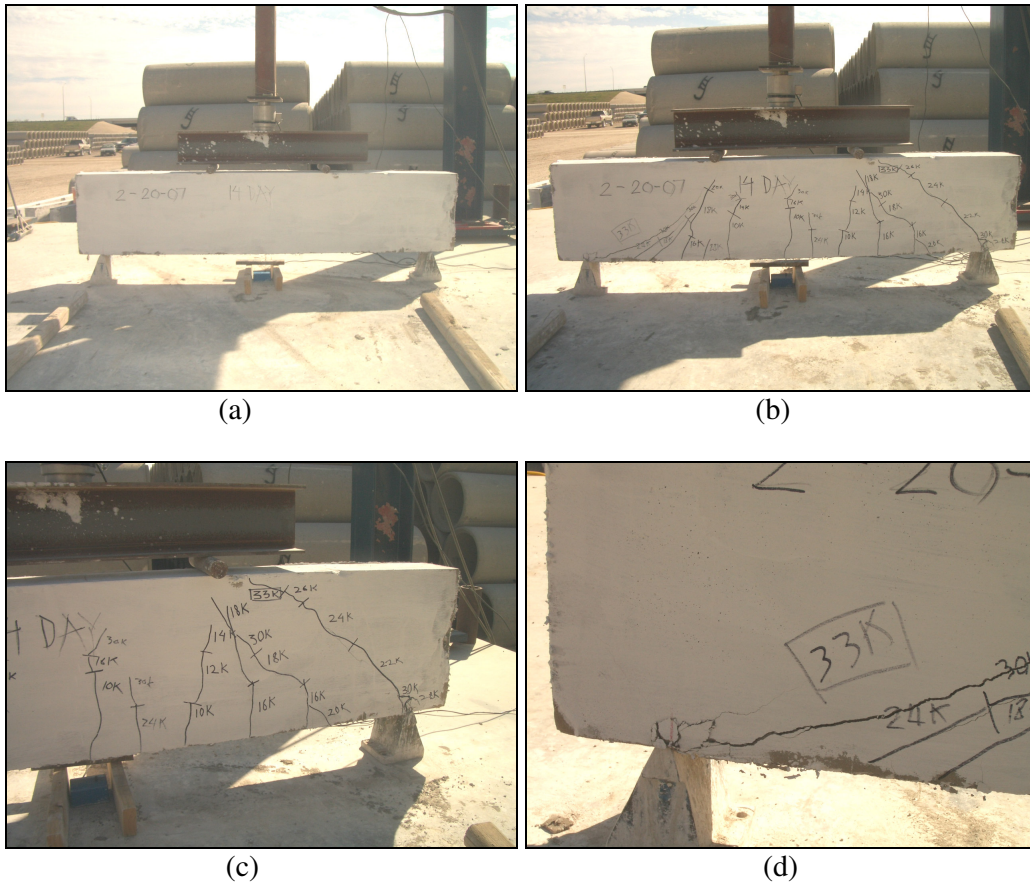


Figure B.57 Ductile lightweight concrete beam with reinforcement cast on 2/27/07 for 14 day test; (a) before test, (b), (c), and (d) cracks on the beam after test

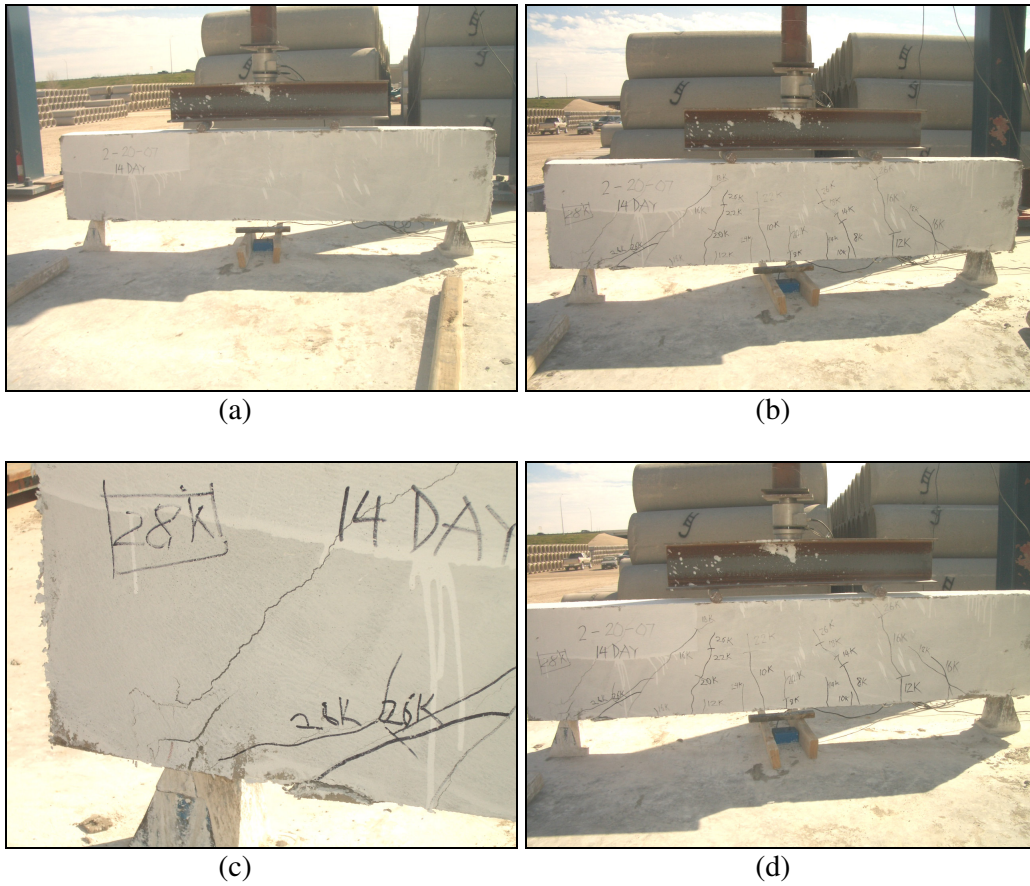


Figure B.58 Ductile lightweight concrete beam with reinforcement cast on 2/27/07 for 14 day test; (a) before test, (b), (c), and (d) cracks on the beam after test

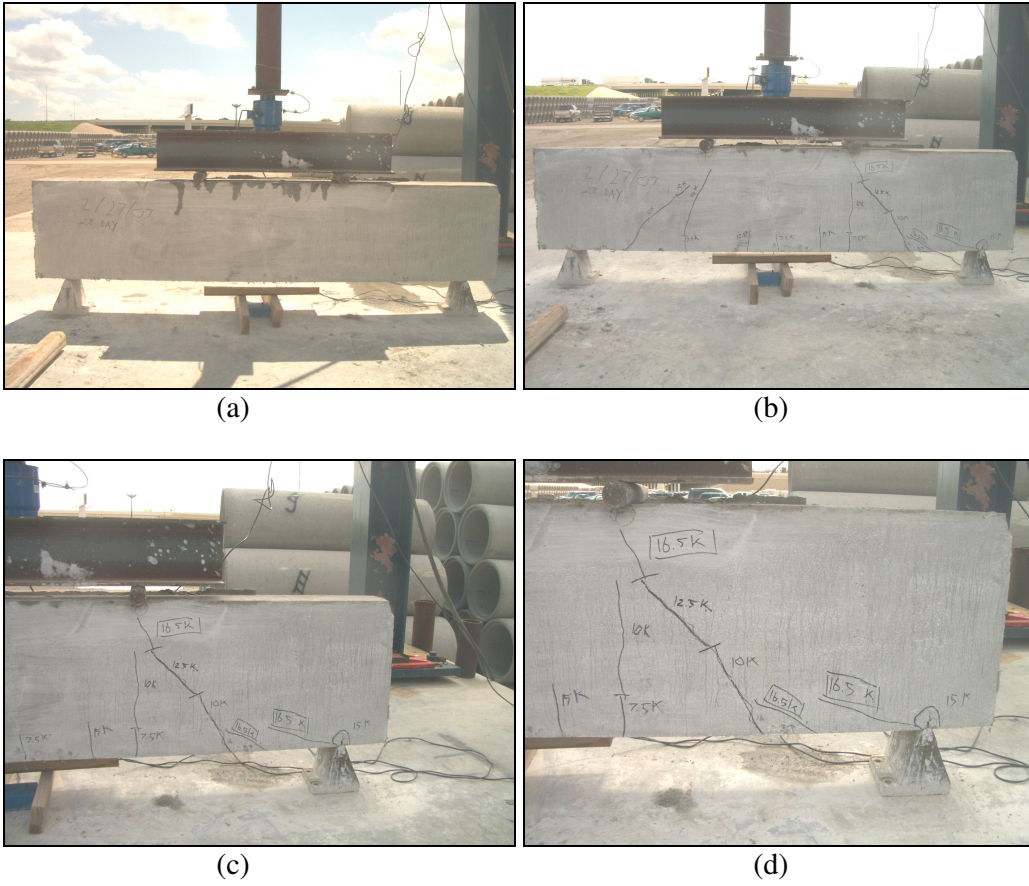


Figure B.59 Ductile lightweight concrete beam with reinforcement cast on 2/27/07 for 28 day test; (a) before test, (b), (c), and (d) cracks on the beam after test

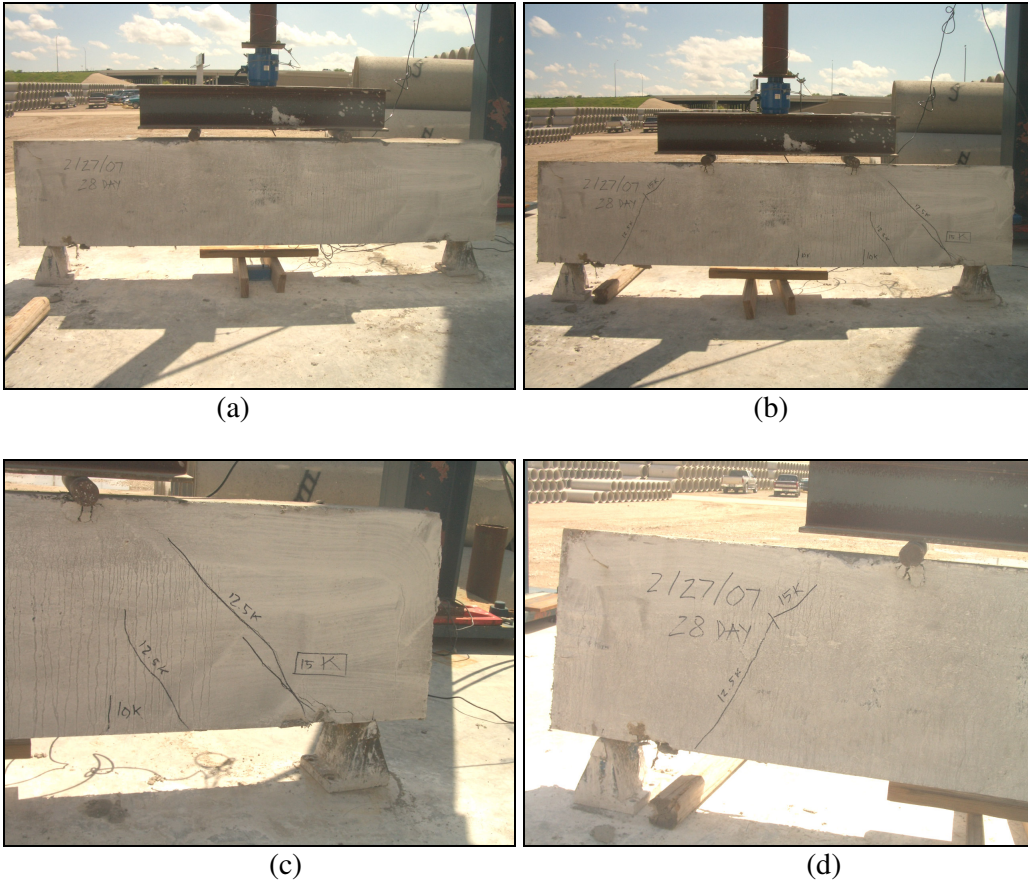


Figure B.60 Ductile lightweight concrete beam with reinforcement cast on 2/27/07 for 28 day test; (a) before test, (b), (c), and (d) cracks on the beam after test

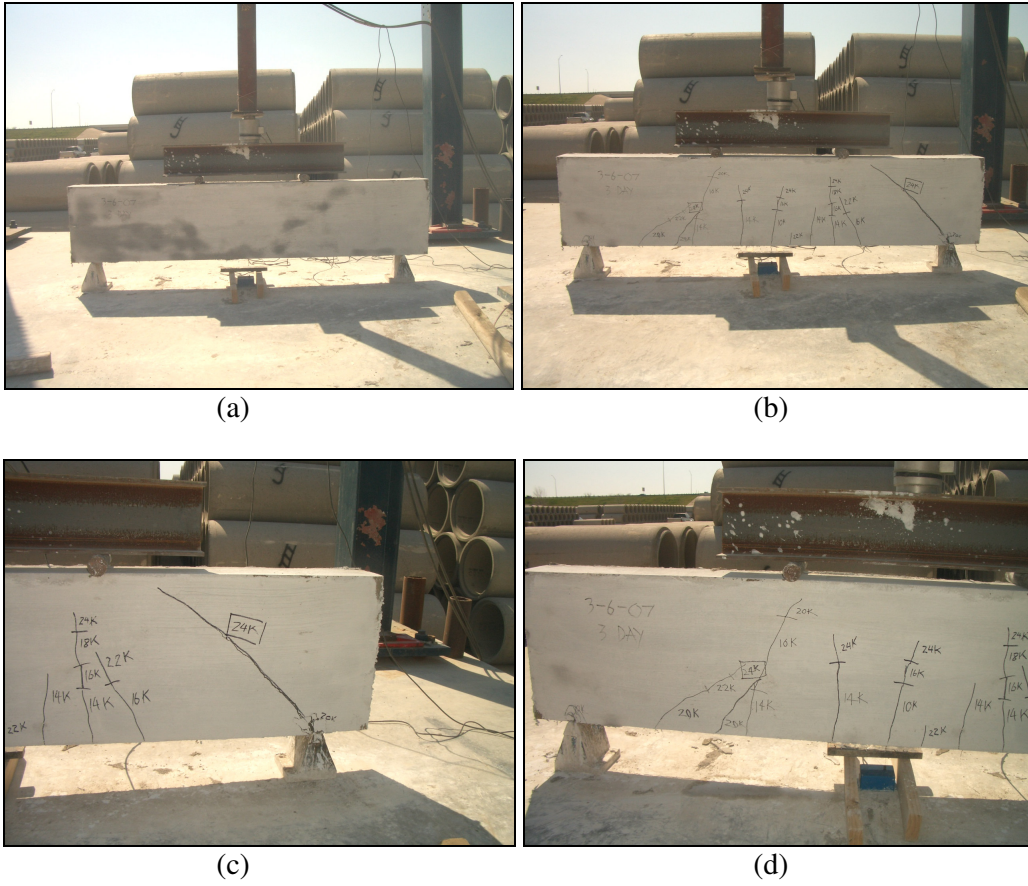


Figure B.61 Ductile lightweight concrete beam with reinforcement cast on 3/6/07 for 3 day test; (a) before test, (b), (c), and (d) cracks on the beam after test



(a)



(b)

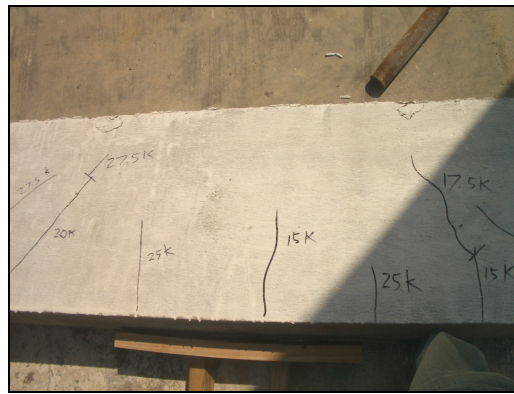


(c)

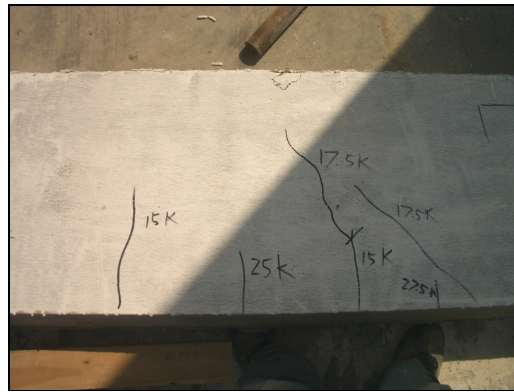
Figure B.62 Ductile lightweight concrete beam with reinforcement cast on 3/6/07 for 3 day test; (a) before test, (b), and (c) cracks on the beam after test



(a)



(b)



(c)

Figure B.63 Ductile lightweight concrete beam with reinforcement cast on 3/6/07 for 7 day test; (a) before test, (b), and (c) cracks on the beam after test





(a)



(b)



(c)

Figure B.64 Ductile lightweight concrete beam with reinforcement cast on 3/6/07 for 14 day test; (a) before test, (b), and (c) cracks on the beam after test

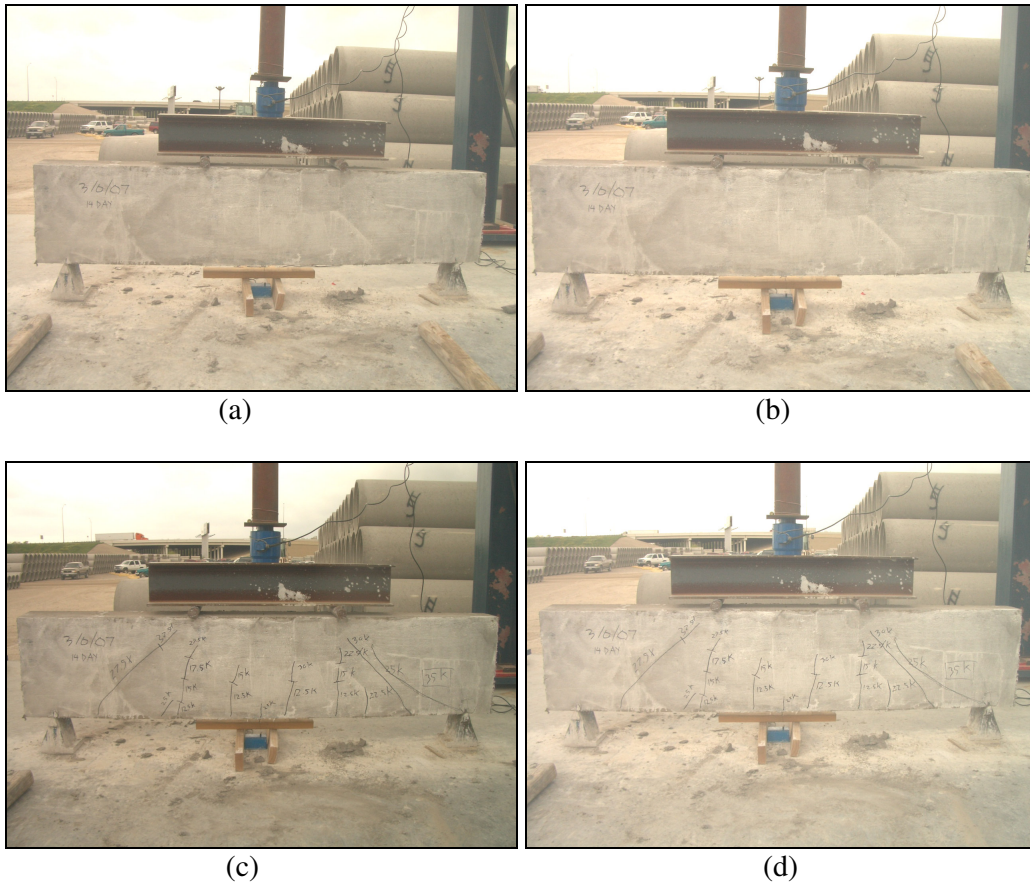


Figure B.65 Ductile lightweight concrete beam with reinforcement cast on 3/6/07 for 14 day test; (a) before test, (b), (c) and (d) cracks on the beam after test

APPENDIX C

WALL TEST, PICTURE BEFORE AND AFTER TESTING,  
AND DRAWING OF EACH PANEL

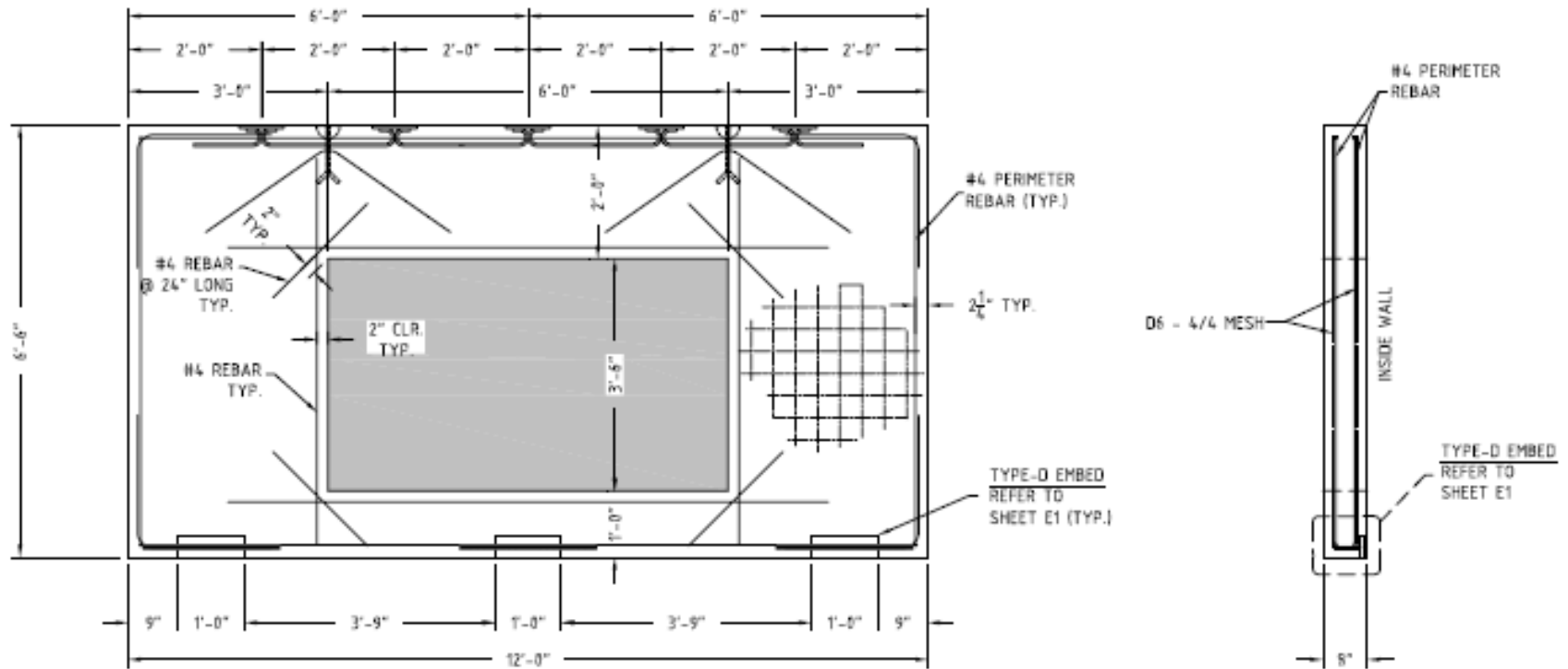


Figure C.1 Detail drawing for concrete panel with door opening

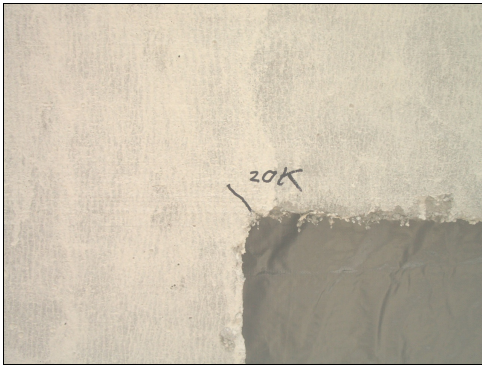
Experimental Report for Wall Panel with window opening Test on 6/18/2007



Figure C.2 Wall panel before testing



(a)



(b)



(c)

Figure C.3 Non-measurable cracks at the middle and both corners of wall opening at 20 kips; (a) crack at middle span, (b) and (c) cracks at the corners of opening

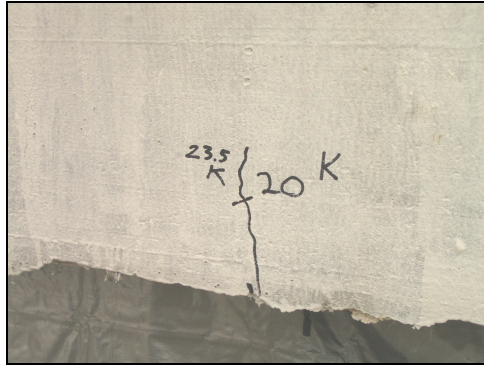


Figure C.4 Crack at the middle of wall becomes longer at 23.5 kips

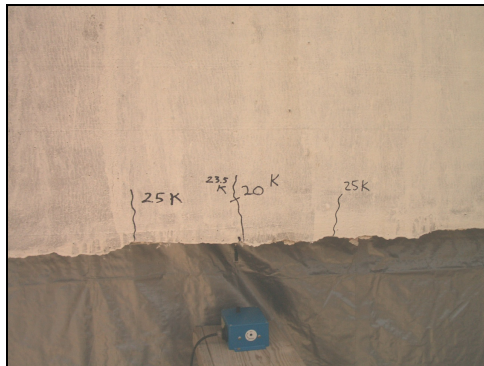


Figure C.5 Cracks at left and right of the middle crack at 25 kips

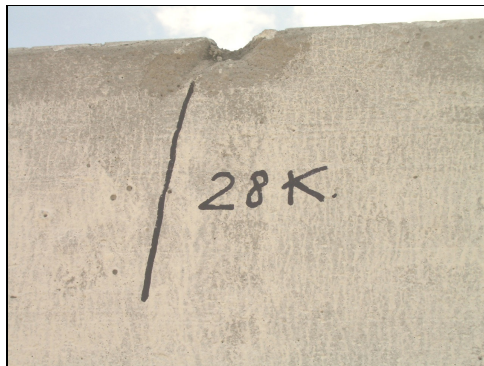


Figure C.6 Crack for negative moment at top of wall at 28 kips

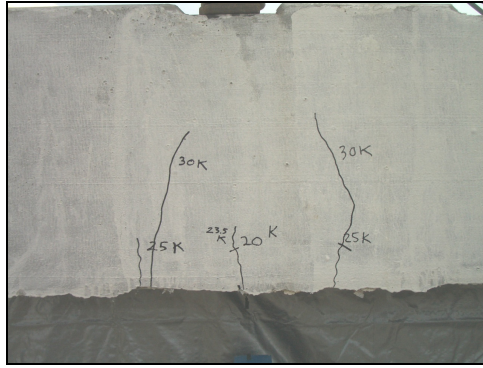


Figure C.7 Initial flexural cracks at 25 kips extend longer at 30 kips

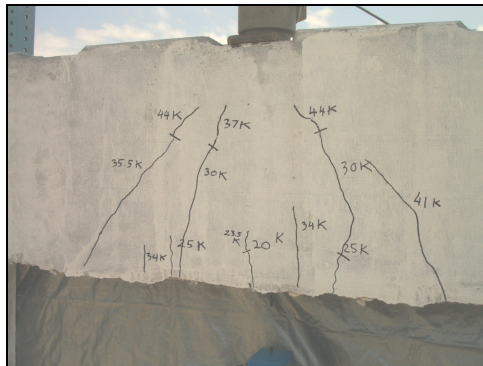


Figure C.8 Flexural cracks occur around the middle of wall until 44 kips



Figure C.9 Wall lost stiffness at 50 kips

After that trying load until the wall fails



Figure C.10 The wall lost all of stiffness at load 98 kips

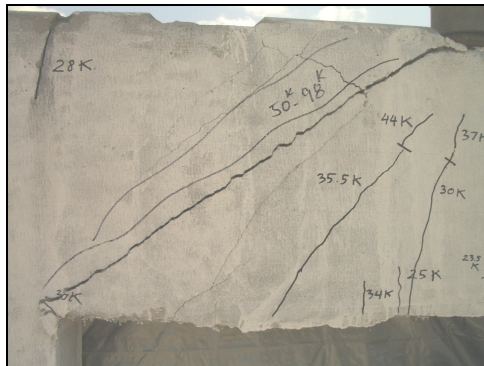


Figure C.11 Big crack 45 degree at the corner of the opening occur at failure load 98 kips



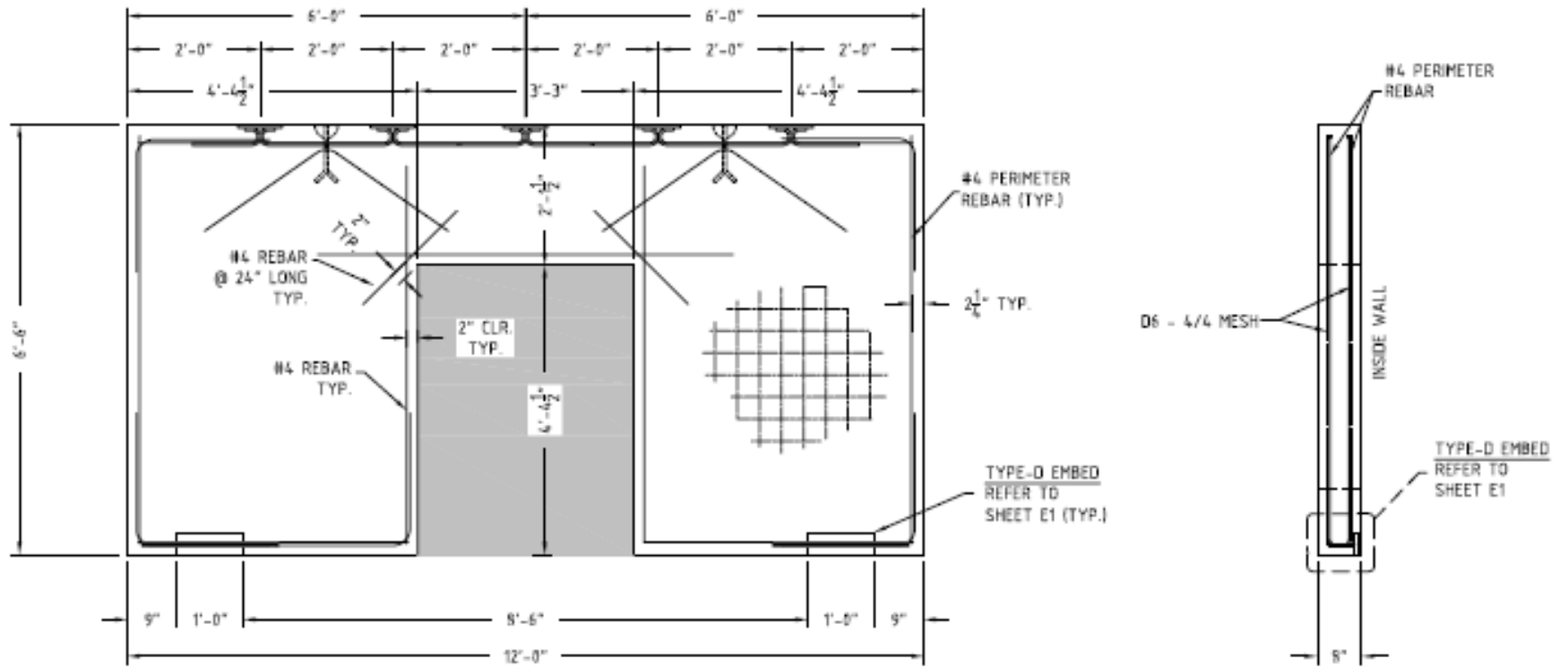


Figure C.12 Detail drawing for concrete panel with window opening

**Experimental Report for Wall Panel with door opening Test on 6/21/2007**



Figure C.13 Set up equipment for wall with door opening test



Figure C.14 The first cracks at the middle of wall opening at 28 kips



Figure C.15 Find another flexural crack at the left of the first crack at 34 kips

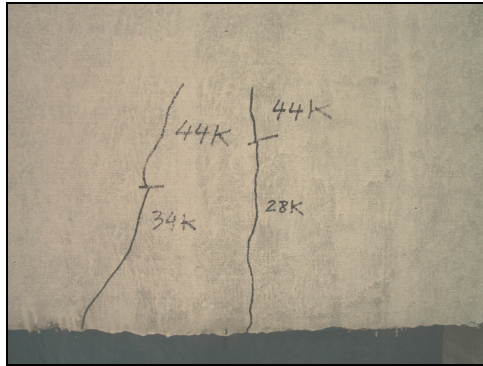


Figure C.16 The initial cracks become longer at 44 kips

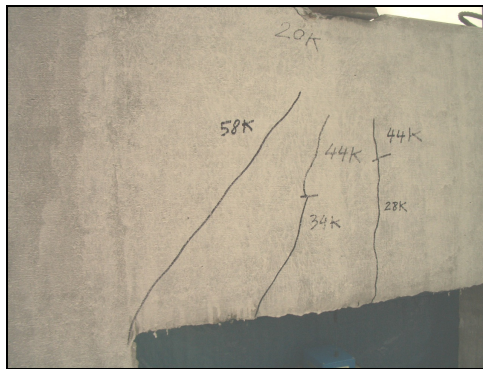


Figure C.17 The 45 degree crack at the corner of opening was found at 58 kips

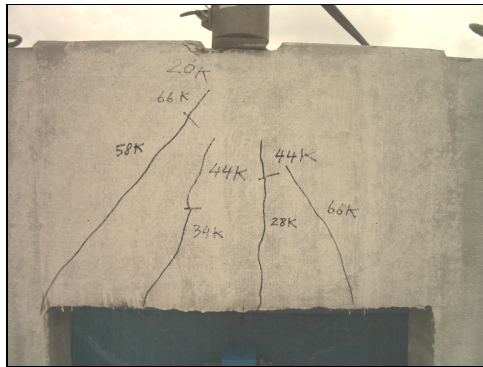


Figure C.18 At 66 kips, crack at the corner of opening became larger and new crack occur at the right hand side of wall

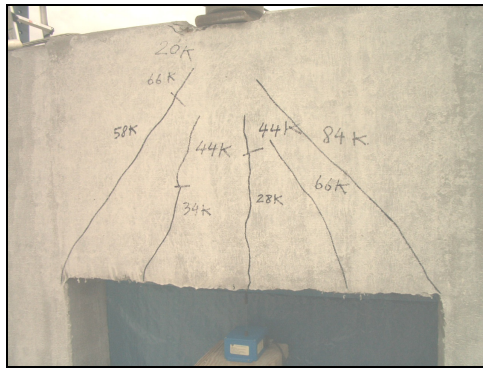
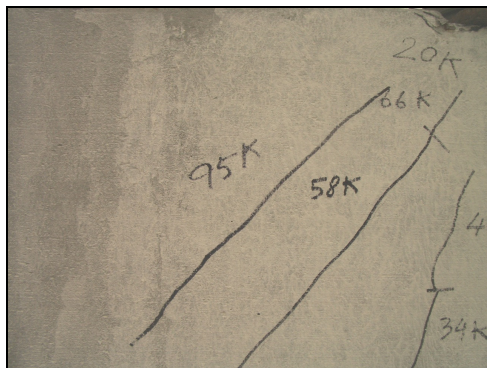


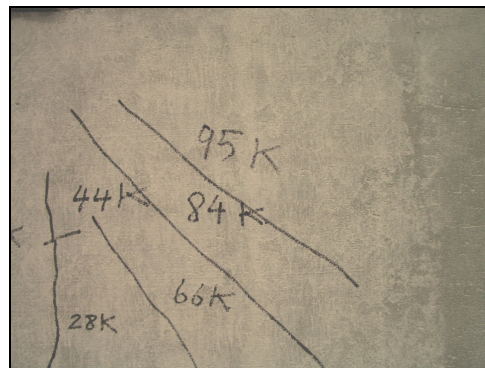
Figure C.19 Found another 45 degree crack at the right corner of opening at 84 kips



(a)



(b)

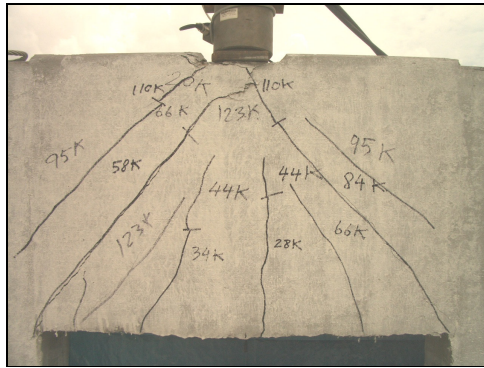


(c)

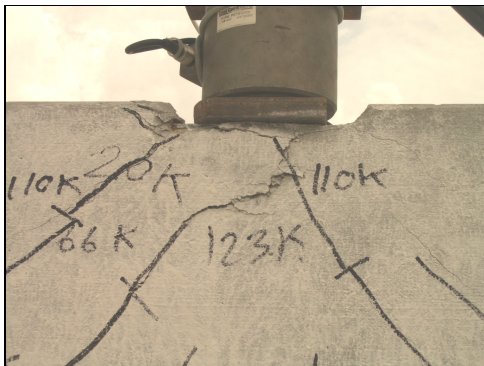
Figure C.20 New cracks occurred at the left and right hand side at 95 kips; (a), (b), and (c) cracks on the panel before ultimate load



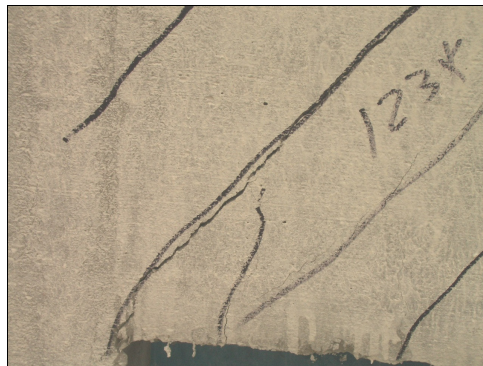
Figure C.21 At 110 kips, some cracks became longer to reach position of load point



(a)



(b)



(c)

Figure C.22 Wall panel fail at load around 123 kips ;  
(a), (b), and (c) cracks on the panel at ultimate load

## REFERENCES

- American Society for Testing Materials (2005), “ASTM C 39: *Standard Test Method for Compressive Strength of Cylindrical Concrete Specimens*” Philadelphia, PA.
- American Society for Testing Materials (2005), “ASTM C 78: *Standard Test Method for Flexural Strength of Concrete*” Philadelphia, PA.
- American Society for Testing Materials (2005), “ASTM C 234: *Standard Test Method Comparing Concretes on The Basis of The Bond Developed with Reinforcing Steel*” Philadelphia, PA.
- ABAQUS, 2005. “ABAQUS version 6.5,” ABAQUS, Inc., Pawtucket, RI.
- Mun, K.J. (2007), “Development and tests of lightweight aggregate using sewage sludge for nonstructural concrete”, *Construction and Building Materials*, Vol. 21, pp. 1583–1588.
- Gesog˘lu, M., Ozturan, T., and Guneyisi, E. (2007), “Effects of fly ash properties on characteristics of cold-bonded fly ash lightweight aggregates” *Construction and Building Materials*, Vol. 21, pp.869–1878.
- Unal, O., Uygunog˘ lu, T., and Yildiz, A. (2007), “Investigation of properties of low-strength lightweight concrete for thermal insulation”, *Building and Environment*, Vol.42, pp. 584–590.
- Teo, D.C.L., Mannan, M.A., Kurian V.J., and Ganapathy, C. (2007), “Lightweight concrete made from oil palm shell (OPS): Structural bond and durability properties”, *Building and Environment*, Vol. 42, pp. 2614–2621.
- Pioro, L.S., and Pioro, I.L. (2004), “Production of expanded-clay aggregate for lightweight concrete from non-selfbloating clays”, *Cement & Concrete Composites*, Vol. 26, pp. 639–643.
- Qiao, X.C., Ng, B.R., Tyrer, M., Poon, C.S., and Cheeseman, C.R. (2006), “Production of lightweight concrete using incinerator bottom ash”, *Construction and Building Materials*.
- Topcu, I.B., Uygunog˘ lu, T. (2007), “Properties of autoclaved lightweight aggregate concrete”, *Building and Environment*, Vol. 42, pp. 4108–4116.
- Mannan, M.A. , Alexander, J., Ganapathy, C., and Teo, D.C.L. (2006), “Quality improvement of oil palm shell (OPS) as coarse aggregate in lightweight concrete”, *Building and Environment*, Vol. 41, pp. 1239–1242.

Topcu, I.B., Odler, I. (1996), "SEMI LIGHTWEIGHT CONCRETES PRODUCED BY VOLCANIC SLAGS", *Cement and Concrete Research*, Vol. 27, No. 1, pp. 15-21.

Miled, K., Roy, R.L., Sab, K., and Boulay, C. (2004), "Compressive behavior of an idealized EPS lightweight concrete: size effects and failure mode", *Mechanics of Materials*, Vol. 36, pp. 1031–1046.

Kewalramani, M.A., and Gupta, R. (2006), "Concrete compressive strength prediction using ultrasonic pulse velocity through artificial neural networks", *Automation in Construction*, Vol. 15, pp. 374 – 379.

Qasrawi, H.Y. (2000), "Concrete strength by combined nondestructive methods Simply and reliably predicted", *Cement and Concrete Research*, Vol. 30, pp. 739-746.

Rajamane, N.P., Peter, J.A., and Ambily, P.S. (2007), "Prediction of compressive strength of concrete with fly ash as sand replacement material", *Cement & Concrete Composites*, Vol. 29, pp. 218–223.

Elfahal, M.M., Krauthamme, T., Ohno, T., Beppu, M., and Mindess, S. (2005), "Size effect for normal strength concrete cylinders subjected to axial impact", *International Journal of Impact Engineering*, Vol. 31, pp. 461–481.

## BIOGRAPHICAL INFORMATION

Ake Piyamaikongdech was born October 16, 1982 in Bangkok, the capital city in Thailand. He finished his school level in 2000 with the major courses of mathematics and science. Then, in 2004 he received his bachelor degree in Civil Engineering at the Chulalongkorn University, one of the most famous universities in Thailand. After his graduation, he started working for the company “Thai Takenaka International Co.,Ltd.” in the area of site engineering for two year. He worked at the site of construction of several factories in Eastern Seaboard industrial area as a field engineer. His main duties were to control the construction processes, coordination with sub-contractors, control quality of works, budget control, construction schedule, and construction documents.

Afterward, he entered the graduate program in Structural and Applied Mechanics at the University of Texas at Arlington (UTA) where he did research under Dr. Ali Abolmaali instruction as a Master of Science in Civil Engineering ductile lightweight concrete and finite element models.